HINGE ZONE TIE SPACING IN REINFORCED CONCRETE TILT-UP FRAME PANELS

by

MICHAEL DEW

B.Sc. (ENG) (CIVIL) University of Cape Town, 1997

A THESIS SUBMITTED IN PARTIAL FULFILLMENT
OF THE REQUIREMENTS FOR THE DEGREE OF

MASTER OF APPLIED SCIENCE

in

THE FACULTY OF GRADUATE STUDIES

Department of Civil Engineering

We accept this thesis as conforming
to the required standard

THE UNIVERSITY OF BRITISH COLUMBIA

April 2000

In presenting this thesis in partial fulfilment of the requirements for an advanced degree at the University of British Columbia, I agree that the Library shall make it freely available for reference and study. I further agree that permission for extensive copying of this thesis for scholarly purposes may be granted by the head of my department or by his or her representatives. It is understood that copying or publication of this thesis for financial gain shall not be allowed without my written permission.

Department of CIVIL ENGINEERING

The University of British Columbia
Vancouver, Canada

Date 18 APRIL 2000

DE-6 (2/88)

ABSTRACT

Tilt-up concrete buildings have concrete walls, supported on a concrete floor slab, and a light weight roof system. The exterior concrete walls, which are typically 190 mm thick with two layers of reinforcement, are cast on the floor slab and then lifted into position. Recently two storey panels with large window openings at both ground and first floor levels have become popular. The result is that the wall panels, which form lateral load resisting system, have become more like frames than walls. Given that the panels are typically only 190 mm thick, the members have very high depth to width ratios. The performance under cyclic earthquake loading of reinforced concrete frame members with these depth to width ratios is not well understood. Furthermore, since the code was written with more traditional cross sections in mind, the tie spacing rules it provides are not necessarily applicable to tilt-up frame panels.

The frame panels are designed so that all inelastic deformations during an earthquake will result from flexural hinging in the frame members. The research reported in this thesis investigated the effect of hinge zone tie spacing on the displacement ductility of reinforced concrete tilt-up frame panels. The results of tests done on six full scale quarter frame panels with three different tie spacings are presented. The test specimens contained typical longitudinal reinforcement and were dimensionally representative of typical tilt-up frame panels.

It was found that hinge zone tie spacing can determine the mode of failure and have a significant effect on panel ductility. The hinge zone tie spacings tested were 100 mm, 200 mm and 300 mm. The mode of failure for the 200 mm and 300 mm specimens was buckling of the longitudinal steel reinforcement in compression after the cover concrete had spalled. The 100 mm tie spacing was sufficiently close to prevent buckling of the longitudinal reinforcement after loss of the cover concrete. The 100 mm specimens failed via either local out of plane buckling of the entire hinge zone reinforcement cage, or by pullout of the longitudinal beam steel resulting from loss of bond within the hinge zone.

It was found that the ultimate load attained and maintained during the ductile range was influenced by the tie spacing. The 100 mm and 200 mm tie spacing specimens attained and maintained a maximum bending moment similar to the ultimate flexural strength calculated assuming a maximum compressive strain in the concrete of 0.0035. The 300 mm tie spacing specimens only attained and maintained a bending moment approximately equal to that at first yielding of the longitudinal steel.

Since the ductilities for the different tie spacings were calculated using different strength assumptions they are not directly comparable, nevertheless the full frame displacement ductilities achieved for the 100 mm, 200 mm and 300 mm tie spacings were 5.7, 3.9 and 4.7 respectively.

TABLE OF CONTENTS:

LIST OF TABLES

LIST OF FIGURES

ACKNOWLEDGMENTS

Research assistantship was provided by the Natural Sciences and Engineering Research Council through a research grant to Dr. R.G. Sexsmith. Further funding was provided in the form of the St. John's College Charles C C Wong Memorial Fellowship. Generous donations were made by local contractors and suppliers in terms of materials and time for the construction of the panels. Special thanks are extended to the following companies for their contributions:

- Beedie Construction Co Ltd. for the construction of the panels.
- Cut Rite Steel for the donation of and fixing of the panel reinforcement.
- LaFarge Canada Inc. for the donation of the concrete.
- Phoenix Trucking for the donation of shipping services.
- Richform Construction Supply Co. Ltd. for the supply of the coil rods cast into the Specimen.
- Steels Industrial Products Ltd. for donating the lifting inserts.
- Sterling Crane for the lifting of the panels.

A committee consisting of representatives from Structural Engineering Consultants of British Colombia (SECBC) consulting firms was formed to guide the testing program. The task of the committee was to identify the issues of concern to designers involved with tilt-up buildings, and to ensure the testing program was designed such that these issues were addressed. The committee was chaired by Gerry Weiler of Weiler Smith Bowers (WSB) Consulting Structural Engineers, and the following people attended the meetings in which the testing program was planned and/or reviewed.

Dr. Robert Sexsmith	UBC
Dr. Perry Adebar	UBC
Michael Dew	UBC
James Lam	Bianco Lam
Patrick Lam	CWMM
Kevin Lemieux	Weiler Smith Bowers
Tim Loo	Omnicron
Jim Mutrie	JKK
Ron Thompson	Read Jones Christofferson
Gerry Weiler	Weiler Smith Bowers

Thanks are extended to the members of the SECBC committee for their involvement in this research and I would personally like to thank Dr. Sexsmith for his help as my thesis supervisor and Gerry Weiler for the guidance and support he provided over the course of this research project.

1 INTRODUCTION

1.1 Origin of interest

In the past tilt-up concrete construction has been popular for warehouses and other buildings in which rectangular panels with few or no openings were appropriate. Tilt-up construction is however being increasingly used for two storey office buildings. For these buildings architects prefer panels with large window openings at both ground and first floor levels. The result is that many modern tilt-up panels are more like frames than walls.

Since the panels are typically only 190 mm thick and the depths of the frame members can range between 800 mm and 1500 mm, the resulting frame members have depth to width ratios of between 4:1 and 8:1. In contrast, traditional concrete frame members have depth to width ratios of between 1:1 and 2:1. The code was written with traditional concrete cross sections in mind and some of the rules for tie spacings in the expected hinge regions are given in terms of member dimensions. When the code rules are applied to the members of tilt-up frame panels, the rules which are given in terms of least member dimensions almost always control. Thus the applicability of the code rules to the members of tilt-up frame panels is questioned.

The relationship between hinge zone tie spacing and the displacement ductility of frames with members having depth to width ratios in excess of 2:1 has not been extensively tested. It was therefore decided to test a set of frame panel specimens under cyclic loads to evaluate what amount of transverse reinforcement is necessary in order to provide acceptable seismic resistance. The same size of reinforcing bars were used in all of the tests, but the spacing of the ties within the expected hinge region was varied.

1.2 Procedure of investigation

A literature review was done and revealed that little testing has been done to investigate the relationship between tie spacing and ductility of frame members with large depth to width ratios. A key issue was to decide what hinge zone tie spacings should be tested. In order to determine what tie spacings have been previously tested a literature review was done and the results of the review have been outlined in chapter 3.

Six full scale test specimens which represented one quarter of a full frame panel were tested. All of the specimens were subjected to the same pattern of cyclic loading, applied at the bottom of the leg. Measurements which enabled the plotting of load vs. leg displacement graphs were recorded. Since it is reasonable to assume that all of the plastic deformation of the frame occurs in hinges which form in the leg members, the plastic displacement of the frame was estimated from the load vs. leg displacement plots.

Measurements which enabled the estimation of the elastic stiffness's of the frame members were also taken. Given the elastic stiffness's of the frame members, the frame yield displacement was obtained. Using the frame yield displacement, and the plastic displacements from the load vs. leg deflection plots, the displacement ductility of a full frame panel with the respective hinge zone tie spacing was estimated. Thus it was possible to observe the effect of hinge zone tie spacing on the ductility of tilt-up frame panels.

1.3 Scope and limitations

Since the test specimens were expensive to construct and transport, it was considered reasonable to expect six specimens to be produced. It was decided to test three different hinge zone tie spacings, testing two specimens for each tie spacing. Thus the results of the testing done in this thesis cannot be considered to statistically significant, but do provide an indication of how the ductility of the frame members of tilt-up frame panels is related to hinge zone tie spacing.

The following variables were kept constant in all of the test specimens; concrete strength, reinforcement grade, longitudinal reinforcement configuration, non hinge zone tie spacing, load sequence characteristics.

A limitation of the test setup adopted was that the axial load present in actual tilt-up frame panels was not modeled. The results of this thesis are therefore only applicable to tilt-up frame panels in which the axial forces are sufficiently low such that they do not significantly effect ductility.

Tilt up panels with typical dimensions and large window openings may be vulnerable to possible out of plane or lateral torsional buckling. This might be especially true for tall panels which are not laterally supported at mid-height by an intermediate floor. This is not a common design condition, but buckling should be considered when this situation does occur. It was decided that the lateral buckling of the panels is a separate issue which is too large to be incorporated into the current study. Lateral buckling of the frames is considered to be an unacceptable mode of failure since it would result in the collapse of the wall with little warning. If lateral stability is considered to be a problem, it would be necessary to ensure that all panels are provided with adequate lateral support. In laterally supported panels, the development of plastic hinges would be the critical failure mode and hence the results of the tests proposed for this research will be useful.

1.4 Plan of development

The thesis report begins with an outline of the problem in chapter 2. A literature review which researched previous work on this topic is contained in chapter 3. The details of the tests are described in chapter 4 and

the observations, results and interpretation of results are covered in chapters 5, 6 and 7 respectively. The conclusions drawn from the test series are listed in chapter 8.

There are five figures which are referenced many times throughout the thesis. For convenience these figures have been placed together in Appendix I and have been numbered I-1 to I-5.

2 PROBLEM DEFINITION

2.1 Description of type of panel being researched

Tilt-up concrete buildings have concrete walls, supported on a concrete floor slab, and a light weight roof system. Roof systems typically consist of structural steel beams, open web steel joists and steel decking. The exterior concrete walls, which are typically 190 mm thick with two layers of reinforcement, are cast on the floor slab and then lifted into position. The walls, which also serve as the exterior face of the building, are temporarily braced until the roof is constructed. In the completed building, the concrete walls resist vertical loads as well as lateral loads from wind and/or earthquakes. The roof acts as a flexible diaphragm, transferring the lateral loads to the perimeter concrete shear walls. The vertical and lateral loads are transferred from the walls to the concrete floor slab via steel connections which are formed by welding together steel plates which are embedded into each of the walls and the floor slab. The connection between the panel and the floor slab prevents translation, but offers very little rotational restraint. This connection between the wall and the floor slab is therefore considered a pin connection for analysis purposes.

Tilt up wall panels with large openings at the first and ground floor levels are becoming increasingly popular. The two large openings result in a panel which is more like a frame than a wall, see Figure I-1a in Appendix I.

Given that the panels are typically only 190 mm thick, the shear resisting system consists of reinforced concrete frames which have members with very high depth to width ratios. The legs typically have depth to width ratios between 4:1 and 5:1, and the beams can have depth to width ratios as high as 8:1. The performance under cyclic earthquake loading of reinforced concrete frame members with these depth to width ratios is not well understood.

2.2 Expected mode of failure

To investigate the mode of failure of frame panels, typical loads were applied to a panel of typical dimensions, (Figure I-1 of Appendix I), with typical reinforcement (Figure I-3 of Appendix I).

Given the connections have sufficient strength and that lateral torsional buckling of the whole frame panel is prevented, failure of the tilt-up wall system will occur via shear, or preferably via flexural hinging in the frame members. For the preferred mode of flexural hinging, in order to determine in which members hinging will occur, it is necessary to compare the bending moments in the frame members as the loads are increased to the flexural capacities of the frame members.

In typical tilt-up frame panels the beam members have significantly deeper cross sections than the leg members and the flexural capacities of the beam members are correspondingly higher. As increasingly large lateral loads, and corresponding vertical loads, are applied to the tilt-up frame panels, the bending moments in the legs of the panel reach their flexural capacity before the bending moments in the beam reach the beam flexural capacity. Therefore failure of the panel will occur via hinging of the leg members. A full quantitative description of the development of the hinges is given in section 4.2.

2.3 Design procedure currently being applied

Assuming the roof to panel and panel to floor connections have sufficient strength, failure of the tilt-up system will occur via flexural hinging in the frame members of the panels. Design forces for tilt-up buildings are generally calculated using a force reduction factor, R, of approximately 2. CSA A23.3-94[1] specifies that a force reduction factor of exactly 2 be used. Therefore, according to CSA A23.3-94[1] the frame panels should be designed and detailed such that they provide sufficient ductility to justify the use of a force reduction factor of 2.

Since the panels with large openings described above are, according to clause 23.5.3 of CSA A23.3[1], effectively frames, designers in the Vancouver, Canada, region are currently applying the plastic hinge detailing rules applicable to frame members requiring nominal ductility (Clause 21.9 of CSA A23.3[1]).

2.4 Applicability of code rules currently being applied

The design and detailing guidelines given in the code provisions of the American Concrete institute, and the Canadian Standards Association, were derived with traditional concrete cross sections in mind i.e. members with depth to width ratios of 1:1 or 2:1. Therefore the applicability of the rules provided by these codes for the design and detailing of tilt-up frame members which have depth to width ratios of 4:1 to 8:1 is questioned. In particular the rules for the spacing of ties in the expected hinge regions are of concern. Cross sections of typical tilt-up frame members are shown in Figure I-3 of Appendix I. It is clear that these cross sections are very different from the square cross sections of traditional concrete frame members.

The research for this thesis began with a careful study of CSA A23.3[1] and of the Concrete Design Handbook of the Canadian Portland Cement Association[20]. The study included an evaluation of how the code was interpreted in the design of an actual tilt-up frame building constructed on Vancouver Island. The main findings of this study are stated below. All references to the "code" refer to CSA A23.3[1].

When the current code hinge zone tie spacing rules are applied to tilt-up frame members (code[1] clauses 21.9.2.1 and 21.9.2.2), the spacing rules given as a fraction of the least member dimension often control.

Since the tilt up frame members have cross sections very different to the cross sections the code was written for, the applicability of these rules is questioned. The rules for how far the hinge zone ties should be extended down the member (code[1] clauses 21.9.2.1 and 21.9.2.2) are also given in terms of member dimensions. The hinge zone distance for typical tilt-up frame panels is twice the member depth from the joint in the case of beams. These rules may be overly conservative for the members of tilt-up frame panels which have very deep sections. The d/2 rule for tie spacing in the non hinge zones of beams (code[1] clause 21.9.2.1.3) often results in a very large spacing, 700 mm for the frame being considered in this study, for example. This spacing is larger than the maximum spacing for distributed reinforcement in walls, so again the applicability of the code rules is questioned.

The joint detailing rule which limits the maximum bar size passing through joint regions (code[1] clause 21.9.2.4.4) is very easily satisfied. This is a result of the large joint sizes. However, the ease with which this requirement is satisfied is an indication that the code was not intended for the section dimensions typically found in tilt-up frame panels.

The conclusion of the study done on CSA A23.3[1] and the Concrete Design Handbook of the Canadian Portland Cement Association[20] was that the code rules are not necessarily applicable to tilt-up frame panels. In particular it was concluded that experimental research into what tie spacings should be used in the hinge zones of tit-up frame members would be useful.

3 LITERATURE REVIEW

3.1 Aim of review

The objective of this research project was to determine the relationship between hinge zone tie spacing and the displacement ductility of tilt-up frame panels. Tie spacing effects the ductility of the frame members because it will determine when, if at all, the longitudinal steel will buckle in compression. Since the load carrying capacity of a member is likely to drop when the longitudinal reinforcement buckles, buckling often marks the end of the ductile range. Although a large amount of testing involving buckling of compression reinforcement has been done on members with low depth to width ratios, there is not a satisfactory amount of information on members with depth to width ratios commonly used in tilt-up panels. The main aim of the literature review was to look at previous research for guidelines as to what tie spacings should be tested.

Twenty four articles directly related to the testing being done for this research were found. A brief overview of each of the 24 relevant articles is provided below in date sequence. The relevance to the tests being done for this research is commented on. The contents of the article are given in regular font and the additional comments relevant to this research are shown in italics. The ratio of tie spacing to longitudinal bar diameter, called the S/D ratio, is commonly used to describe tie spacing. In some of the cases in which the authors did not mention S/D ratios in their articles, these ratios have been calculated and included in the comments in italics.

3.2 Summaries of relevant articles

G. Agrawal, L Tulin, K. Gerstle (1965)[4]

"Response of doubly reinforced concrete beams to cyclic loading"

Journal of American Concrete Institute, 62-51, P823-834

Three beams with a 3" wide 4" deep cross section were tested under cyclic loading. The beams were longitudinally reinforced with #4 bars. Each beam had two longitudinal bars, one at the top and one at the bottom. Transverse reinforcement consisted of 1/4" rectangular ties at 2.6" spacing. No buckling failures occurred.

These tests suggest that S/D ratios of 2.6/0.5 = 5.2 are adequate to prevent buckling of the longitudinal reinforcement. However only three beams were tested and the scaling may influence the results. Furthermore since there was relatively little tensile reinforcement, the compressive stresses in the concrete would have been small and therefore the outward pressure on the longitudinal steel from the bulging of the concrete in compression would have been low.

N. Burns, C. Seiss (1966)[5]

"Plastic hinging in reinforced concrete"

Journal of Structural Engineering, ASCE, vol. 92 # ST5, Oct. P45-64

Cyclic (not reverse) testing was done on 39 under-reinforced beams (no axial load) which had aspect ratios of 2:1. The beams were simply supported and the load was applied at midspan. In 18 of the beams the load was applied through a column stub which was cast integrally on the top of the beam at midspan. The column stub was intended to model the beam/column joint. In the other 21 specimens the load was applied through a column stub which was cast integrally on the top and the bottom of the beam. Again the intent of the column stub was to model the beam/column joint.

The 6" x 12" cross sections were longitudinally reinforced with #6 and/or #8 bars. The transverse reinforcement consisted of #3 rectangular ties at 6" spacing.

Buckling of longitudinal bars preceded failure, but this only occurred once the cover had spalled. Once the cover had been lost, "bulging" of the core contributed to the buckling of the longitudinal steel. It was found that #6 and #8 bars buckled within a 6" spacing.

#6 (19 mm) at 6" (152 mm) and #8 (25 mm) bars at 6" (152 mm) spacings give S/D ratios of 8 and 6 respectively.

N. Burns, C. Seiss (1966)[6]

"Repeated and reverse loading in reinforced concrete"

Journal of Structural Engineering, ASCE vol. 92 #ST5, Oct. P65-78

Three beams with 2:1 aspect ratios were tested under reverse cyclic loading. The beams had the same properties as the set of 21 specimens described in the previous reference i.e. this is a second paper from the same set of experimental tests. This second paper was written to describe the effect of reverse cyclic loading as opposed to cyclic loading applied in one direction only which was covered in the first paper. Buckling failures did occur and again buckling took place over one 6" tie spacing.

#6 (19 mm) bars at 6" (152 mm) centers gives an S/D ratio of 152/19=8

W. Ruiz, G. Winter (1969)[16]

"Reinforced concrete beams under repeated loads"

Journal of Structural Engineering, ASCE vol. 95 #ST6, June, P1189

18 simply supported beams with a 8" wide and 11" deep cross section were tested under cyclic loading. The reinforcing properties as well as the loading patterns were varied. Six of the 18 specimens had compression steel and ties at the critical section, while the other 12 had only tension steel. The tensile steel consisted of either 2 or 3 bars which were either #6 or #7 bars. Where compression steel was used, it consisted of a single bar placed at the midpoint of the top side of the rectangular stirrups. Buckling of the single compression bars was observed.

Since stirrups are not very effective in restraining bars at a mid point of one of their sides, it is not surprising that these bars buckled. Given the very different reinforcement configurations in this test, compared to those of the tilt-up panel frame legs, the findings of this paper are not particularly useful for the tilt-up frame panel research.

R. Brown, J Jirsa (1971)[7]
"Reinforced concrete beams under load reversals"
Journal of American Concrete Institute, 68-39, P380-390
Twelve beams with a 6" x 12" cross section were tested under cyclic loading. The beams were longitudinally reinforced with four #6 or #8 bars, one in each corner. Transverse reinforcement consisted of #3 closed stirrups at 2" spacing. No buckling failures occurred. It was found that increasing the number of stirrups to improve confinement increased the number of cycles to failure.

These tests indicate that S/D ratios of 2/0.75 = 2.7 are adequate to prevent buckling of the longitudinal reinforcement. Since no buckling failures were observed an indication of how close this S/D ratio is to the limit was not obtained, but it is likely that an S/D ratio of 2.7 is substantially lower than would be required to prevent buckling of the longitudinal reinforcement. Ties spaced with an S/D ratio of 2.7 would however offer a large amount of confinement.

J. Wight, M. Sozen (1975)[17]
"Strength decay of reinforced concrete columns under shear reversals"
Journal of Structural Engineering, ASCE, vol. 101 #ST5, May, P1053
The 12 specimens tested had aspect ratios of 2:1. Reinforcement consisted of four #6 longitudinal bars, one in each corner of the #2 or #3 rectangular stirrups. The main focus of this research was to investigate the shear behavior under cyclic loading and not much emphasis was placed on the buckling of the longitudinal steel. The authors recommended that the tie spacing should be less than 1/4 of the depth of the beam, but it seems that this is recommended as a shear consideration as opposed to a reinforcement stability consideration.

N. Gosain, R. Brown, J. Jirsa (1977)[8]

"Shear requirements for load reversal in reinforced concrete members"

Journal of Structural Engineering, ASCE, vol. 103 #ST4, July, P1461

This paper summarizes and comments on experimental tests done by other researchers. The paper suggests that a S/D ratio of 6 should be used where buckling of longitudinal reinforcement over a single tie spacing needs to be prevented. The paper mentions other studies (Berto and Popov EERC Report 75-15) which suggested that s/d ratios of between 6 and 8 would be acceptable. The paper also describes the mechanics of buckling of longitudinal reinforcement bars in compression.

C. Scribner, J. Wight (1980)[9]

"Strength decay of reinforced concrete beams under load reversal"

Journal of Structural Engineering, ASCE, vol. 106 #ST4, April, P861

14 T-shaped specimens were tested under cyclic loading. The T-shaped specimens represented the beam and columns of a concrete frame. Eight of the specimens were at 1/2 scale and the other six were full scale. A reverse cyclic load was applied to the beam of the specimen and the effect of tie spacing on the behavior of the hinge which formed in the beam was observed.

A number of buckling failures of the #6 and #8 longitudinal bars were observed. These tests indicated that large ties are needed to prevent the buckling of longitudinal reinforcement. It is mentioned that ties as large as the longitudinal reinforcement would be adequate. Buckling often occurred over 3 or 4 tie spacings which suggested that the ties act as elastic supports rather than rigid supports between which buckling takes place. Tie stiffness is therefore very important.

The authors drew the following conclusions from the tests:

- The longitudinal steel only buckled once the cover reinforcement had been spalled.
- Larger ties are more effective than smaller ties in delaying the buckling of longitudinal reinforcement.
- Beam twist or shear deformations, which result in relative displacement of the compression bar over the spalled region, lead to buckling at reduced loads.

The comment that ties as large as the longitudinal reinforcement should be used is probably conservative since the code says that ties need be only half as large as the longitudinal bars. The test set-up used by Scribner and Wight was similar to the test setup used for the testing reported in this thesis.

B. Scott, R. Park, M. Priestley (1982)[18]

"Stress strain behavior of concrete confined by overlapping hoops at low and high strain rates"

Journal of American Concrete Institute, 79-2, P13-27

Twenty five 450 mm square, 1200 mm high, columns were tested. The specimens had between 8 and 12 longitudinal bars and the transverse reinforcement consisted of a varied arrangement of square and/or octagonal steel hoops. The loading applied was monotonic compression and it was either concentrically or eccentrically applied. The loading rate was varied to investigate the effect of strain rate on strength. The tests performed indicated that a S/D ratio of 2.7 to 4.9 was adequate to delay buckling until another mode of failure took place.

The loading used in the above tests was pure axial compression and therefore the S/D ratios derived would not be applicable to the tilt-up frame members in which flexure dominates.

C. Scribner (1986)[10]

"Reinforcement buckling in reinforced concrete flexural members"

Journal of American Concrete Institute, 83-85, P966-973

This paper contained details on buckling mechanics of compression reinforcement. Tests were done and it was found that even large closely spaced ties did not always prevent buckling of the longitudinal bars at large flexural displacements. Buckling over one and more tie spacings was observed. It was found that if buckling over more than one tie spacing is to be prevented, the tie diameter should be at least half of the longitudinal bar diameter.

It was queried whether the large flexural displacements at which longitudinal bar buckling takes place are realistic. This query is valid because the drift requirements required for serviceability are 1.5% of interstorey height. The author felt that since other parts of the code are based on large displacement tests the tie spacing requirements for longitudinal bar buckling should also be based on large displacement tests.

The author felt that for the purposes of an analytical model for buckling over multiple tie spacings, it would be good to assume that buckling takes place over 3 tie spacings. The plastic hinge region is generally d/2 long, where d is the depth of the hinging member. Ties are likely to be spaced at approximately d/4. The first tie is typically a half tie spacing from the support i.e. d/8. The fourth tie will

therefore typically be at d/8 + (3 x d/4) = 7/8d i.e. near the end of the hinge region. The first and fourth ties are likely to be well held, the first one is near the support and the fourth one is in or near an area where the concrete has not spalled. Buckling is therefore likely to take place between the first and the fourth ties, over a distance of 3/4d i.e. 3 times the tie spacing of d/4.

M. Papia, G. Russo, G. Zingone (1988)[11]
"Instability of longitudinal bars in RC columns"
Journal of Structural Engineering, ASCE, vol. 112 #2, P445
A mathematical model was developed to predict the behavior of reinforcing bars in compression. Uniaxial compression tests on reinforced concrete specimens were done to check the accuracy of the model. The model represented the ties as elastic springs such that buckling over more than one tie spacing could be evaluated.

In the tests it was found that when buckling occurs over many tie spacings, the ties are damaged and this results in a loss of confinement which leads to a premature failure of the concrete. Tie stiffness is therefore important. Failure under uniaxial compression will always involve the buckling of the longitudinal steel, no matter what the tie spacing, and no recommendations for tie spacings were given.

M. Saatcioglu, G Ozcebe (1989)[12]
"Response of RC columns to simulated seismic loading"
Structural Journal of American Concrete Institute, 86-s1, P3-12
Fourteen full scale columns were tested under slowly applied lateral load reversals. The columns were tested under a range of axial loads. One of the main aims of the tests was to investigate the effect of axial load on the seismic behavior of RC columns. It was found that as the axial load was increased the yield load of the column increased but the ductility decreased. The opposite was found to be true for axial tension i.e. the yield was reached sooner but the columns were more ductile. It was found that an axial load equal to 20% of the design axial load capacity had a significant effect on the behavior and ductility of the column.

The longitudinal steel consisted of 25 mm bars and the ties were at 150 mm c/c. No buckling of longitudinal reinforcement was observed. Further tests were done with ties at 75 mm and 50 mm c/c. The closer spacings were used to improve confinement. The 75 mm spacing gave similar results to the 150 mm spacing, but the 50 mm spacing gave significantly more ductility.

The axial loads in the legs of tilt-up frame panels will typically be less than 10% of the nominal axial compressive capacity, (see section 4.1.4). This is less than the 20% value which was found to have a significant effect on ductility. These tests indicate that an S/D ratio of 150/25 = 6 is adequate to prevent buckling of the longitudinal reinforcement.

S. Mau, (1990)[13]

"Effect of tie spacing on inelastic buckling of reinforcing bars"

Structural Journal of American Concrete Institute, 87-S69, P671-677

A finite element study to predict the buckling behavior of reinforcing bars was done. The study used the stress strain behavior for typical high yield steel. The critical S/D ratio was found to be in the range of 5-7 depending on the stain hardening behavior of the steel. If the S/D ratio is less than the critical value, and the ties have adequate stiffness to prevent buckling over many tie spacings, then the longitudinal bars will not buckle but will follow the stress strain curve for the steel. If the S/D ratio is greater than the critical S/D ratio, then as the longitudinal bars reach yield they will become unstable and buckle. It was found that strain hardening may delay buckling of the longitudinal steel if the S/D ratio is close to the critical S/D ratio.

The tilt-up panel tests will have a minimum S/D ratio of 5. This paper indicates that this spacing should be adequate to prevent buckling.

G. Monti, C Nuti (1992)[14]

"Non-linear cyclic behavior of reinforcement bars including buckling"

Journal of Structural Engineering, ASCE, vol. 112 #12, P3268

Tests were done on steel reinforcing bars i.e. not on reinforced concrete members. These test results were used to check a mathematical model which was developed to predict the behavior, including buckling, of longitudinal reinforcing bars in compression in reinforced concrete members. The bars were tested by loading lengths of reinforcing bar in compression. The tests done indicated that a S/D ratio less than 5 is required to avoid buckling problems.

Since the test specimens were clamped at their ends, the test would only represent buckling over a single tie spacing. Furthermore these bar test results can only be used to predict the behavior of reinforcing bars restrained by ties, if it is assumed that the fixity applied to the longitudinal bars by the ties is the same as the fixity applied to the test specimen bars by the testing machine. The tilt-up panel tests will have a

minimum S/D ratio of 5. Therefore the tests reported in the above mentioned paper suggest that this ratio should be adequate to prevent buckling.

A. Azizinamini, S. Baum Kuska, P. Brungardt, E. Hatfield (1994)[15]
"Seismic behavior of square high strength concrete columns"
Structural Journal of American Concrete Institute, 91-S33, P336-345
Nine 2/3 scale columns were tested. The test columns had #6 bars running longitudinally. The maximum spacing of the #3 transverse reinforcement bars was 2 5/8". Buckling of the longitudinal reinforcement preceded failure. When the spacing was decreased from 2 5/8" to 1 5/8" the maximum deflection increased by 40%. It was found that so long as the axial load is less than 20% of the axial load capacity reasonable ductilities are achieved. It was found that the hinge region extended to a distance equal to the depth of the beam from the support.

The 2 5/8" spacing gives a S/D ratio of 66/19 = 3.5 and the 1 5/8" spacing gives a S/D ratio of 41/19 = 2.2. The S/D ratios required to prevent buckling in these tests are lower than those found in the other literature. This is as a result of the high axial loads used in the tests. It is likely that S/D ratios as low as 3.5 would not be required in tilt-up frame panels where axial loads are less than 10% of their nominal axial load capacity.

S. Pantazopoula (1998)[19]
"Detailing for reinforcement stability in RC members"
Journal of Structural Engineering, ASCE, vol. 124 #6, P623-P641
The author analyzed a database of over 300 columns tested under cyclic, axial and/or flexural, loading. Based on the tests a mathematical model to predict critical tie spacing was formulated. This paper also contains a description of compression reinforcement buckling mechanics.

It was reported that buckling may only take place at strains 5 times the yield strain, but this depends on the tie arrangement effectiveness and on the composite action of the rebar and the concrete. The author found that experimental reports for axial strain at buckling vary widely and this, according to the author, is as a result of different test set-ups as well as the subjective judgment of when buckling takes place i.e. usually done by eye. Involved mathematical equations which use concrete strains to predict critical tie spacing are provided.

3.3 Conclusions of literature review

All of the testing reported in the literature was performed on members with depth to width ratios of less than 2:1. A number of different load configurations were used in the tests reported in the literature. Members were subjected to monotonic, cyclic or reverse cyclic loading and the loads were axial and/or flexural. Although the load configurations and test specimens were widely varied it is felt that they will give some indication of what type of behavior can be expected in the testing of this research.

The following conclusions were drawn from the literature review:

- Buckling of the longitudinal reinforcement only occurs once the cover concrete has spalled. In some cases the buckling and spalling occur simultaneously.
- The longitudinal bars will only buckle once they have yielded in compression.
- Strain hardening of the longitudinal steel may delay buckling.
- Bulging of the core concrete in compression results in an outward force being exerted on the longitudinal steel. This contributes to buckling.
- Buckling can take place over one or more than one tie spacing.
- It was found that buckling over a single tie spacing began to occur when the ratio of tie spacing to longitudinal bar diameter (S/D ratio) reaches 6 to 8.
- S/D ratios of 4 to 5 were found to be adequate to prevent buckling of the longitudinal reinforcement even at high flexural displacements.
- Buckling failures occur over more than one tie spacing when the ties are not large enough to restrain the longitudinal steel. In order to prevent this it was found that the tie thickness should not be less than half of the longitudinal bar thickness.
- Axial load does have an effect on ductility and axial loads equal to 20% of the axial compressive capacity of the member were found to have a significant effect on ductility. A discussion on the effect of axial load on the ductility of tilt-up frame panel members is contained in section 4.2.2.

4 MODE OF FAILURE, TEST SPECIMEN, SET-UP AND PROCEDURE, AND MATERIAL PROPERTIES

An investigation into the mode of failure of tilt-up frame panels is outlined in section 4.1. The selection of the test specimen properties, the test set-up and the testing procedure are explained in sections 4.2, 4.3 and 4.4 respectively. The properties of the test specimen materials are provided in section 4.5.

4.1 Determination of mode of failure

Failure of the tilt-up wall system will often occur via flexural hinging in the frame members. In order to study the exact mode of failure, a typical frame panel was considered. The dimensions of the frame panel studied are shown in Figure I-1a in Appendix I and the reinforcement considered for the test specimen is shown in Figure I-3 of Appendix I.

It was expected that failure of the tilt-up frame panels would occur via the formation of flexural hinges in the legs below the lower beam. In order to confirm this, the following was done: flexural capacities of the leg and beam members were calculated by doing layer analyses using the typical frame section properties shown in Figures I-1 and I-3 of Appendix I. The flexural capacities from the layer analyses were then compared to the frame bending moments obtained from a linear elastic analysis using loads large enough to cause yielding of the frame members.

In order to calculate the flexural capacities of the frame members the yield strength of the reinforcing steel used to construct the specimens was required. Since no tests were done on the reinforcing steel until after the testing of the panels, the yield strength was estimated to be 450 MPa for the purposes of these calculations. (The tests done later on the reinforcement indicated it to have a yield strength of 453 MPa.) Layer analyses were done to determine the yield moments of the frame members assuming the strain in the bottom reinforcement to be 450/200 000 = 0.00225. The top strain was then varied until an axial load equal to zero was obtained and the corresponding moment was assumed to be the yield moment.

A spreadsheet was developed to perform these yield moment calculations. The spreadsheet assumed the steel to have bi-linear stress strain behavior and used the tension stiffening model proposed by Collins and Mitchell[21] using the tensile cracking stress of the concrete. The concrete compression force model proposed by Collins and Mitchell[21] was used to calculate the compressive force in the concrete. All of the material performance factors were assumed to be equal to 1.

The spreadsheet calculations for the yield moments of the leg and the beam are contained in Tables 1-3. Table 1 contains the yield moment calculation for the leg of the typical frame panel considered. The leg reinforcement considered is shown in Figure I-3 of Appendix I. Table 2 contains the yield moment calculation for the beam of the typical frame panel considered. The beam reinforcement is shown in Figure I-3 of Appendix I. Table 3 contains the yield moment calculation for the beam of a frame panel reinforced as shown in Figure I-3 of except using 10M bars for the distributed instead of the 15M bars shown in Figure I-3.

Knowing the yield moments of the frame members, vertical and transverse loads (with typical relative proportions) were applied to the frame and increased until yield moments were reached in either the legs or the beams. This procedure indicated that flexural hinges will form in the legs below the lower beam joint before yielding begins in the beams. The first yield bending moment diagram is shown in Figure I-1b in Appendix I. Note that the moments in the top of the legs are, on average, equal to the calculated yield moment of 271 kNm, see Table 1. The full frame analysis for first yielding, including all relevant input and output, is contained in Appendix II. In SAAP 2000, the computer program used for the frame analysis, U refers to displacement and R refers to rotation. The displacements are given in meters (m) and the rotations in radians. P is axial load, V is shear, T is torsion and M3 is the moment about the Y axis. The forces and moments have units of Newtons (N) and Newton.meters (Nm) respectively. In the joints definition section, the joint restraints are described by six numbers which are each either zero or one. A zero indicates that the restraint was not applied while a one indicates that it was applied. The first three numbers refer to translation in the X, Y and Z directions respectively, and the last three refer to rotation about the X, Y and Z axes respectively. In the material properties section, special materials called "legmat" and "beammat" were defined with moduli of elasticity's such that the stiffnesses of the legs and beams were in proportion.

For the frame structure of Figure I-1a, by comparing the shear forces from the frame analysis to the shear capacities of the members, it is clear that flexural hinges will form prior to shear failure of the frame members, therefore shear failure will not be critical and flexural hinging will be the controlling mechanism. The shear resistances offered by the concrete, Vc, are very close to the shear loads in the legs and beams of the panels. Therefore only a minimum amount of transverse reinforcement would be required for shear strength. However, substantially more than minimum transverse reinforcement is used since it is required to prevent the buckling of the longitudinal reinforcement. Contribution to shear strength is a secondary purpose of the transverse reinforcement.

Since joint failure was not considered to be an issue, the joint regions were modeled using infinitely stiff short frame members in the computer analysis.

TABLE 1 - YIELD MOMENT CALCULATION FOR LEG

(REINFORCED AS SHOWN IN FIGURE I-3 OF APPENDIX I)

fc' (MPa)= 30 Ect(MPa) = 30124.7 ult strain = -0.00199

fr (MPa) =	1.81
str@cracking	6.0084E-05
alpha1=	0.7
alpha2=	1

Depth to bot strain (mm)= 740
Width of C flange (mm) = 190
d to bot of flange (mm) = 800
Width of web (mm) = 190
Depth to CA (mm) = 400

Top strain -8.51780E-04
Bot.strain 2.26500E-03
Beta1 0.694375614
Alpha1 0.528094952
c (mm) 202.2334589
phi 4.212E-06

Axial force (N)

conc C	-422878
conc T	89697
steel	331386
	-1.794E+3

Moments (Nmm)

conc C	139323521
conc T	5.67E+6
steel	125946115
	270934962

Moment (kNm) = 271

CONCRETE FORCES

Comp (N) -422.702E+3 (rectangular stress block)

10 LAYERS OF CONCRETE IN COMPRESSION: Shrinkage strain: 0.00E+00

Layer	Depth	strain cf	f (MPa)	d to bot of layer	Area	N (N)	lever (mm)	M (Nmm)
1	10.1	-809.19E-6	-19.4	20.2	3842	-74639	-390	29100726
2	30.3	-724.0E-6	-17.8	40.4	3842	-68574	-370	25349389
3	50.6	-638.8E-6	-16.2	60.7	3842	-62088	-349	21696005
4	70.8	-553.7E-6	-14.4	80.9	3842	-55180	-329	18166154
5	91.0	-468.5E-6	-12.5	101.1	3842	-47850	-309	14785418
6	111.2	-383.3E-6	-10.4	121.3	3842	-40099	-289	11579380
7	131.5	-298.1E-6	-8.3	141.6	3842	-31926	-269	8573621
8	151.7	-212.9E-6	-6.1	161.8	3842	-23331	-248	5793723
9	171.9	-127.8E-6	-3.7	182.0	3842	-14315	-228	3265268
10	192.1	-42.6E-6	-1.3	202.2	3842	-4877	-208	1013837
					38.42E+3	-422.88E+3		139323521

TENSILE FORCES - See C&M P135 for equation &143 for area

zone	d to cent.	strain cf	f (MPa)	Area	N (N)	lever (mm)	M (Nmm)
1	740	0.002265	0.614	32300	19826	340	6740753
2	520	0.0013384	0.697	43700	30455	120	3654560
3	280	0.0003275	0.902	43700	39417	-120	-4729987
4	60	-0.0005991	0.000	32300	0	-340	0
5		-0.0008518	0.000	0	0	-400	0
6		-0.0008518	0.000	0	0	-400	0
7		-0.0008518	0.000	0	0	-400	0
					89.70E+3		5.67E+6

STEEL FORCES

Layer	AREA	fy	Depth	strain from phi	strain sf	MPa	N (N)	lever (mm)	M (Nmm)
1	600	450	740	0.002265	0.002265	450.0	270000	340	91800000
2	400	450	520	0.001338	0.001338	267.7	107071	120	12848541.41
3	400	450	280	0.000328	0.000328	65.5	26203	-120	-3144404.76
4	600	450	60	-0.000599	-0.000599	-119.8	-71888	-340	24441978.81
				-0.000852	-0.000852	0.0	0	-400	0
				-0.000852	-0.000852	0.0	0	-400	0
				-0.000852	-0.000852	0.0	0	-400	0
				-0.000852	-0.000852	0.0	0	-400	0
				-0.000852	-0.000852	0.0	0	-400	0
				-0.000852	-0.000852	0.0	0	-400	0
				-0.000852	-0.000852	0.0	0	-400	0
				-0.000852	-0.000852	0.0	0	-400	0
							3.31E+05		1.26E+08

TABLE 2 - YIELD MOMENT CALCULATION FOR BEAM

(REINFORCED AS SHOWN IN FIGURE I-3 OF APPENDIX I)

fc' (MPa)= 30 Ect(MPa) = 30124.7 ult strain = -0.00199

fr (MPa) =	1.81
str@cracking	6.0084E-05
alpha1=	0.7
alpha2=	1

Depth to bot strain (mm)= 1340
Width of C flange (mm) = 190
d to bot of flange (mm) = 1400
Width of web (mm) = 190
Depth to CA (mm) = 700

Top strain -6.84420E-04
Bot.strain 2.26500E-03
Beta1 0.688226997
Alpha1 0.442109542
c (mm) 310.9502207
phi 2.201E-06

Axial force (N)

conc C	-539471
conc T	128450
steel	409234
	-1.786E+3

Moments (Nmm)

conc C	319635005
conc T	11.29E+6
steel	251283135
	582208049

Moments (kNm) = 583

CONCRETE FORCES

Comp (N) -539.296E+3 (rectangular stress block)

10 LAYERS OF CONCRETE IN COMPRESSION: Shrinkage strain: 0.00E+00

Layer	Depth	strain cf	f (MPa)	d to bot of layer	Area	N (N)	lever (mm)	M (Nmm)
1	15.5	-650.20E-6	-16.4	31.1	5908	-96833	-684	66277445
2	46.6	-581.8E-6	-15.0	62.2	5908	-88419	-653	57769122
3	77.7	-513.3E-6	-13.5	93.3	5908	-79586	-622	49523590
4	108.8	-444.9E-6	-11.9	124.4	5908	-70335	-591	41579899
5	139.9	-376.4E-6	-10.3	155.5	5908	-60666	-560	33977095
6	171.0	-308.0E-6	-8.6	186.6	5908	-50577	-529	26754228
7	202.1	-239.5E-6	-6.8	217.7	5908	-40070	-498	19950344
8	233.2	-171.1E-6	-4.9	248.8	5908	-29145	-467	13604491
9	264.3	-102.7E-6	-3.0	279.9	5908	-17801	-436	7755718
10	295.4	-34.2E-6	-1.0	311.0	5908	-6038	-405	2443073
					59.08E+3	-539.47E+3		319635005

TENSILE FORCES - See C&M P135 for equation &143 for area

zone	d to cent.	strain cf	f (MPa)	Area	N (N)	lever (mm)	M (Nmm)
1	60	-0.0005524	0.000	39900	0	-640	0
2	380	0.000152	0.993	42750	42460	-320	-13587075
3	700	0.0008563	0.766	42750	32741	0	0
4	1020	0.0015607	0.673	42750	28759	320	9202984
5	1340	0.002265	0.614	39900	24491	640	15674000
6		-0.0006844	0.000	0	0	-700	0
7		-0.0006844	0.000	0	0	-700	0
					128.45E+3		11.29E+6

STEEL FORCES

Layer	AREA	fy	Depth	strain from phi	strain sf	MPa	N (N)	lever (mm)	M (Nmm)
1	600	450	60	-0.000552	-0.000552	-110.5	-66282.77	-640	42420972.9
2	400	450	380	0.000152	0.000152	30.4	12159	-320	-3890756.78
3	400	450	700	0.000856	0.000856	171.3	68506	0	0
4	400	450	1020	0.001561	0.001561	312.1	124853	320	39952918.93
5	600	450	1340	0.002265	0.002265	450.0	270000	640	172800000
				-0.000684	-0.000684	0.0	0	-700	0
				-0.000684	-0.000684	0.0	0	-700	0
				-0.000684	-0.000684	0.0	0	-700	0
				-0.000684	-0.000684	0.0	0	-700	0
				-0.000684	-0.000684	0.0	0	-700	0
				-0.000684	-0.000684	0.0	0	-700	0
				-0.000684	-0.000684	0.0	0	-700	0
							4.09E+05		2.51E+08

TABLE 3 - YIELD MOMENT CALCULATION FOR BEAM

(REINFORCED AS SHOWN IN FIGURE I-3 OF APPENDIX I, EXCEPT ASSUMING 10M DISTRIBUTED BARS INSTEAD OF 15M)

fc' (MPa)= 30 Ect(MPa) = 30124.7 ult strain = -0.00199

fr (MPa) =	1.81
str@cracking	6.0084E-05
alpha1=	0.7
alpha2=	1

Depth to bot strain (mm)= 1340
Width of C flange (mm) = 190
d to bot of flange (mm) = 1400
Width of web (mm) = 190
Depth to CA (mm) = 700

Top strain -5.86554E-04
Bot.strain 2.26500E-03
Beta1 0.684808481
Alpha1 0.387826776
c (mm) 275.6329917
phi 2.128E-06

Axial force (N)

conc C	-417380
conc T	92278
steel	323303
	-1.799E+3

Moments (Nmm)

conc C	252588076
conc T	13.12E+6
steel	225474190
	491183300

Moments (kNm) = 492

CONCRETE FORCES

Comp (N) -417.266E+3 (rectangular stress block)

10 LAYERS OF CONCRETE IN COMPRESSION: Shrinkage strain: 0.00E+00

Layer	Depth	strain cf	f (MPa)	d to bot of layer	Area	N (N)	lever (mm)	M (Nmm)
1	13.8	-557.23E-6	-14.4	27.6	5237	-75613	-686	51886952
2	41.3	-498.6E-6	-13.1	55.1	5237	-68812	-659	45323267
3	68.9	-439.9E-6	-11.8	82.7	5237	-61738	-631	38962517
4	96.5	-381.3E-6	-10.4	110.3	5237	-54392	-604	32827235
5	124.0	-322.6E-6	-8.9	137.8	5237	-46774	-576	26939957
6	151.6	-263.9E-6	-7.4	165.4	5237	-38882	-548	21323217
7	179.2	-205.3E-6	-5.9	192.9	5237	-30719	-521	15999549
8	206.7	-146.6E-6	-4.3	220.5	5237	-22283	-493	10991488
9	234.3	-88.0E-6	-2.6	248.1	5237	-13574	-466	6321569
10	261.9	-29.3E-6	-0.9	275.6	5237	-4593	-438	2012326
					52.37E+3	-417.38E+3		252588076

TENSILE FORCES - See C&M P135 for equation &143 for area

zone	d to cent.	strain cf	f (MPa)	Area	N (N)	lever (mm)	M (Nmm)
1	60	-0.0004589	0.000	39900	0	-640	0
2	380	0.0002221	0.950	28500	27084	-320	-8666897
3	700	0.0009031	0.758	28500	21597	0	0
4	1020	0.001584	0.670	28500	19106	320	6113931
5	1340	0.002265	0.614	39900	24491	640	15674000
6		-0.0005866	0.000	0	0	-700	0
7		-0.0005866	0.000	0	0	-700	0
					92.28E+3		13.12E+6

STEEL FORCES

Layer	AREA	fy	Depth	strain from phi	strain sf	MPa	N (N)	lever (mm)	M (Nmm)
1	600	450	60	-0.000459	-0.000459	-91.8	-55064.697	-640	35241406.28
2	200	450	380	0.000222	0.000222	44.4	8884	-320	-2842824.21
3	200	450	700	0.000903	0.000903	180.6	36123	0	0
4	200	450	1020	0.001584	0.001584	316.8	63361	320	20275608.07
5	600	450	1340	0.002265	0.002265	450.0	270000	640	172800000
				-0.000587	-0.000587	0.0	0	-700	0
				-0.000587	-0.000587	0.0	0	-700	0
				-0.000587	-0.000587	0.0	0	-700	0
				-0.000587	-0.000587	0.0	0	-700	0
				-0.000587	-0.000587	0.0	0	-700	0
				-0.000587	-0.000587	0.0	0	-700	0
				-0.000587	-0.000587	0.0	0	-700	0
							3.23E+05		2.25E+08

The assumption of flexural hinging taking place in the legs may not always be true. In this case the maximum beam moment of 429 kNm obtained from the linear elastic analysis is less than the yield moment for the beam which was calculated to be 583 kNm, see Table 2. However, if 10M bars were used for distributed reinforcement in the beam instead of 15M bars, the beam yield moment would reduce to 492 kNm, see Table 3. This would still result in hinges in the legs before yielding begins in the beam. However this may not always be the case and the flexural strengths of the members should always be compared to the expected moments to determine where failure will occur. All regions in which hinging is expected should be detailed accordingly.

The cover concrete will spall as flexural hinging begins and a drop in flexural capacity is expected when the longitudinal steel buckles in compression. After the cover concrete has spalled, the remaining core concrete in compression will "bulge out" between the ties, pushing on the longitudinal compression reinforcing bars and inclining them to buckle. The tendency of the longitudinal reinforcing bars to buckle in compression will be affected by the spacing of the ties in the hinge region and on whether or not the bars have already been yielded in tension. Prior yielding in tension results in a decrease in stiffness, known as the Baushinger effect, and this will increase the likelihood of buckling. Further details on the mechanics of failure involving buckling of longitudinal reinforcement in compression can be found in References 8 and 10.

4.2 Test specimen details

4.2.1 Classification of transverse reinforcement

There is a question as to whether it is strictly correct to describe the ties and stirrups in the frame members as confinement reinforcement. Concrete under large compressive stresses will strain significantly in the transverse direction unless it is confined. Lateral ties or "confinement reinforcement" is used to hold the concrete together to prevent expansion. This increases the effective compressive strength of the concrete. Since the ties in the legs of the panels are not resisting a compression failure of the concrete, they should not be classified primarily as "confinement" reinforcement. The primary purpose of the stirrups and ties is to prevent the buckling of the longitudinal bars under cyclic loads and it would therefore be more correct to describe the transverse reinforcement as "anti-buckling" reinforcement. The stirrups will also provide confinement to the concrete core, so the ties and stirrups are acting partially as confinement steel. A third purpose of the transverse reinforcement is to provide shear resistance.

4.2.2 Test panel configuration

Test specimen properties were selected such that the test specimen would exhibit the same failure mechanisms that would take place in real tilt-up frame panels i.e. plastic hinging in the leg of the panel. The test panel dimensions are shown in Figure 1.

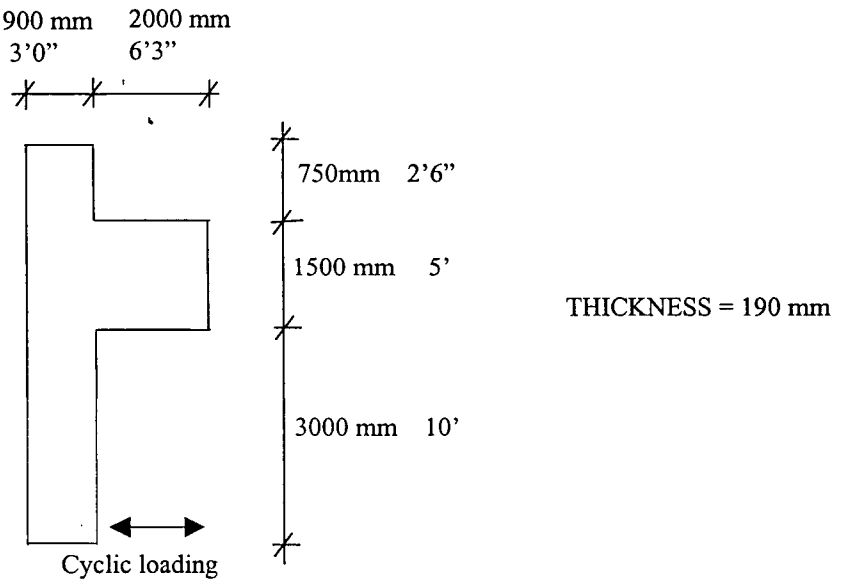

FIGURE 1 - TEST PANEL DIMENSIONS

Since the failure mode in the real frame panels would be the formation of flexural hinges in the legs of the panel, it is important that this also be the failure mechanism in the test panel. The proposed test specimen is proportioned to have a flexural hinge failure. The interaction of the column in which the hinge forms with the adjacent joint region is equally important. The proposed test specimen includes the joint region and therefore the column joint interaction will be well modeled.

Although the eventual failure mechanism would involve the formation of a plastic hinge in the lower leg of the frame, it would be beneficial to observe the level of damage in the joint and adjoining column and beam when failure occurred in the leg. Therefore a test specimen which included a portion of the frame beam was used.

The final test panel shape is shown in Figure I-2 in Appendix I. In order to ensure that the shear to moment ratios in the leg and in the beam would be exactly the same as in the real panel it was necessary to apply the reactions at the inflection points of the bending moment diagram under lateral loads, see Figure I-1b of Appendix I. Trucking restrictions limited the length of the beam of the test specimen. Therefore a

steel extension beam was used to ensure the beam reaction was applied at the inflection point of the bending moment diagram. The stiffness of the steel extension beam is significantly less than that of the concrete beam. However, since the test setup is statically determinate the member forces are not affected. Another advantage of the statically determinate test set-up was that a single force measurement would enable the computation of shear forces and bending moments at all points in the test specimen.

The axial load present in tilt-up frame panels was not modeled in the test since it would have significantly complicated the test to model the axial loads accurately. Axial compression delays yielding but decreases ductility. Conversely, axial tension results in earlier yielding but more ductility. The maximum axial compression in the frame legs at failure is of the order of 350 kN. The maximum axial tension in the frame legs at failure is of the order of 50 kN. (See frame analysis contained in Appendix II.) The nominal axial compressive capacity of a 190 mm x 800 mm concrete section with four 20M bars and four 15M bars longitudinally is 3380 kN. Therefore tension in the frame legs is likely to be less than 5% of the nominal axial compressive capacity, and the compression in the frame legs is likely to be about 10% of the nominal axial compressive capacity. Saatcioglu & Ozcebe[12] found that an axial load of 20% of the member axial compressive capacity had a significant effect on the behavior and ductility of the 14 full scale columns they subjected to slowly applied lateral load reversals. However Azizinamini et al[15] found that as long as the axial load is less than 20% of the axial capacity of the member, reasonable ductilities were achieved in the nine 2/3 scale columns they tested under reverse cyclic loading. The panels were tested without axial load in the legs as the axial loads were sufficiently low so as not to significantly effect the ductility results.

The model was not scaled. Scaling problems include a lack of reinforcing steel in smaller sizes and the difficulties involved in scaling of concrete (the coarse aggregate can be scaled down but then the size ratio of the large to small aggregate is changed.) Furthermore given that the size of defects in concrete is generally independent of the size of the coarse aggregate, in the scaled down specimen a given defect would have a larger effect than it would have had in a full size test specimen.

The reasons for testing a full size test were, therefore:

- good representation of behavior and failure of real structure.
- opportunity to observe behavior of "non-failure regions" as failure is approached.

Six test specimens, with the same concrete outline, but different reinforcement configurations were tested.

4.2.3 Cross sectional dimensions and details of the test specimens

The longitudinal steel in the legs of frame panels is proportioned to resist bending moments caused by eccentrically applied gravity loads, and in plane bending moments caused by lateral loads from wind or

seismic loads. Longitudinal reinforcement details which are typical for tilt-up frame panel legs were used for the test panels (see Figure I-3 in Appendix I).

A specimen with a 190 mm wide and 800 mm deep leg, longitudinally reinforced as shown in Figure 2, was tested.

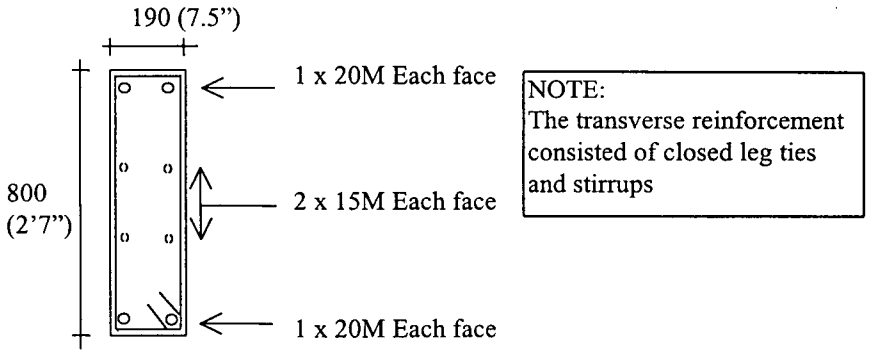

FIGURE 2 - LEG REINFORCEMENT

The reinforcement configuration for the whole test specimen is shown in Figure I-3 in Appendix I. The strictest code rules (Clause 21.9.2.2.1 of reference 1 and clause 21.10.5.1 of reference 2) result in a tie spacing of half the least member dimension. In a typical panel, 190 mm thick, the resulting spacing is 95 mm. Previous research[5,6,7,8,1213,14] has found that tie spacing to longitudinal bar diameter ratios (S/D ratios) of between 5 and 8 are adequate to prevent buckling of longitudinal steel. Given that 20M bars are the largest bars commonly used in the legs of tilt-up frame panels, a tie spacing of 100 mm would be adequate, according to the most conservative previous research, to prevent premature buckling of the longitudinal reinforcement. Designers have used hinge region tie spacings of between 95 mm and 300 mm. Since six test specimens were available it was decided to test three different tie spacings, with two specimens per spacing.

The tie spacings tested were 100 mm (S/D = 5), 200 mm (S/D = 10) and 300 mm (S/D = 15). In the test specimens these tie spacings started 1m below the beam joint and were extended up through the joint and into the leg above the beam. Below the hinge region, and in the beam, a tie spacing of 400 mm was used. All transverse reinforcement consisted of closed leg ties or stirrups.

Shear stresses in the frame members are generally low and minimum shear reinforcement is sufficient as far as shear strength is concerned.

4.3 Test setup

4.3.1 Positions of supports for the test specimens

In order for the tests to be representative of the behavior of real portal frame panels it was necessary to choose a support configuration which would give similar member forces to those found in a full panel loaded until failure. The test specimen setup is shown in Figure I-2 of Appendix I.

A frame analysis was done to determine the bending moments and shear and axial forces at first yielding of the prototype frame members. Since the longitudinal reinforcement of the members was pre-defined, the yield bending moments could be calculated. The method by which this was done is explained in section 4.1. The loads on the frame were increased until moments large enough to cause yielding were reached. Yielding occurred first in the legs, just below the lower header beam. The loads which were large enough to cause yielding and the resulting bending moment diagram are shown in Figure I-1b in Appendix I. The self weight of the frame members was also considered in the analysis. The full yield analysis input and results are contained in Appendix II.

The position and type of supports applied to the test panel were chosen such that the member forces in the test panel were as close to those determined for the full panel as possible. It was found that this could best be achieved by placing a hinge support at the inflection point in the upper column, point A in Figure 3, and a roller support near the inflection point in the lower header beam, point B in Figure 3.

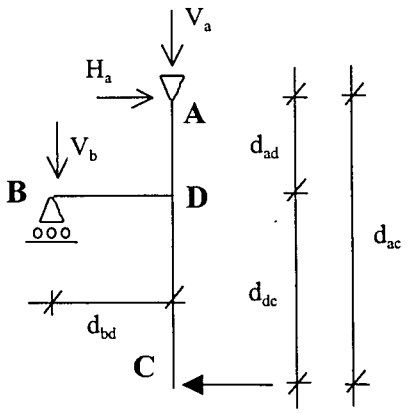

Summing moments about A:
load x d_{ac} = V_b x d_{bd}

Therefore V_b = load x d_{ac} / d_{bd}

M_{db} = V_b x d_{db}
= load x d_{ac}
Therefore the moment in the beam does not depend on d_{ad}, d_{dc} or d_{bd}

FIGURE 3 - TEST SETUP FORCES

Member BD has been referred to as the "beam" of the test specimen in the discussion below i.e. it represents the lower beam in the real panel.

Since leg DC will be made the same length as in the leg in the real panel, the moment and shear forces in it will be the same as in the real structure. As shown in Figure 3, the moment in the beam at point D does not

depend on the length of the beam i.e. it only depends on length d_{ac}. Therefore, given that the hinge at A is at the inflection point of the bending moment diagram and that the length of the leg is the same as in the real structure, the bending moment in the beam will be exactly the same as in the real structure. Since M_{db} and M_{dc} are the same as in the real structure, moment equilibrium of the joint implies that the M_{da} , the moment in the upper column, will be exactly the same as in the real structure.

As length d_{bd} is increased the reaction V_b, and therefore the shear force in the beam, will decrease. Since, as shown in Figure 3, the moment in the beam does not depend on length d_{bd}, it is possible to vary length d_{bd} until the reaction V_b is such that the shear force in the beam is the same as in the real panel.

Therefore the following can be said about the test panel:

1. The distribution of moments in the test panel will be the same as in the actual structure (This is very important since the mode of failure is flexural hinging).
2. All the shear forces, apart from the shear forces in member DA, will be the same as in the real structure. The error in the shear force in member DA is not considered to be critical.
3. The axial forces in the test panel are not the same as in the real structure, but since only column DA, which is not expected to fail, has any axial force at all, this is considered to be acceptable because the axial forces in the real structure are low.

As can be seen from the shear force diagrams contained in Appendix II, the shear forces vary along the length of the beam. Since it would not be practical to change the length d_{bd} in the test every time the load direction changes, d_{bd} has been chosen to be representative of the shear forces in the beam throughout the loading sequence.

It was found that the length d_{bd} required to give a representative shear force in member bd was in excess of 4m. Since it would not be practical or economical to have a test specimens with beams 4m long, an attachable steel extension beam was used to increase the length of the beam. The stiffness differences between the concrete and steel members will be of no consequence because the test set-up is statically determinate.

4.3.2 Hardware required for the test

In some cases the hardware required for the tests was available, and in other cases it had to be manufactured. The hardware, as positioned in the final test setup, is shown in Figure I-2 in Appendix I. The Drawings from which the hardware was constructed are shown in Appendix III.

The panel was tested on the strongfloor in the structures lab at UBC. The panel was tested in a "lying down" position and was supported 300 mm above the strong floor. The test panel rested on low friction teflon pads to ensure that minimal jacking force was used to resist friction during testing. A jack with a 100 kip (445 kN) load capacity and a 24" (620 mm) stroke was used to load the test specimen at the bottom of the leg, 2900 mm below the bottom of the beam.

A horizontal thrust support was required for the jack. Since the jacking force was reasonably low, up to 140 kN, and was applied quite close to the floor, about 300 mm, the strength requirements for the jack support were not very large. A column stub was modified and bolted to the floor to serve as a thrust support for the jack.

A steel extension beam was attached to the end of the beam of the test specimen. The roller support at the end of the steel extension beam, point B in Figure 3, was provided by placing rollers, which were found in the structures lab, between the steel beam and horizontal thrust supports. Thrust supports were placed on either side of the steel extension beam.

A hinge connection was required at the top of the column such that free rotation, but no translational movement, was permitted. The part of the hinge attached to the top of the column was connected to threaded bars which were cast into the test specimen.

4.4 Testing procedure

4.4.1 Loading procedure

Using the leg reinforcement shown in Figure I-3 of Appendix I, the yield force was calculated to be approximately 93 kN (f_y = 450 MPa, f_c' = 30 MPa). The specimens were loaded using sequences consisting of three cycles. A cycle, which would begin at zero displacement, consisted of a push in one direction followed by a pull in the opposite direction, and then a return to zero displacement. The reverse cyclic loading sequence shown in Figure I-4 of Appendix I was followed. The displacement at 75 kN was multiplied by 4/3 to predict the yield displacement, d, which was used as the basis for the rest of the loading which was done under displacement control. It is important to note that the 75 kN displacement used to calculate the yield displacement, was the 75 kN displacement for the test panel in the test set-up. This would be different to the 75 kN displacement for the leg alone and different to the 75 kN displacement of the full frame panel. Similarly the predicted yield displacement i.e. 4/3 times the 75 kN displacement, is the test panel yield displacement.

4.4.2 Data recording

Load and displacement readings from the jack were electronically captured. A LVDT was placed at the top of the leg to measure the movement of the top of the leg. The only information it was essential to measure was the load and deflection readings from the jack and the deflection readings at the top of the leg. With this information it was possible to plot the load deflection diagrams for the leg and hence determine the panel ductilities corresponding to the respective tie spacings. However other readings were also taken during the test. At each load increment concrete strains on opposite sides of the beam were electronically recorded using LVDT's. This enables the plotting of the moment curvature diagram for the beam which allows the elastic stiffness of the beam to be estimated.

The deflections recorded by the jack included deflections resulting from deformations occurring in the beam of the test specimen. The rotation of the joint was required to calculate the deflection of the LEG of the test specimen. This rotation was calculated using the deflection measured at the top of the leg and assuming rigid body motion of the joint region about the hinge connection shown in Figure I-2 in Appendix I. As a check on the rotations a laser pointer was glued to the center of the joint and the movement of the laser dot on a piece of paper 8m away from the pointer was measured. Using the movement of the laser dot it was possible to calculate the rotation of the joint at each load stage. A comparison of the joint rotations obtained from each of the methods is made in chapter 6.

At each load increment concrete strains on opposite sides of the leg in the hinge zone were electronically recorded using LVDT's, and mechanically recorded using dial gauges. From the strain measurements it is possible to obtain curvatures and hence plot moment curvature diagrams for the hinge regions of the specimens.

The strains were typically measured over 400 mm of the hinge zone. In some cases the 400 mm measuring length extended into the joint region and in other cases it started and finished within the leg. In order to attach the strain measuring apparatus to the test specimen the following method was used: 100 mm long steel studs were cut from 10 mm diameter round bar. The studs were hammered into holes which had been drilled into the top face of the test specimens. Horizontal bars which spanned the 400 mm gauge length were attached to the top of the studs using 90° clamps. Where dial gauges were used, the gauges were attached to steel studs which were inserted into the top of the test specimen as described above. Where LVDT's were used, the LVDT's were held in plastic clamps which were epoxy glued to the specimen. A number of the photographs contained in Appendix IV show the placement of the strain measuring apparatus on the test specimens. The effectiveness of these methods of measuring strain is described in chapter 6.

4.5 Material properties

4.5.1 Concrete properties

The specified 28 day strength of the concrete was 30 MPa. The test panels were cast from the same batch of concrete that was used to cast the panels being used for the actual building on site. Deltiac Testing and Engineering LTD did the quality control testing for the concrete used in the panels. The average 28 day strength reported by Deltiac was 33.0 MPa.

Six cylinders were cast and tested in the materials laboratory at the University of British Columbia (UBC). These six cylinders were cured under exactly the same conditions as the panels. One of the six cylinders was tested on the same day as each of the six test specimens were tested. The results from these tests are contained in Table 4 below. Casting took place on Wednesday the 14th of July 1999 and the test panels and the cylinders were moved to the structures laboratory at UBC on the 21st of July 1999.

Table 4 - RESULTS OF CONCRETE TESTING DONE AT UBC

Cylinder #	Date	Age (days)	Strength (MPa)
1	**7 September**	**55**	**21.3**
2	**21 September**	**69**	**25.3**
3	**29 September**	**77**	**21.9**
4	**5 October**	**83**	**21.6**
5	**20 October**	**98**	**23.8**
6	**4 November**	**113**	**23.9**

It is clear from Table 4 that the 28 day strength of the cylinders tested at UBC would have been significantly less than 30 MPa. However the curing of the cylinders tested at UBC was the same as the curing of the test panels and these particularly dry curing conditions may have contributed to the low strengths shown in Table 4.

The cylinders were removed from their plastic molds when the formwork was stripped from the test panels i.e. three days after casting. The cylinders then spent four days outdoors before being moved into the structures lab at UBC, where they were placed alongside the test panels. These dry and exposed curing conditions would partly account for the low strengths of the cylinders tested at UBC. An additional reason for low strength could be that the cylinders cast on site may not have been adequately compacted. A concrete strength of 30 MPa was assumed in the yield load calculations. However, it was found that the yield load calculation was not very sensitive to the concrete strength assumed for the calculation.

4.5.2 Reinforcing steel properties

A number of pieces of the 20M bar used in the legs were cut from the test panels for testing. The yield strain of the 20M bars was required in order to calculate the yield moment of the leg, see section 4.1.

Since the first four pieces tested behaved similarly, no additional tests were done. Table 5 below summarizes the results of the tests.

Table 5 - REINFORCING STEEL TEST RESULTS

TEST PANEL #	Yield Strength (MPa)	Ultimate Strength (MPa)	Elongation (%)
2	**449.5**	**726**	**15.5**
2	**453.7**	**732**	**14.0**
3	**451.6**	**727**	**13.5**
3	**455.7**	**743**	**15.5**

The yield strength was determined by 0.5% extension under load.

5 OBSERVED BEHAVIOR DURING TESTING

Unless otherwise indicated, all the figures referenced in this chapter can be found in Appendix IV.

Load sequences names like "3d" are often used. This means that the maximum displacements of that load sequence were equal to 3 times the yield displacement. In order to understand the explanations given in this chapter it is important to have a full understanding of the load cycles and load sequences described in section 4.4.1. Again it is noted that the yield displacement is the yield displacement for the system, and therefore includes the elastic displacement of the steel extension beam.

Table 6 indicates at which load stages the spalling of cover and buckling of reinforcement took place for each of the test specimens. A full description of the behavior of the individual test specimens follows.

5.1 Behavior common to all specimens

The behavior of all the specimens was similar prior to yielding of the longitudinal steel. This is not surprising given that the longitudinal reinforcement was the same in each of them.

Assuming a modulus of rupture stress of 3.29 MPa (Equation 8-8 of Reference 1) the cracking load was estimated, using the transformed section, to be 26 kN. The first flexural cracks appeared during the 25 kN load sequence and by the end of the 25 kN load sequence typically only one or two small flexural cracks had formed. In order to ensure that the positions of the cracks were visible in the photographs, lines were drawn with a marker pen over the cracks on the specimens. Therefore what might appear to be large cracks are actually the marker pen lines. The crack thicknesses are indicated by the numbers alongside the cracks.

By the end of the 50 kN load sequence cracks as large as 0.35 mm had formed and the spacing of cracks in the future hinge zone was typically 150 mm to 200 mm. The 50 kN load sequence ended with the 12th load cycle. The cracking in the first 100 mm specimen at the end of the 12th cycle is shown in Figure IV-1 of Appendix IV. The extent of cracking shown in Figure IV-1 is typical of the cracking in all of the specimens at the end of the 50 kN load stage.

TABLE 6 - TEST SPECIMEN BEHAVIOR

Load Stage	Jack Load (kN)	100 mm ties		200 mm ties	300 mm ties	
		first specimen	second specimen		first specimen	second specimen
0	0					
1	25					
2	-25					
3	25					
4	-25					
5	25					
6	-25					
7	50					
8	-50					
9	50					
10	-50					
11	50					
12	-50					
13	75					
14	-75					
15	75					
16	-75					
17	75					
18	-75					
19	d					
20	-d					
21	d					
22	-d					
23	d					
24	-d					
25	1.5d					
26	-1.5d					
27	1.5d					
28	-1.5d					
29	1.5d					
30	-1.5d					
31	2d					
32	-2d					
33	2d					
34	-2d					
35	2d				Spalling	Spalling & Buckling (outside)
36	-2d				Spalling	Spalling & Buckling (inside)
37	3d			Spalling	Buckling (outside)	
38	-3d			Spalling	Buckling (inside)	
39	3d			Buckling (outside)		
40	-3d			Buckling (inside)		
41	3d	Spalling	Spalling			
42	-3d	Spalling	Spalling			
43	4d					
44	-4d					
45	4d	Beam steel bond failure				
46	-4d					
47	4d		Vert. crack into beam			
48	-4d					
49	300 mm		Buckling of entire			
50	-300 mm		reinforcement cage			

At the end of the yield displacement load sequence cracks as large as 2.0 mm had formed and the spacing of cracks in the future hinge zone was typically 100 mm to 150 mm. The yield displacement load sequence ended with the 24th load cycle. The cracking in the first 100 mm specimen at the end of the 24th load cycle is shown in Figure IV-2 of Appendix IV. The extent of cracking shown in Figure IV-2 is typical of the cracking in all of the specimens at the end of the yield displacement load cycle.

The largest crack shown in Figure IV-2 is 1.8 mm wide and runs from the beam leg intersection diagonally into the joint. In all of the specimens the largest flexural crack at any given load stage would start at the leg beam intersection and run diagonally into the joint region. It is of interest to note that this large crack would be partially controlled by the diagonal 15M bars which are placed at the leg beam intersection, see Figure I-3 of Appendix I. The code intention for these diagonal bars was to control shrinkage cracks, but clearly they will also have an effect on the location of the flexural hinge.

After yielding of the longitudinal steel the specimens with different tie spacings behaved differently but there was still some common behavior. Even though the longitudinal steel started yielding during the 1d load sequence, the earliest the cover ever spalled was at the end of the 2d load sequence, this occurred in both of the 300 mm specimens. The cover of the 200 mm tie spacing specimens spalled in the 3d load sequence. The extent of cracking in the 200 mm tie spacing specimen at the end of the 2d load sequence is shown in Figure IV-3 of Appendix IV. It can be seen from Figure IV-3 that the cracking on the outside of the leg extended up into the joint region. Figure IV-3 also shows the extent of cracking in the joint region and in the part of the beam adjacent to the joint.

As would be expected, there was more diagonal cracking in the specimens with larger tie spacings. As shown in Figure IV-3 of Appendix IV, at the end of the 2d load sequence there was a 1.25 mm diagonal crack in the 200 mm tie spacing specimen. Since the shear is constant along the length of the leg and the tie spacing was increased to 400 mm in the part of the leg more than 1m from the joint, there was more shear cracking in the region of the leg below the area detailed for ductility.

The hinge regions (regions of yielding) appeared to extend approximately 800 mm below the joint, and up into the joint. The large 4.5 mm crack visible in Figure IV-3 of Appendix IV formed approximately 250 mm into the joint region. It is therefore clear that the zone of yielding of the longitudinal reinforcement extended well into the joint region.

5.2 Behavior of 100 mm tie spacing specimens

5.2.1 1st Specimen

The cover first spalled during the third cycle of the 3d loading sequence. Severe cracks, many in excess of 3 mm, were present in the joint region during hinging and the crushing and tensile straining of concrete associated with the hinging extended into the joint region. By the end of the 4d load sequence the cover had extensively spalled, especially on the outside face leg. It can be seen from Figure IV-4 in Appendix IV that by the end of the 4d load sequence, which ended with load cycle 48, the cover had spalled over 7 tie spacings (700 mm), and had extended 2.5 tie spacings (250 mm) into the joint region.

During the third cycle of the 4d load sequence the bottom longitudinal beam reinforcement, which is anchored in the part of the joint just above the top of the leg, underwent a bond failure and pulled out of the joint. This bond failure occurred as a consequence of the repeated cyclic loading causing excessive tensile straining in the lower region of the joint. The large crack associated with this bond failure can be seen in Figure IV-5 of Appendix IV.

The pullout of the longitudinal beam bar led to a failure, with corresponding drop in capacity, in the "pushing" direction. However there was no failure in the pulling direction. When the leg was pulled the large crack closed and the hinge continued to develop for the pulling direction. However, even though no failure was observed, the load reached with each successive load cycle at the same displacement was reduced. This is largely as a result of the Baushinger effect i.e. as the steel was yielded again and again, the stiffness decreased more and more. The result being that with each successive straining of the steel to give the same displacement, the load would be successively lower.

Since the jack had only a 600 mm stroke the specimen could only be deflected 300 mm either way. It was therefore not possible to see if the specimen would maintain its "pulling" capacity at higher displacements. Since failure had already taken place in one direction it was decided that it would not be worthwhile to move the jack such that the specimen could be "pulled" further.

By the end of the test, the region in which cover had spalled on the outside face had grown considerably compared to when the pullout of the longitudinal beam bars occurred. The spalling just prior to the beam steel pullout is shown in Figure IV-4 of Appendix IV and the spalling at the end of the test is shown in Figure IV-6. (It can also be seen in Figure IV-6 how the large crack visible in Figure IV-5 closed when the specimen was pulled.) Figure IV-6 shows that the region of spalling at the end of the test extended over 10 tie spacings (1000 mm), extending 400 mm into the joint and 600 mm down the leg. It is clear from this

photograph that 100 m ties are very effective for preventing buckling of the longitudinal steel even at very high strains.

5.2.2 2nd Specimen

The cover spalled during the third cycle of the 3d loading sequence. Bond failure of the bottom longitudinal beam steel was not the primary cause of failure in the second 100 mm tie spacing specimen. A large crack did form, running from the leg beam intersection, extending vertically up the beam joint interface. Figure IV-7, which was taken at the end of the first push of the 4.3 d load sequence, shows the spalling of the concrete and the crack extending vertically up into the beam.

There was not a significant decrease in load carrying capacity in the pushing direction with the formation of this vertical crack. Before full bond failure occurred, the face concrete spalled off the leg and all eight of the longitudinal bars in the leg (four on each face) buckled out of plane. All the longitudinal bars in the hinge zone buckled in the same mode and in the same direction. The out of plane buckling of the whole hinge zone reinforcement cage is clearly shown in Figure IV-8.

The first bars to buckle were the top face distribution reinforcement bars. These bars are not restrained from buckling by the ties since they are in the center of the long side of the ties, see Figure I-3 of Appendix I. Since the leg buckled up it is likely that the top face distribution bars buckled before the bottom face distribution bars. It is likely that the top face distribution bars buckled first because the quality of the top face concrete would be lower than the quality of the bottom face concrete i.e. as a result of bleeding and more exposed early curing conditions. Once the top distribution bars had buckled out of plane there was a tendency for the whole hinge zone reinforcement cage to undergo local out of plane buckling. The ties prevent in plane buckling of the outside longitudinal bars but are ineffective if all the longitudinal bars buckle in the same direction.

5.3 Behavior of 200 mm tie spacing specimens

5.3.1 1st Specimen

The first 200 mm tie spacing specimen was the first of the six specimens tested. A number of problems occurred during the first test.

The first major problem was with the load calibration in the computer. The load scale was set incorrectly and the maximum load the computer could read was 96.8 kN. Unfortunately this load was very close to the expected yield load and by the time the problem was detected the specimen had yielded and the yielding portion of load deflection plot had not been recorded.

A second problem occurred when the pushing direction roller supports (see Figure I-2 of Appendix I) moved 20 mm during the first load cycle of the 1.5d load sequence. The moving of the support was a result of the bolts connecting the support to the strong floor not being sufficiently tensioned. Since the roller supports were only pushed in one direction, it was possible to fill in the 20 mm gap and continue. However during the first cycle of the 2d load sequence the hinge support (see Figure I-2 of Appendix I) moved. Since the hinge support was required to carry loads in two directions it would slide forward and back as the loading continued. Therefore the specimen was loaded to failure by pushing it in one direction. The resulting test was therefore one in which a specimen with a 200 mm tie spacing was subjected to a degree of cyclic loading and then pushed monotonically until failure.

This test gave an indication of how cyclic loading reduced the ability of the specimen to achieve the maximum displacement. By comparing the maximum displacement of this 200 mm tie spacing specimen, which had a relatively small amount of cyclic loading, to the maximum displacement of the 200 mm tie spacing specimen which was subjected to increasing cyclic loads to failure, the effect of cyclic loading on maximum displacement achieved could be observed.

Failure in the 200 mm tie spacing specimen loaded monotonically to failure occurred via buckling of the longitudinal steel which occurred after the concrete had spalled. After failure had occurred the loads which the specimen could resist were significantly less and it was therefore possible to apply cyclic loads once again i.e. the loads were too low to cause sliding of the supports. After a few cycles the longitudinal steel ruptured in tension. The steel on both sides of the specimen leg ruptured.

For subsequent tests, bigger, stronger bolts were used and the jacking force was significantly increased to ensure there were no further sliding problems.

5.3.2 2nd Specimen

The failure of the specimens with hinge zone ties spaced at 200 mm was similar in nature to the failure of the specimens with ties spaced at 300 mm. Therefore the failure observations for the second 200 mm specimen have been considered in section 5.4 alongside the observations of the 300 mm specimens.

5.4 Behavior of 300 mm (and 2nd 200 mm) tie spacing specimens

5.4.1 Overall behavior of specimens

The failure of the second 200 mm tie spacing specimen and both of the 300 mm tie spacing specimens were all controlled by in plane buckling of the outside longitudinal bars. Buckling always occurred over one tie spacing. The behavior of the 300 mm and the 2nd 200 mm tie spacing specimens is summarized in Table 7.

Table 7 – Summary of behavior of 200 mm and 300 mm tie spacing specimens

	200 mm specimen	1st 300 mm specimen	2nd 300 mm specimen
Start of spalling.	1st cycle of 3d sequence	3rd cycle of 2d sequence	3rd cycle of 2d sequence
Buckling of steel on outside face.	2nd cycle of 3d sequence	1st cycle of 3d sequence	3rd cycle of 2d sequence
Buckling of steel on inside face.	2nd cycle of 3d sequence	1st cycle of 3d sequence	3rd cycle of 2d sequence

5.4.2 Specific behavior of 200 mm tie spacing specimen

Although the first buckling of the longitudinal steel in the 200 mm tie spacing specimen occurred during the 2nd cycle of the 3d load sequence, this initial buckling was not very severe. See Figure IV-9 of Appendix IV. It can be seen from Figure IV-9 that the buckling took place in a plane at 45° to the face of the leg. Although in Figure IV-9 it appears that only the bottom bar has buckled, the top bar has also buckled, but since it has buckled towards the camera, this buckling is not clear. Although there was a decrease in load carrying capacity associated with this initial buckling, the decrease was not very large.

Figure IV-10 of Appendix IV shows the extent of buckling on the outside face of the member after the pushing portion of the first cycle of the 4d load sequence. By this stage the buckling was severe with a correspondingly large decrease in load carrying capacity. Again it is noted that buckling always occurred over one tie spacing.

Although it happened once the load carrying capacity had dropped significantly, it is interesting to note that the longitudinal steel ruptured in tension. Shortly after the rupturing of the longitudinal steel the cover on the face of the leg spalled and the face reinforcing bars on the top face of the specimen buckled up. This buckling was similar to that observed in the second 100 mm tie spacing specimen although in this case out of plane buckling of the whole reinforcement cage did not take place.

5.4.3 Specific behavior of first 300 mm tie spacing specimen

As can be seen from the times of spalling and buckling in Table 7, the buckling of the longitudinal steel in the 300 mm tie spacing specimens occurred in the same cycle, or one cycle after, the cover spalled. The rapid succession of spalling and buckling can be seen by referring to Figures IV-11, IV-12 and IV-13 in Appendix IV. Figure IV-11 shows the first 300 mm tie spacing specimen at the end of the 2d load sequence. At this stage the cracking was quite severe and a small amount of surface cover had spalled on the inside face of the leg.

Figure IV-12 shows the spalled cover and buckled reinforcement on the outside face of the leg at the end of the pushing half of the first cycle of the 4d load sequence i.e. just half a load cycle after the picture in Figure IV-11 was taken. As in the 200 mm tie spacing specimen, the buckling took place in a plane at 45° to the face of the leg. Again it appears that only the bottom bar has buckled, but actually the top bar has also buckled.

The spalling of cover and buckling of longitudinal reinforcement on the inside face of the leg took place during load stage 38 i.e. the second half of the first cycle of the 4d load sequence. The damage at load stage 38 is shown in Figure IV-13 of Appendix IV. The rapid succession of spalling and buckling is clear when it is considered that the pictures in Figures IV-11 and IV-13 were taken only one load cycle apart.

5.4.4 Specific behavior of second 300 mm tie spacing specimen

In the second 300 mm tie spacing specimen the succession of spalling and buckling was even more rapid, with both occurring in the same half load cycle i.e. the third cycle of the 2d load sequence. The damage in the specimen at the end of the 1.5d load sequence can be seen in Figure IV-14 of Appendix IV. It is interesting to note the relatively large shear cracks (1.0 mm) in the hinge region. Shear cracks did not form to this extent in the specimens with closer hinge zone tie spacings.

Since the buckling took place immediately after / as spalling occurred, no pictures of the specimen in the spalled but not buckled condition were taken. Figure IV-15 of Appendix IV shows the buckled bars on the outside face of the specimen. Spalling and buckling of the bars on the outside face took place during the first half of the third cycle of the 2d load sequence i.e. load stage 35. Note how by this stage the diagonal shear cracks had increased in width to be 1.8 mm. The longitudinal steel on the inside of the leg buckled during the second half of the third cycle of the 2d load sequence i.e. load stage 36. During the first half of the first cycle of the 3d load sequence a significant amount of damage occurred. Firstly further spalling and buckling took place on the outside of the leg. Secondly, the face cover of the leg spalled and the

longitudinal bars on the face of the leg buckled up. This is clearly shown in Figure IV-16 which was taken at the end of the first cycle of the 3d load sequence i.e. load stage 37.

6. TEST RESULTS - GENERATION OF LEG LOAD DEFLECTION PLOTS

6.1 Assumptions used and plan of presentation of test results

The primary objective of this thesis was to determine the relationship between hinge zone tie spacing and the ductility of full size tilt-up frame panels. It is assumed that the plastic displacement of the full panel results entirely from the plastic rotation of the hinges which form in the top of the legs. Thus the main objective of the tests was to obtain leg load displacement plots for the respective tie spacings. This would provide the plastic displacement capacity of the legs, and therefore the plastic displacement capacity of the entire frame.

The raw load displacement readings from the jack require interpretation and modification since they include deflections resulting from deformation of the steel extension beam. In order to obtain the leg deflection values corresponding to the recorded loads it was necessary to subtract deflections resulting from deformation of the parts of the test specimen other than the leg from the jack deflection readings. Referring to Figure I-2 of Appendix I, the joint would move laterally when load was applied to the bottom of the leg because the support at the end of the beam was a roller support. This lateral movement would be included in the deflections recorded by the jack. Furthermore, the deformation of the test specimen beam as well as the steel extension beam would also contribute to rotation of the joint. This joint rotation would result in deflections at the bottom of the leg which would also be included in the deflections measured by the jack. Since it was necessary to obtain LEG load deflection plots, these deflections which originated from outside of the leg would have to be subtracted from the deflections measured by the jack.

In order to calculate the magnitude of the bottom of leg deflections resulting from firstly lateral movement of the joint and secondly from joint rotations, it was necessary to calculate top of leg deflections. The computation of top of leg deflections is explained in section 6.2. The plotting of leg load vs. deflection graphs is explained in section 6.3.

Strain measurements were recorded during the tests so that moment curvature plots could be generated. The success of the strain recording methods and the interpretation of the results is explained in section 6.4.

Since the computer recorded load and deflection values at either 2 or 5 second intervals, each test had up to 2000 data points. All manipulation of data and calculations were done using Microsoft Excel. Extracts of the recorded test data are contained in Appendix V. The complete set of test data is available from the author at michaeljohndew@hotmail.com.

6.2 Computation of top of leg deflections

6.2.1 Methods of computation of top of leg deflection

Three different methods were used to determine the top of leg deflections. In each of the methods it was assumed that there was rigid body motion of the joint and upper leg of the test specimen (see Figure I-2 of Appendix I). Using this rigid body motion assumption, each of the methods calculated the rotation of the joint and then used the joint rotation to calculate the movement of the top of the leg. Given that there was relatively little cracking in the upper region of the joint and in the leg above the joint, the rigid body motion assumption seems reasonable.

The three methods used to calculate top of leg deflections were as follows:

1. The most basic method involved direct measurement of the movement of the joint region using a regular 300 mm ruler. The ruler was suspended above the specimen and the movement of a line which was drawn on the specimen was recorded. The distance of the measuring point from the hinge of the test setup was recorded and it was used to calculate joint rotation. The joint rotation was then used to calculate the movement of the top of the leg using simple trigonometry.
2. For the second method, a laser pointer was glued to the top of the specimens in the middle of the joint region. The movement of the laser dot was monitored on a piece of paper positioned 8 m away. Using simple trigonometry it was possible to find the of rotation of the joint. The joint rotation was then used to calculate the movement of the top of the leg using the assumption of rigid body motion of the joint and upper leg.
3. Before the third test an extra LVDT became available and for the third to sixth tests, the top of leg deflections were measured using the LVDT. The LVDT recorded the top of leg deflections at 2 second intervals and matched them to corresponding load readings recorded by the jack. The distance of the LVDT from the hinge of the test setup was measured and used to calculate joint rotation. The joint rotation was then used to calculate the top of leg deflection using the assumption of rigid body motion for the joint and top leg.

6.2.2 Top of leg deflection calculations for test # 1, first 200 mm specimen

For test one only method 1 described in section 6.2.1 above was used. However this method was used twice. Firstly the lateral movement of the joint was measured as described above. Secondly, the lateral movement of the connection between the concrete beam of the test specimen and the steel extension beam was measured. Assuming axial rigidity of concrete beam of the test specimen, and using the measured "vertical" (as viewed in Figure I-2 of Appendix I) distance from the hinge of the test setup to the point of measurement, the rotation of the joint was calculated. The joint rotation was then used to calculate top of leg deflection.

The results of the two calculations are shown in Figure 4. The average of the two best fit lines was used to obtain top of leg deflections from the load values recorded by the jack i.e. this equation was programmed into the spreadsheet such that the top of leg deflections for each recorded load could be calculated. This was done in the Excel spreadsheet containing the recorded test data.

6.2.3 Top of leg deflection calculations for test # 2, first 100 mm specimen

Methods one and two described in section 6.2.1 above were used to calculate the top of leg deflections for test 2. The results of the two methods are shown in Figure 5. The average of the best fit lines was used to obtain top of leg deflections from the load values recorded by the jack i.e. this equation was programmed into the spreadsheet such that the top of leg deflections for each recorded load could be calculated. This was done in the Excel spreadsheet containing the recorded test data.

6.2.4 Top of leg deflection calculations for tests #'s 3-6 and evaluation of methods used

All three methods described in section 6.2.1 above were used to calculate the top of leg deflections for tests 3 to 6. The results of the three methods for specimens 3 to 6 are shown in Figures 6 to 9.

Comparing the top of leg deflection results from the three methods revealed the following: The ruler method was reasonably accurate. However an assumption of the ruler method was that the load deflection movement of the top of the leg was the same as the unload deflection movement of the top of the leg. The LVDT load vs. top of leg deflection results indicate that this assumption is not true, see Figures 6 to 9. The LVDT results suggest that as the load was reduced, the beam and joint parts of the test set-up recovered first and the deflections in the leg recovered more slowly.

This could be explained by the greater degree of cracking in the leg compared to the beam. Since the beam had relatively little cracking, once the load was reduced the beam was easily able to return to its original shape. In the leg where the cracking was more severe, as the load was reduced the cracks would not close completely. Only once the load direction had been reversed would the cracks be forced closed. This type of pinched hysteresis loop is typically observed in members with high shear. Although the leg failure was flexurally dominated, there was a degree of shear cracking, particularly below the hinge zone where the tie spacing was 400 mm.

For specimens one and two, the use of the fitted line to calculate the load vs. top of leg deflection involved assuming that the load deflection movement of the top of the leg was the same as the unload deflection movement of the top of the leg. As explained above, this is not a true assumption and as a result the load

Figure 4 - Load vs. Top of Leg Deflection - Test 1, 200mm Ties

TEST 1 DATA, FIRST 200 mm SPECIMEN

Load (kN)	d at ruler (mm)	d at top of leg (mm)	d at beam (mm)	d at top of leg (mm)
	0	0	0	0
25	3	3.3	2	2.9
-25	-3	-3.3	-3	-4.4
25	3	3.3	2	2.9
-25	-3	-3.3	-3	-4.4
25	3	3.3	2	2.9
-25	-3	-3.3	-3	-4.4
50	7	7.8	5	7.3
-50	-7	-7.8	-6	-8.7
50	7	7.8	5	7.3
-50	-7	-7.8	-6	-8.7
50	8	8.9	6	8.7
-50	-8	-8.9	-6	-8.7
75	11	12.3	8	11.6
-75	-11	-12.3	-10	-14.6
75	11	12.3	8	11.6
-75	-11	-12.3	-10	-14.6
75	12	13.4	8	11.6
-75	-13	-14.5	-11	-16
94	15	16.7	12	17.5
-96	-14	-15.6	-13	-18.9
96.8	14	15.6	11	16
-90	-16	-17.8	-13	-18.9
94	15	16.7	11	16

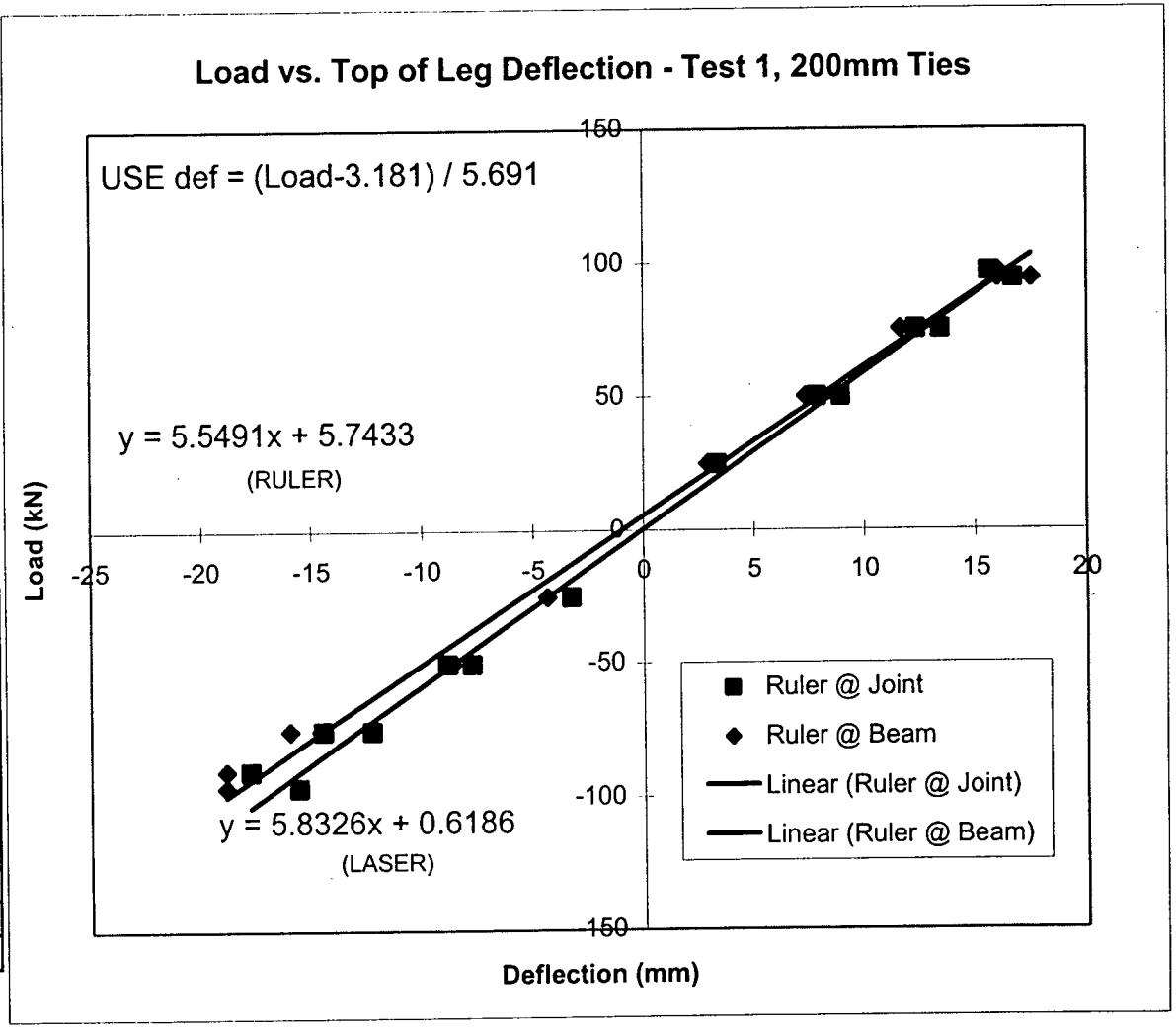

Figure 5 - Load vs Top of Leg Deflection - Test 2, 100mm Ties

TEST 2 DATA, FIRST 100 mm SPECIMEN.

Load (kN)	Rot. of j (Laser) (radians)	d @ top of leg (laser) (mm)	d@ruler @joint (mm)	d @ top of leg (mm)
0			0	0
25	0.001375	3.073125	3	3.03
-25	-0.001	-2.235	-1	-1.01
25	0.001375	3.073125	3	3.03
-25	-0.00113	-2.514375	-3	-3.03
25	0.001375	3.073125	2	2.02
-25	-0.00113	-2.514375	-4	-4.04
50	0.003375	7.543125	7	7.06
-50	-0.00275	-6.14625	-8	-8.07
50	0.0035	7.8225	7	7.06
-50	-0.003	-6.705	-9	-9.08
50	0.003625	8.101875	8	8.07
-50	-0.003	-6.705	-9	-9.08
75	0.005875	13.130625	12	12.11
-75	-0.0045	-10.0575	-12	-12.11
75	0.005875	13.130625	12	12.11
-75	-0.0045	-10.0575	-13	-13.12
75	0.006125	13.689375	12	12.11
-75	-0.00475	-10.61625	-13	-13.12
97	0.008625	19.276875	16	16.14
-97.9	-0.0055	-12.2925	-16	-16.14
93.5	0.0085	18.9975	17	17.15
-89.9	-0.0055	-12.2925	-16	-16.14
96.2	0.0085	18.9975	16	16.14
-89	-0.0055	-12.2925	-15	-15.14
122			21	21.19
-108			-18	-18.16
101			20	20.18
-105			-18	-18.16
106			20	20.18
-104			-18	-18.16
95			22	22.2
-89			-18	-18.16
108			22	22.2
-106			-19	-19.17
105			22	22.2
-100			-19	-19.17

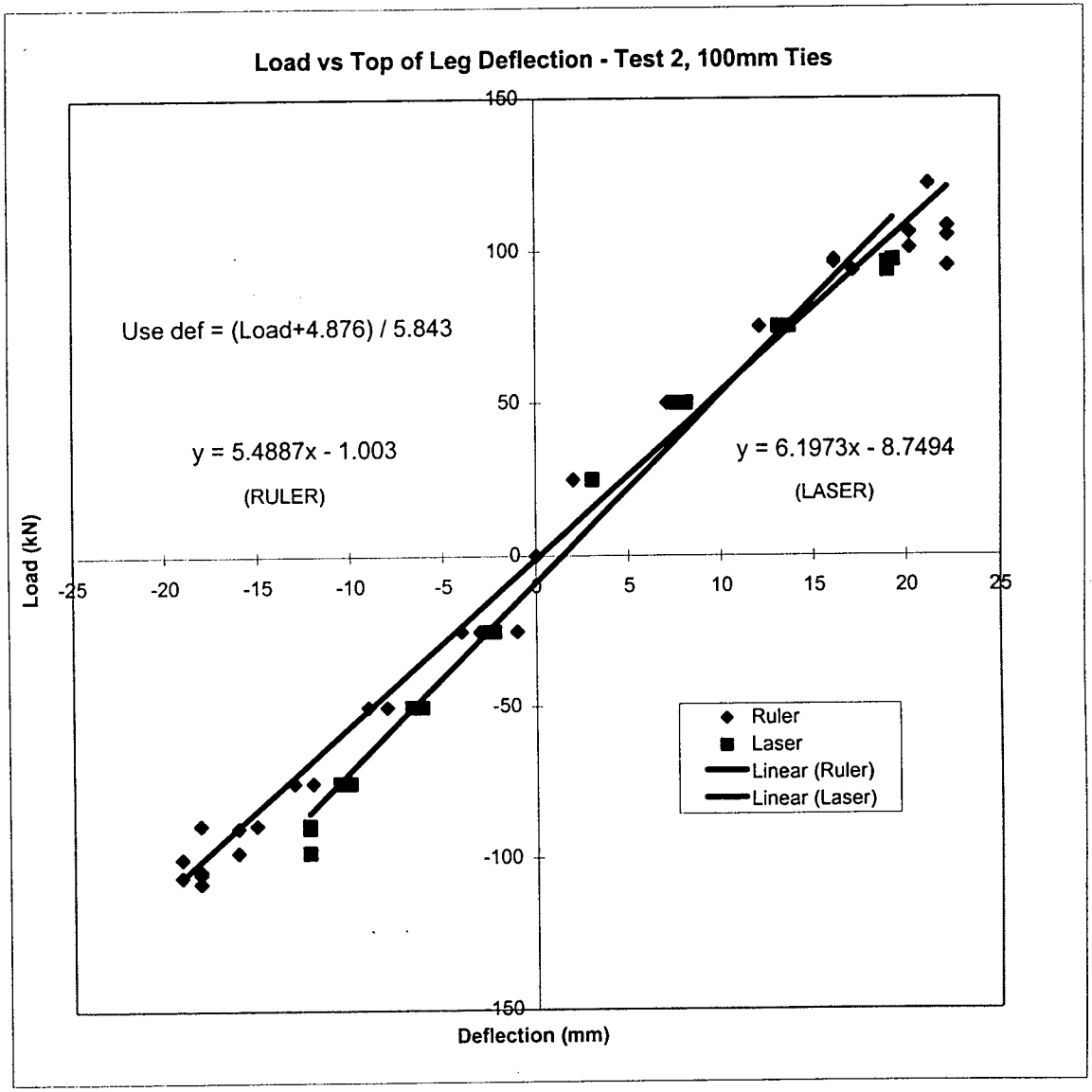

Figure 6 -Load vs Top of Leg Deflection - Test 3, 300mm Ties

TEST 3 DATA, FIRST 300 mm SPECIMEN

Load (kN)	Rot. of jnt (Ruler) (radians)	d @ top of leg (Ruler) (mm)	Rot. of jnt (laser) (radians)	d @ top of leg (Laser) (mm)
0	0	0	0	0
25	0.002048	4.6	0.002125	4.7
-25	-0.000683	-1.5	-0.000875	-2.0
25	0.00273	6.1	0.0025	5.6
-25	-0.001365	-3.1	-0.000875	-2.0
25	0.00273	6.1	0.002375	5.3
-25	-0.002048	-4.6	-0.000875	-2.0
50	0.004778	10.7	0.004625	10.3
-50	-0.003413	-7.6	-0.0025	-5.6
50	0.004778	10.7	0.0045	10.1
-50	-0.004096	-9.2	-0.002875	-6.4
50	0.005461	12.2	0.0045	10.1
-50	-0.004096	-9.2	-0.002875	-6.4
75	0.007508	16.8	0.00625	14.0
-75	-0.006143	-13.7	-0.00425	-9.5
75	0.007508	16.8	0.00625	14.0
-75	-0.006143	-13.7	-0.00425	-9.5
75	0.007508	16.8	0.00625	14.0
-75	-0.006143	-13.7	-0.00425	-9.5
94	0.010239	22.9	0.007375	16.5
-98	-0.007508	-16.8	-0.00525	-11.7
94	0.009556	21.4	0.007375	16.5
-97	-0.008191	-18.3	-0.00525	-11.7
92	0.008873	19.8	0.007375	16.5
-91	-0.008191	-18.3	-0.00525	-11.7
117	0.010921	24.4	0.008875	19.8
-117	-0.009556	-21.4	-0.00625	-14.0
100	0.010921	24.4	0.008875	19.8
-80	-0.007508	-16.8	-0.00525	-11.7
99	0.010921	24.4	0.008625	19.3
-82	-0.008191	-18.3	-0.00525	-11.7
112	0.011604	25.9	0.0095	21.2
-106	-0.008873	-19.8	-0.00625	-14.0
104	0.011604	25.9	0.0095	21.2
-68	-0.008873	-19.8	-0.00575	-12.9
106	0.011604	25.9	0.0095	21.2
-100	-0.009556	-21.4	-0.00625	-14.0
112	0.011604	25.9	0.0095	21.2

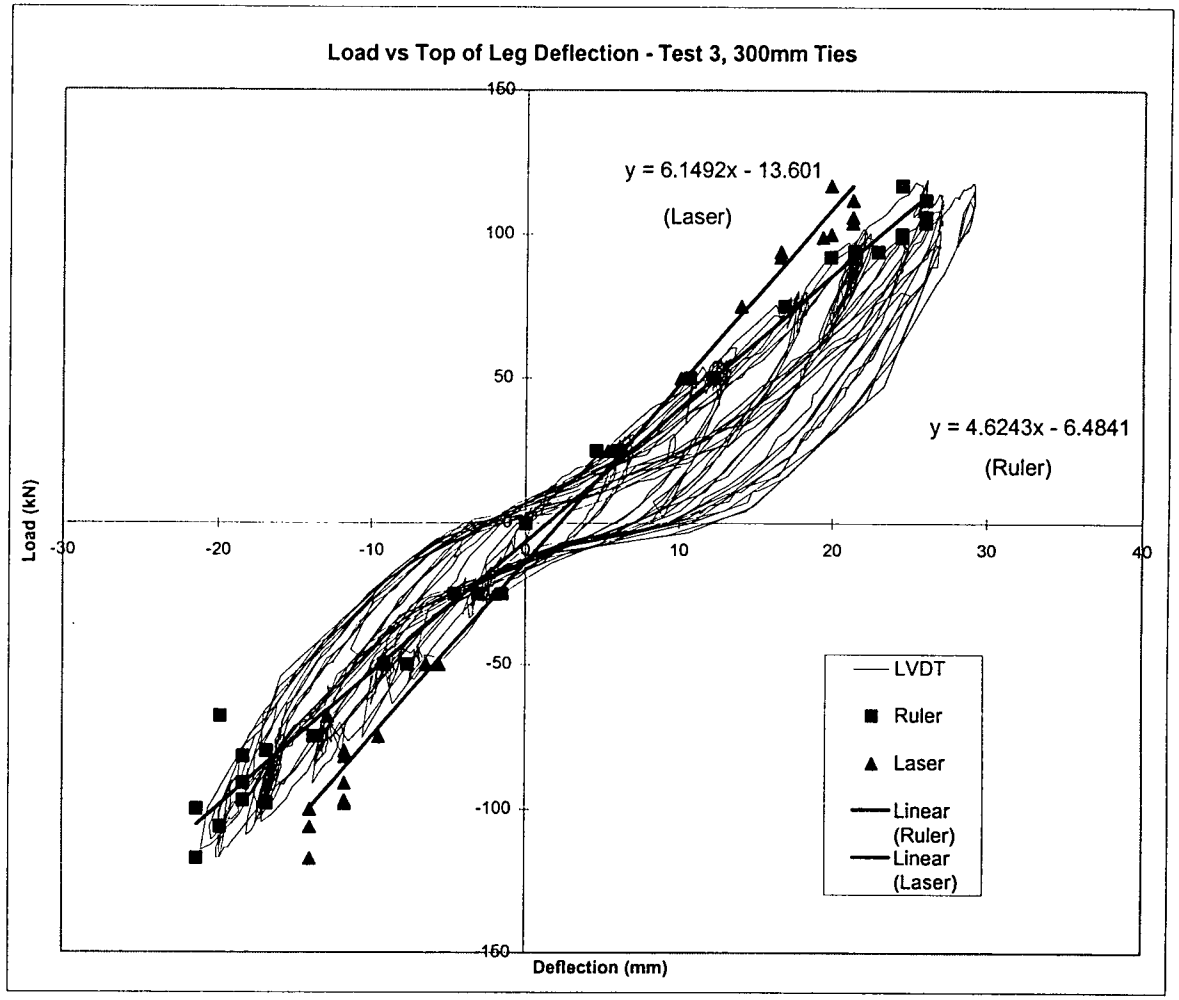

Figure 7 - Load vs Top of Leg Deflection - Test 4, 300mm Ties

TEST 4 DATA, SECOND 300 mm SPECIMEN

Jack Load (kN)	Rot. of jnt (Ruler) (radians)	d @ top of leg (Ruler) (mm)	Rot. of jnt (laser) (radians)	d @ top of leg (Laser) (mm)
0	0	0	0	0
25	0.00177	3.94	0.00125	2.78
-25	-0.00177	-3.94	-0.0015	-3.34
25	0.00177	3.94	0.00125	2.78
-25	-0.00177	-3.94	-0.0015	-3.34
25	0.00118	2.63	0.00125	2.78
-25	-0.00177	-3.94	-0.0015	-3.34
50	0.00354	7.88	0.003375	7.51
-50	-0.00413	-9.19	-0.003375	-7.51
50	0.00413	9.19	0.004	8.90
-50	-0.00472	-10.50	-0.003375	-7.51
50	0.00472	10.50	0.004	8.90
-50	-0.00472	-10.50	-0.003875	-8.62
75	0.00649	14.44	0.006	13.35
-75	-0.00708	-15.75	-0.005625	-12.52
75	0.00649	14.44	0.006	13.35
-75	-0.00708	-15.75	-0.005625	-12.52
75	0.00649	14.44	0.006	13.35
-75	-0.007669	-17.06	-0.006375	-14.18
100	0.008849	19.69	0.00775	17.24
-98	-0.008849	-19.69	-0.007625	-16.97
94	0.007669	17.06	0.007375	16.41
-98	-0.008849	-19.69	-0.007625	-16.97
92	0.008849	19.69	0.007375	16.41
-96	-0.008849	-19.69	-0.007625	-16.97
117	0.010029	22.32	0.009375	20.86
-114	-0.010619	-23.63	-0.00875	-19.47
104	0.010029	22.32	0.009	20.03
-105	-0.009439	-21.00	-0.008125	-18.08
101	0.009439	21.00	0.009	20.03
-100	-0.009439	-21.00	-0.008125	-18.08
117	0.010619	23.63	0.009875	21.97
-117	-0.010619	-23.63	-0.009	-20.03
107	0.010029	22.32	0.009625	21.42
-107	-0.010029	-22.32	-0.00875	-19.47
92	0.009439	21.00	0.009375	20.86
-104	-0.010029	-22.32	-0.00875	-19.47

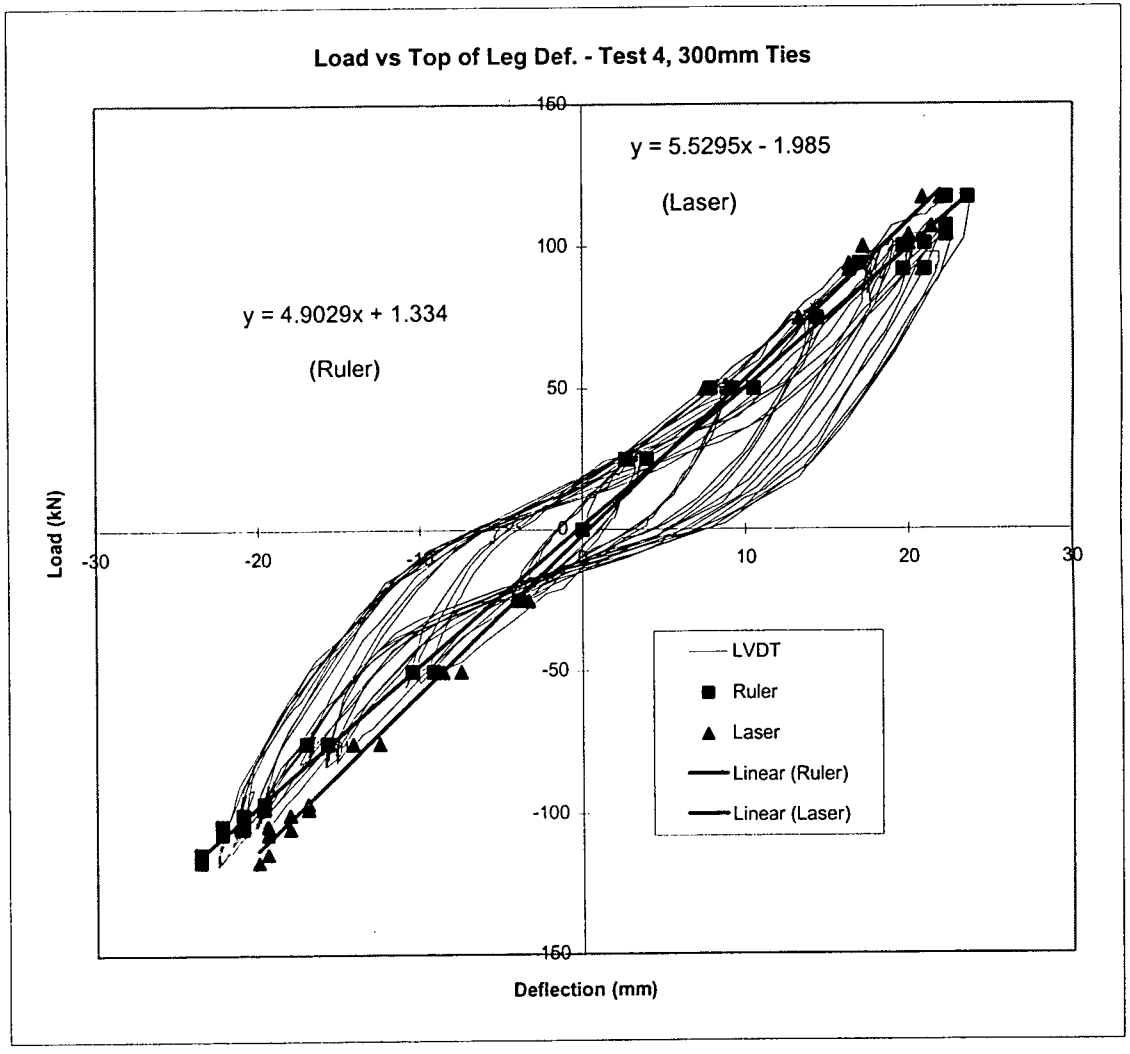

Figure 8 - Load vs Top of Leg Deflection - Test 5, 100mm Ties

TEST 5 DATA, SECOND 100 mm SPECIMEN

Load (kN)	Rot. of jnt (Ruler) (radians)	d @ top of leg (Ruler) (mm)	Rot. of jnt (laser) (radians)	d @ top of leg (Laser) (mm)
0	0	0	0	0
25	0.002055	4.6	0.002	4.5
-25	-0.002055	-4.6	-0.0015	-3.3
25	0.00274	6.1	0.0025	5.6
-25	-0.002055	-4.6	-0.00175	-3.9
25	0.00274	6.1	0.0025	5.6
-25	-0.002055	-4.6	-0.00175	-3.9
50	0.005479	12.2	0.004875	10.8
-50	-0.00411	-9.1	-0.00325	-7.2
50	0.006164	13.7	0.00525	11.7
-50	-0.004794	-10.7	-0.003375	-7.5
50	0.006164	13.7	0.00525	11.7
-50	-0.00411	-9.1	-0.003375	-7.5
75	0.008219	18.3	0.007125	15.9
-75	-0.007534	-16.8	-0.005	-11.1
75	0.008904	19.8	0.00725	16.1
-75	-0.006849	-15.2	-0.005	-11.1
75	0.008219	18.3	0.007625	17.0
-75	-0.007534	-16.8	-0.00525	-11.7
87	0.009589	21.3	0.008125	18.1
-99	-0.008904	-19.8	-0.006625	-14.7
83	0.009589	21.3	0.008125	18.1
-99	-0.009589	-21.3	-0.006625	-14.7
83	0.009589	21.3	0.008125	18.1
-98	-0.009589	-21.3	-0.006125	-13.6
111	0.010958	24.4	0.00875	19.5
-123	-0.009589	-21.3	-0.007625	-17.0
98	0.010958	24.4	0.009625	21.4
-113	-0.010274	-22.9	-0.00725	-16.1
91	0.010274	22.9	0.009625	21.4
-110	-0.010274	-22.9	-0.00725	-16.1
118	0.011643	25.9	0.01	22.3
-129	-0.010958	-24.4	-0.007875	-17.5
109	0.011643	25.9	0.01	22.3
-121	-0.010958	-24.4	-0.007875	-17.5
106	0.010958	24.4	0.010125	22.5
-116	-0.010274	-22.9	-0.00775	-17.2

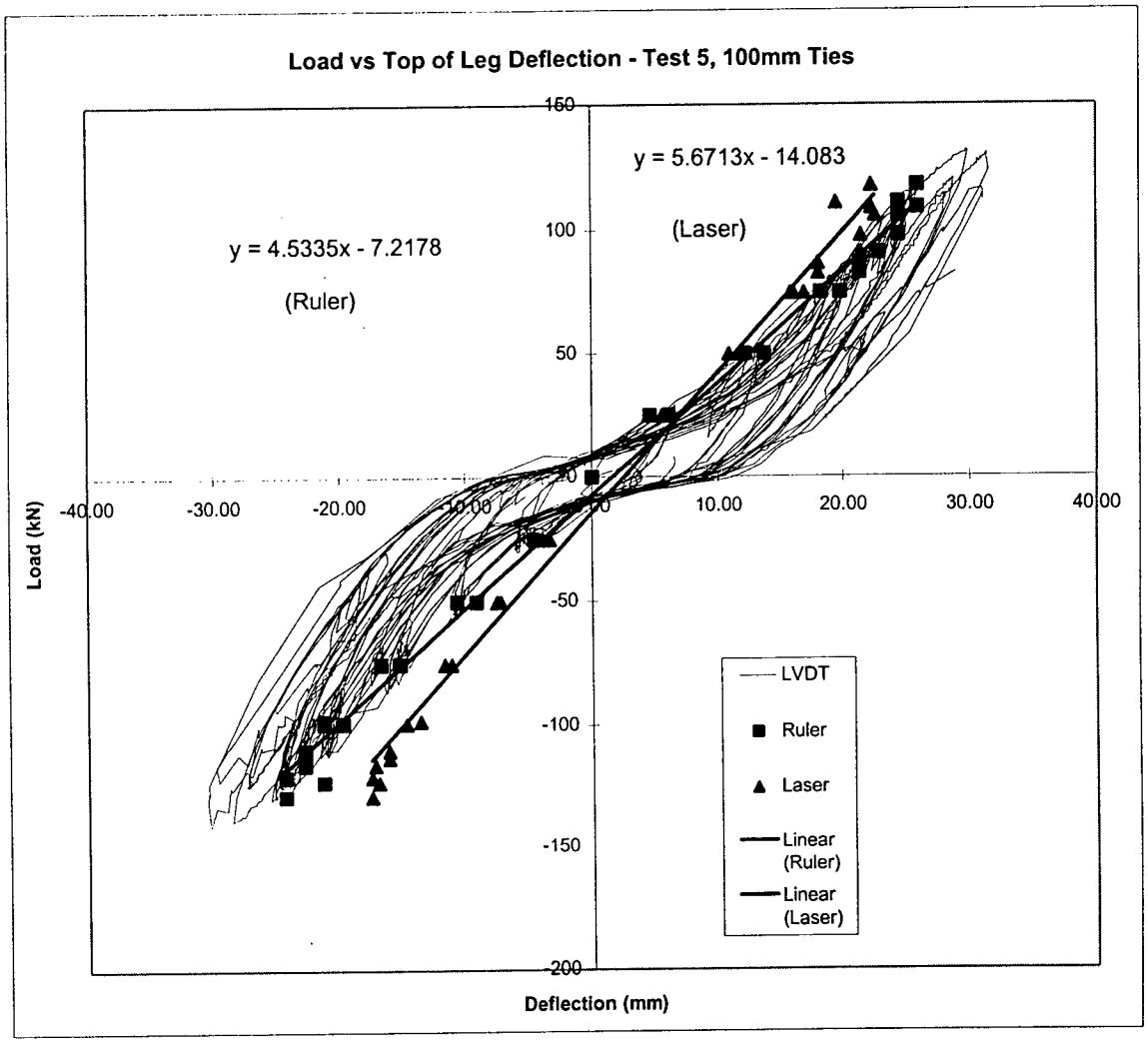

Figure 9 - Jack Load vs Top of Leg Def. - Test 6, 200mm Ties

TEST 6 DATA, SECOND 200 mm SPECIMEN

load (kN)	Rot. of jnt (Ruler) (radians)	d @ top of leg (Ruler) (mm)	Rot. of jnt (laser) (radians)	d @ top of leg (Laser) (mm)
0	0	0	0	0
25	0.00244	5.4	0.00187	4.2
-25	-0.00195	-4.3	-0.0015	-3.3
25	0.00244	5.4	0.00187	4.2
-25	-0.00195	-4.3	-0.0015	-3.3
25	0.00244	5.4	0.00187	4.2
-25	-0.00195	-4.3	-0.00175	-3.9
50	0.00537	11.9	0.00425	9.5
-50	-0.00439	-9.8	-0.00325	-7.2
50	0.00537	11.9	0.0045	10.0
-50	-0.00439	-9.8	-0.00375	-8.3
50	0.00537	11.9	0.0045	10.0
-50	-0.00439	-9.8	-0.00375	-8.3
75	0.00732	16.3	0.00612	13.6
-75	-0.00537	-11.9	-0.00462	-10.3
75	0.00732	16.3	0.00612	13.6
-75	-0.00585	-13.0	-0.005	-11.1
75	0.00732	16.3	0.0065	14.5
-75	-0.00634	-14.1	-0.00537	-11.9
94	0.00878	19.5	0.00762	17.0
-101	-0.00781	-17.4	-0.00662	-14.7
91	0.00878	19.5	0.00762	17.0
-100	-0.00732	-16.3	-0.00662	-14.7
74	0.00829	18.4	0.00737	16.4
-100	-0.00732	-16.3	-0.00662	-14.7
118	0.01073	23.9	0.00962	21.4
-117	-0.00829	-18.4	-0.00737	-16.4
104	0.01024	22.8	0.00912	20.3
-111	-0.00829	-18.4	-0.00737	-16.4
101	0.01024	22.8	0.00912	20.3
-108	-0.00829	-18.4	-0.00737	-16.4
107	0.01122	25.0	0.01	22.3
-119	-0.00878	-19.5	-0.00775	-17.2
106	0.01122	25.0	0.01	22.3
-114	-0.00878	-19.5	-0.00775	-17.2
105	0.01122	25.0	0.01	22.3
-107	-0.00829	-18.4	-0.00775	-17.2
123	0.01268	28.2	0.01162	25.9
-118	-0.00878	-19.5	-0.00825	-18.4

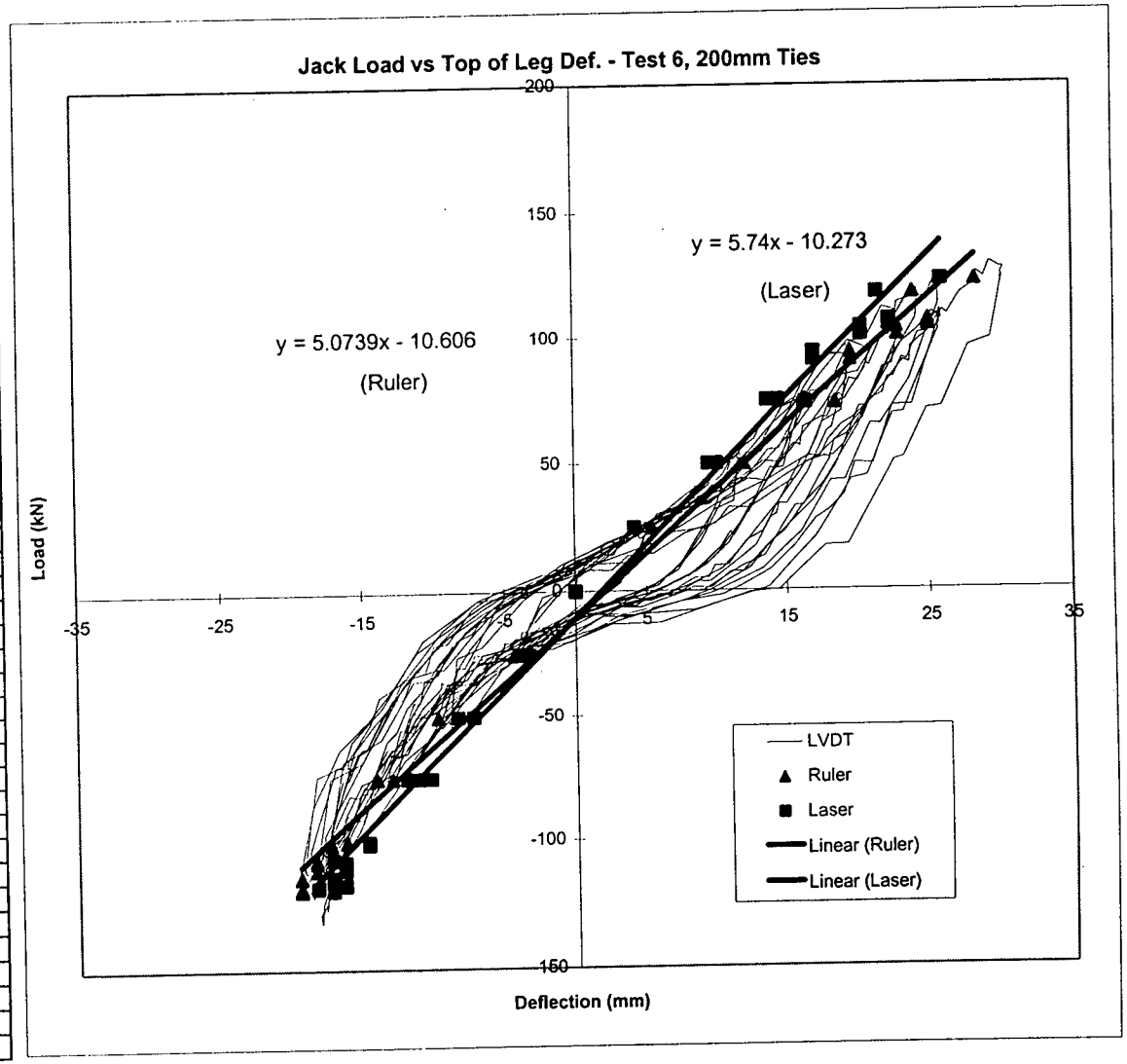

deflection shape of the leg will not be correct. Since the ruler measurements were taken during the loading stage, the line fitted to the ruler measurements will be accurate for loading, but inaccurate for unloading. Therefore the loading part of the leg load deflection diagram will be accurate but the unloading part will not. The result of the error is that the unloading part of the leg load deflection plots for tests one and two are steeper than they should be. This effect can be observed by comparing the load deflection plots of the first and second tests to the load deflection plots of the third to sixth tests, see Figure I-5 of Appendix I to compare test 2 to tests 3 to 6.

Since it was clear that the top of leg deflection results obtained from the LVDT at the top of the leg were the most accurate, they were used to calculate the bottom of leg deflections for specimens 3 to 6. The top of leg deflection equations obtained from the ruler and laser data points were not used for specimens 3 to 6 but are shown in Figures 6 to 9 for comparison purposes.

6.3 Plotting of load vs. leg deflection graphs

6.3.1 Method of plotting of load vs. leg deflection graphs

As explained above, in order to obtain the leg deflection it was necessary to subtract the following quantities from the deflection value recorded by the jack:

1. Deflection resulting from lateral movement of the joint.
2. Deflection resulting from rotation of the joint.

The magnitude of the sum of the above quantities was calculated as follows:

- The distance from the center of the hinge to the top of the leg, L_{joint}, was constant for all of the tests (2225 mm).
- The distance from the center of the hinge to the point of force application at the bottom of the leg, L_{jack}, was constant for all of the tests (5125 mm).
- The top of leg deflection calculated as described in section 6.2 above was multiplied by the ratio L_{jack}/L_{joint} to obtain dsys, the "system" displacement at the bottom of the leg i.e. displacement resulting from lateral movement of the joint, d_{joint}, as well as from rotation of the joint, d_{rot}.

The quantities used in this calculation are illustrated in Figure 10.

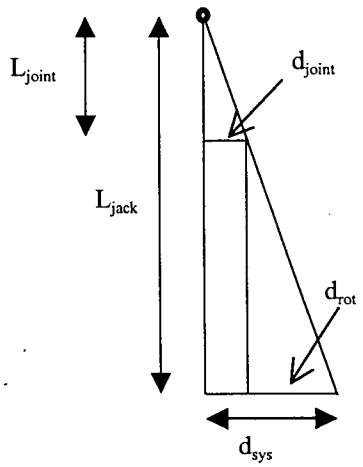

FIGURE 10 - LEG DISPLACEMENT DIAGRAM.

It is clear from Figure 10 that the total displacement at the bottom of the joint, d_{sys}, resulting from non leg deformations, is equal to d_{joint} plus d_{rot}. The calculation of d_{sys} was done in excel and subtracted from the deflection recorded by the jack to obtain the leg deflection. Thus it was possible to plot load vs. leg deflection graphs.

6.3.2 Load deflection graph for test #1, first 200 mm specimen

As explained in chapter 5, a number of problems were experienced during test # 1, the first 200 mm specimen. The results of test #1 are not considered in the analyses done in chapter 7. The load vs. LEG deflection plot for test #1 is shown in Figure 11.

6.3.3 Load deflection graphs for test #'s 2-6

The load vs. LEG deflection plots for test #'s 2-6 are shown in Figure 12 as well as in Figure I-5 of Appendix I. These plots are analyzed and interpreted in chapter 7.

6.4 Interpretation of stain readings taken during testing

6.4.1 Effectiveness of strain measuring method

Concrete strains were measured in the hinge region of the legs and in the beams of the specimens. The method by which the LVDT's and dial gauges were attached to the specimens was explained in section 4.4.2. The strain readings obtained at low loads, before significant cracking had occurred, appeared to be reasonably good. However once severe flexural cracks had developed this method of recording strains proved to be ineffective. The flexural cracks had a tendency to pass through the holes into which the inserts had been placed. It is possible that the drilling which was done to create the insert holes caused microcracking of the concrete around the holes resulting in an area of damaged concrete which "attracted"

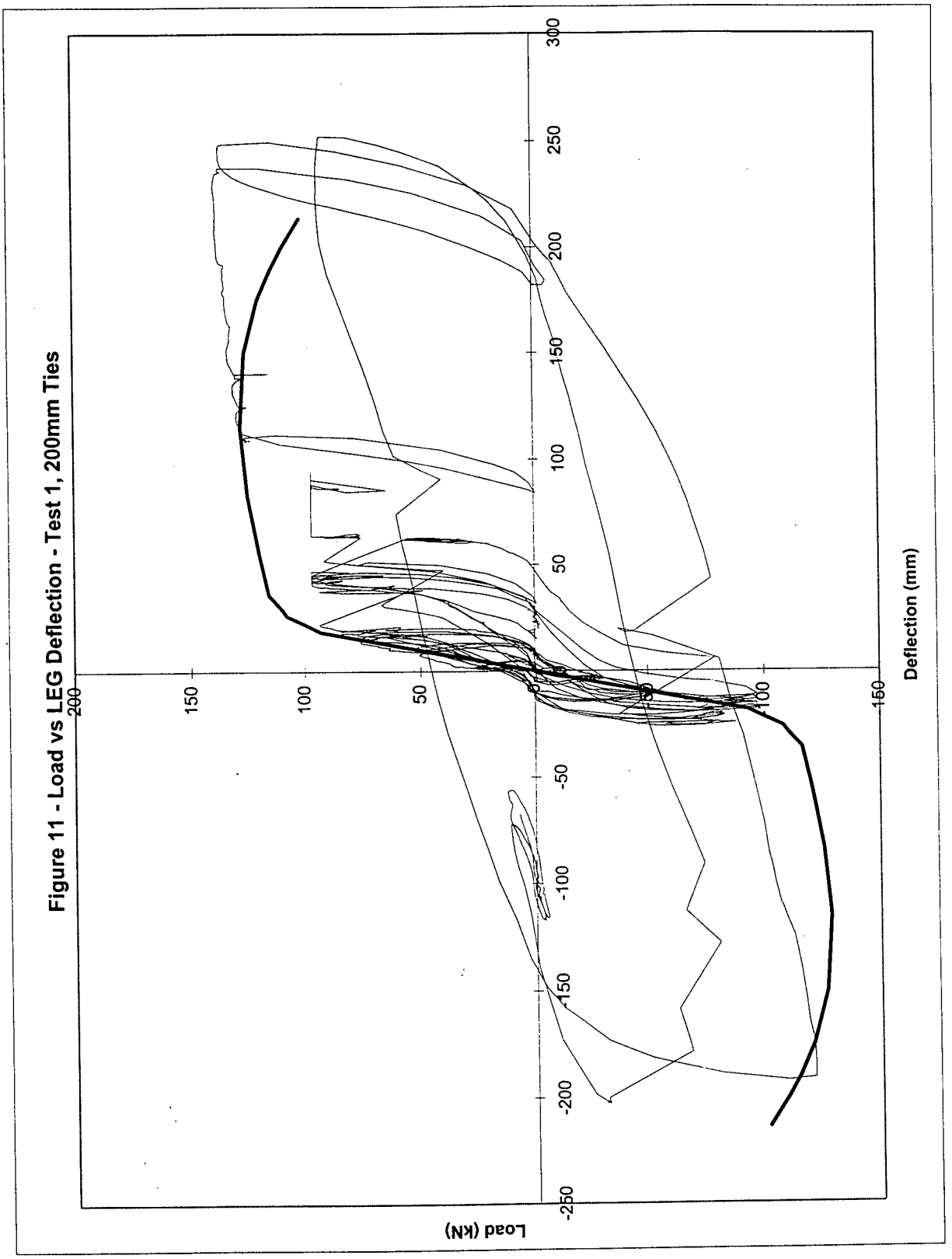
Figure 11 - Load vs LEG Deflection - Test 1, 200mm Ties
Load (kN)
Deflection (mm)
200
150
100
50
-50
-100
-150
-200
-250
300
250
200
150
100
50
-50
-100
-150

Figure 12 - Load vs. Leg Deflection - Tests 2 - 6

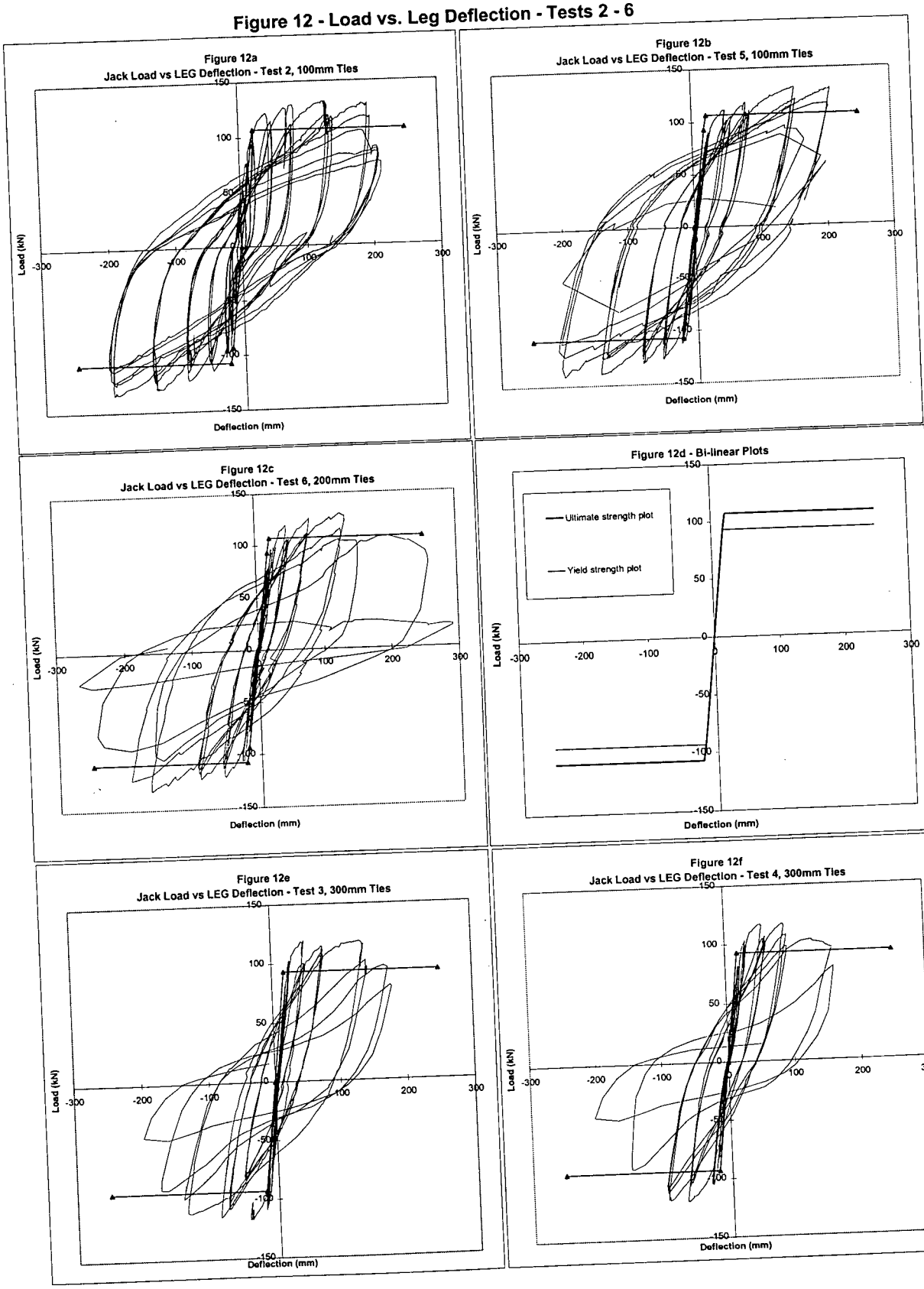

flexural cracks. The result of the cracks passing through the holes was that the inserts became loose. Since the gauge length for the strain readings was typically only 400 mm, even a small amount of movement would ruin the results.

6.4.2 Hinge zone strain readings

Since there was severe cracking in the hinge zone, the problems with the strain measuring system described in section 6.4.1 above were particularly severe. The results were in fact so erratic that they have not been presented.

6.4.3 Beam strain readings

Since there was a lesser degree of flexural cracking in the beam, the results of the beam strain measurements were reasonably good. The strains measured on the top and bottom of the beam were used to obtain curvature values which were used to plot a moment curvature plot for the beam. The process by which the readings from the LVDT's at the top and bottom of the beam were translated into a moment curvature plot was as follows:

1. Displacement values were recorded by the LVDT's at either 2 or 5 second intervals.
2. The zero load displacements measured by the LVDT's at the beginning of the test were subtracted from the LVDT displacements at each recorded load to give displacements relative to zero load.
3. The displacements were divided by the gauge length, typically 400 mm, to give strain values.
4. The differences between the strains at the top and bottom of the beam were divided by the distance between the LVDT's at the top and bottom of the beam. The resulting value was the curvature of the beam at the given load.
5. Using the corresponding load recorded by the jack, the roller reaction was found by summing moments about the hinge of the test set-up, see Figure I-2 of Appendix I. This was possible since the test setup was statically determinate. The moment associated with the curvature calculated in step 4 above, was assumed to be equal to the roller reaction multiplied by the distance from the roller to the center of the gauge length of the LVDT's at the top and bottom of the beam.
6. The moment curvature graph was plotted using the curvature values from step 4 and moment values from step 5.

Beam strains were recorded using LVDT's in tests one and six. However, it seems that one of the LVDT's recording the beam strain readings in test number one was faulty and therefore the results were discarded. The beam strain readings from test number six were well recorded and the resulting moment curvature plot is shown in Figure 13.

Figure 13 - Beam Moment Curvature -Test 6, 200mm Ties

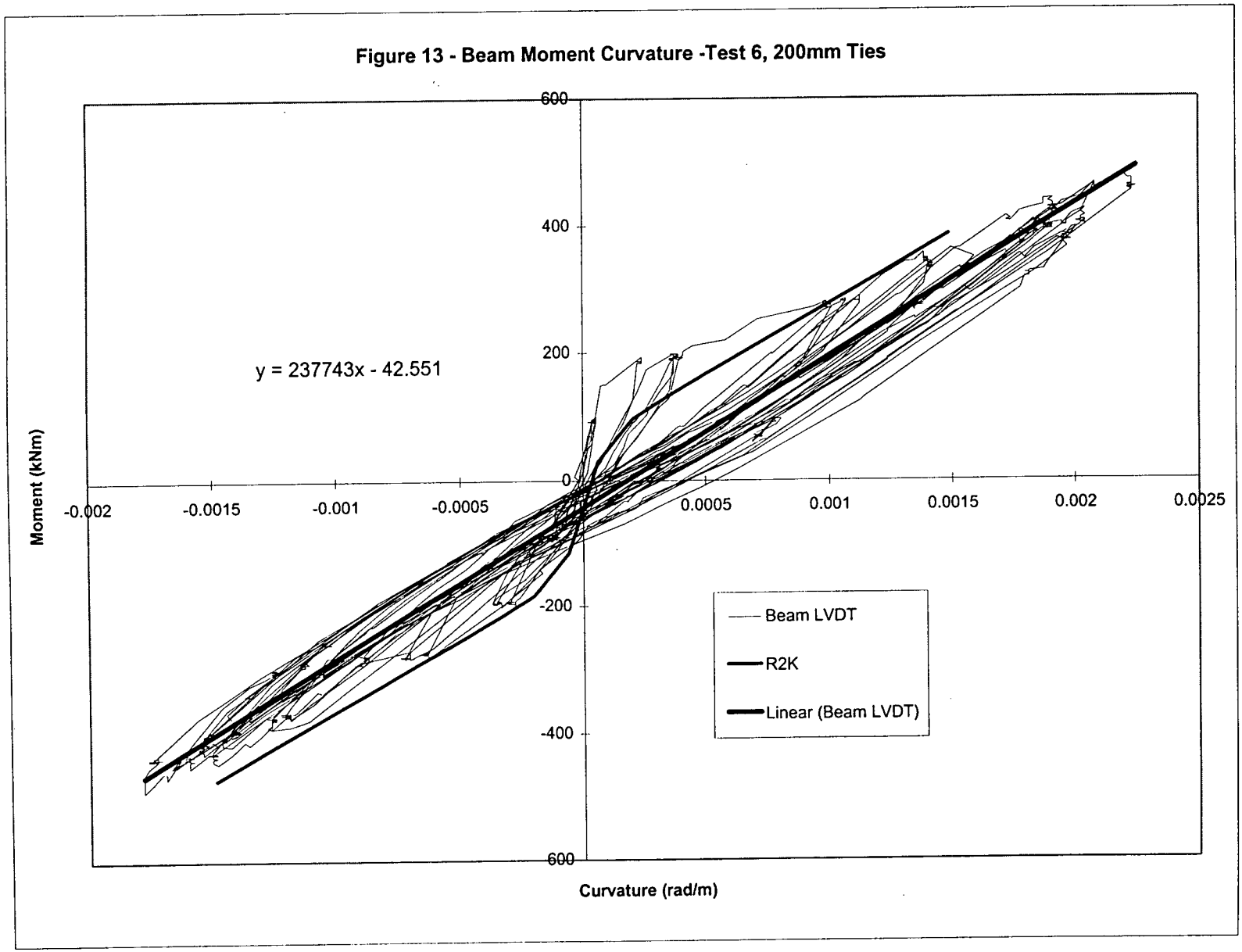

The plot in Figure 13 also contains the response of the beam section predicted using Response 2000[22]. The gradient of the post cracking prediction of Response 2000[22] agrees well with the line fitted through the moment curvature values recorded from the beam during test 6.

From the gradient of the beam moment curvature plot the beam stiffness could be estimated. It was fortunate that the beam moment curvature plot could be generated because the elastic stiffness obtained from this plot was used in the elastic analysis to determine the yield displacement of the frame. This is explained further in chapter 7.

7 INTERPRETATION AND ANALYSIS OF TEST RESULTS

7.1 Plan of presentation for result analysis

As explained in chapter 5 a number of problems were experienced during test #1, the first 200 mm specimen. Therefore the results of that specimen have not been considered in the interpretation and analysis of test results done in this chapter.

In chapter 6 the load vs. leg displacement plots for each of the tests were developed and these plots are shown in chapter 6 and in Figure I-5 of Appendix I. There is information shown on the force displacement plots of Figure I-5 of Appendix I which was not mentioned in chapter 6: the bi-linear plots and the yield points. The calculation of the yield points is explained in section 7.3. and the generation of the bi-linear plots is explained in section 7.4. The calculation of displacement ductility and the corresponding force reduction factors is done in section 7.5.

7.2 Comments on observed test behavior

The load displacement plots from each of the two 100 mm specimens, fig I-5a and I-5b in Appendix I, are similar. Even though the modes of failure were different, failure occurred at similar loads and displacements and this accounts for the similarity of the load displacement hysteresis plots. The load displacement plots from each of the two 300 mm specimens, fig I-5e and I-5f, also appear similar. This is not surprising given that the modes of failure were the same. Although buckling occurred during different load sequences for each of the two 300 mm tie spacing specimens, it occurred only one load cycle apart and therefore the behavior can be assumed to be consistent. Given the consistency of performance of the 300 mm specimens, it is assumed that the 200 mm spacing load deflection plot, Figure I-5c of Appendix I, is representative of 200 mm spacing performance even though only one test result is available.

7.3 Determination of yield point of leg

The load vs. leg deflection plots in Figure I-5 of Appendix I contain small triangular markers which indicate the yield point of the legs.

Since the legs have a significant quantity of distributed reinforcement, see Figure I-3 of Appendix I, the force displacement curve is rounded in the yielding region and does not have a well defined yield point. Therefore, in order to estimate the yield load, the following method which involved the use of a layered analysis to determine the yield moment, was used:

- Tests indicated the steel to have a yield strength of 453 MPa, see chapter 4.
- It was assumed that the strain at a depth of 740 mm was 453/200 000 = 0.002265.
- The top strain was varied until an axial load equal to zero was obtained.
- The corresponding moment (271 kNm) was assumed to be the yield moment.
- Assuming a lever arm of 2.9 m, see Figure I-2 of Appendix I, a yield force of 93 kN was calculated.

Thus the yield load was found via a theoretical calculation, but using the yield strength obtained from tests done on reinforcement taken from the test specimens.

The following method was used to obtain the yield displacement:
The average displacement at approximately 75% of the yield load (70 kN) was found considering the loads and displacements for both directions from all of the tests. In other words, the absolute values of the displacements at 70 kN and at -70 kN for each test specimen were obtained from the test data. The yield displacement was assumed to be equal to 93/70 times the average displacement at 70 kN. As shown in Table 8, the average displacement at 70 kN was found to be 13.8 mm which resulted in a predicted yield displacement of 18.3 mm.

TABLE 8 - ESTIMATION OF YIELD DISPLACEMENT

TEST #	d @ 70 kN (mm)	d @ - 70 kN (mm)	Average (mm)
1	**14**	**-14.3**	**14.2**
2	**10.4**	**-14.7**	**12.6**
3	**17.5**	**-8.1**	**12.8**
4	**16.1**	**-15**	**15.6**
5	**17**	**-8.3**	**12.7**
6	**15.1**	**-14.3**	**14.7**
		Ave. from all tests	**13.8**
		Predicted yield disp.	**18.3**

The yield point was assumed to be at a load of 93 kN and a displacement of 18.3 mm. The yield points were assumed to be the same for each of the test specimens and are shown as triangular markers on the load vs. leg deflection plots of Figure I-5 of Appendix I.

7.4 Development of bi-linear plots and method of determination of plastic displacement of legs
The bi -linear plots were constructed to provide a simple representation of the specimen behavior as well as to allow the determination of the plastic displacement of the legs of the test specimens. Plastic

displacement is calculated by subtracting the yield displacement from the ultimate displacement. The determination of the yield displacement (18.3 mm at 93 kN) was explained in section 7.3. The ultimate displacement is defined as the displacement to which a specimen can be deformed while retaining its load carrying capacity. However, it is noticed from the hysteresis loops, Figure I-5 of Appendix I, that with each successive cycle to the same displacement, the load reached is reduced. This is partly a result of the Baushinger effect and partly a result of the decrease in stiffness of the test specimen as cracking increases. There is typically a large decrease in the load attained between the first and second cycles, while the loads obtained in the second and third cycles are fairly similar. In other words, by the third cycle the decrease has somewhat stabilized.

Load and deflection readings at the peak of each post yielding load cycle in each load sequence were extracted from the test data and are listed in Appendix V. Also contained in Appendix V are plots which show the post yielding cycle peaks. The decrease in load attained with each successive cycle at the same displacement can clearly be seen. It is also clear from the plots that the decrease in load attained stabilizes by the third cycle. Figures 14, 15 and 16 show the absolute values of the load and deflection values for the first, second and third post yielding cycle peaks for the 100 mm, 200 mm and 300 mm test specimens respectively. For the 100 mm and 300 mm specimens, the results for both specimens with the respective tie spacings are plotted.

The ductile range is considered to end when the specimen can no longer maintain a prescribed strength. For a specimen to be considered to be maintaining it's load carrying capacity, it was considered necessary for it to reach the prescribed load capacity on the third cycle of each load sequence. A question arises as to what the prescribed load capacity should be. Referring to Figure 14 for the 100 mm tie spacing specimen, and Figure 15 for the 200 mm tie spacing specimen, it is observed that the third cycle peaks are significantly above the yield load of 93 kN. Furthermore it is likely that in design, the capacity of the leg would be assumed to be larger than the strength corresponding to first yield. Once the lateral forces have been reduced by the appropriate force reduction factor, the longitudinal reinforcement would be designed assuming a maximum compressive strain in the concrete of 0.0035, with a layer analysis. The result would be that the distributed bars, most of which would be yielding, would contribute to the strength and therefore the ultimate moment assumed would be greater than the first yield moment. The calculation of the ultimate strength of the leg of the test specimen is shown in Table 9. It was assumed that there was no tension stiffening as it is unlikely that tension stiffening would be used by a typical engineer when designing the leg of a tilt-up frame panel.

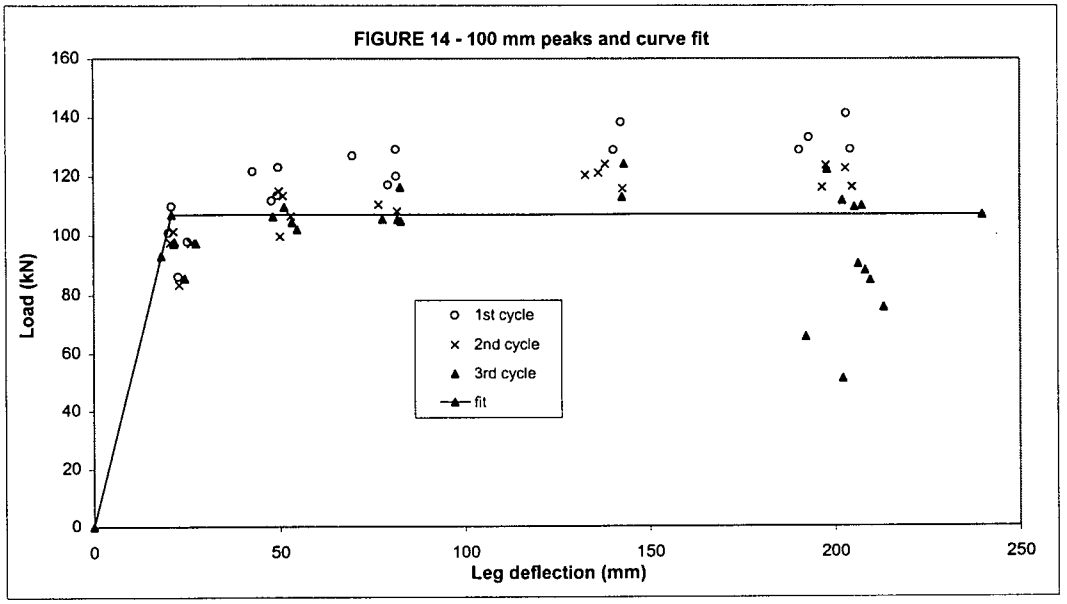
FIGURE 14 - 100 mm peaks and curve fit
Load (kN)
Leg deflection (mm)
1st cycle
2nd cycle
3rd cycle
fit

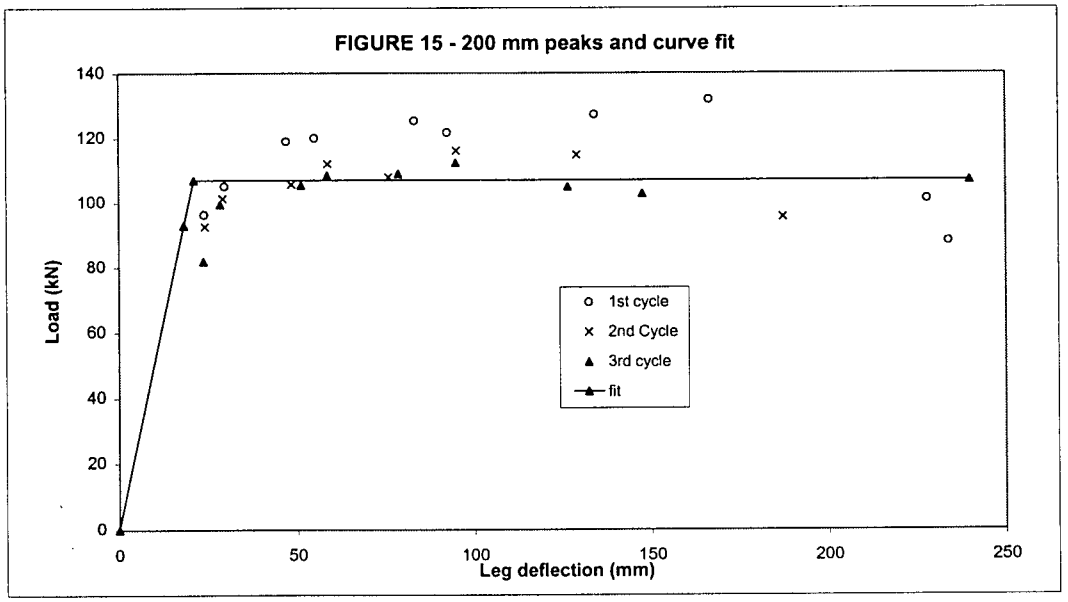
FIGURE 15 - 200 mm peaks and curve fit
Load (kN)
Leg deflection (mm)
1st cycle
2nd Cycle
3rd cycle
fit

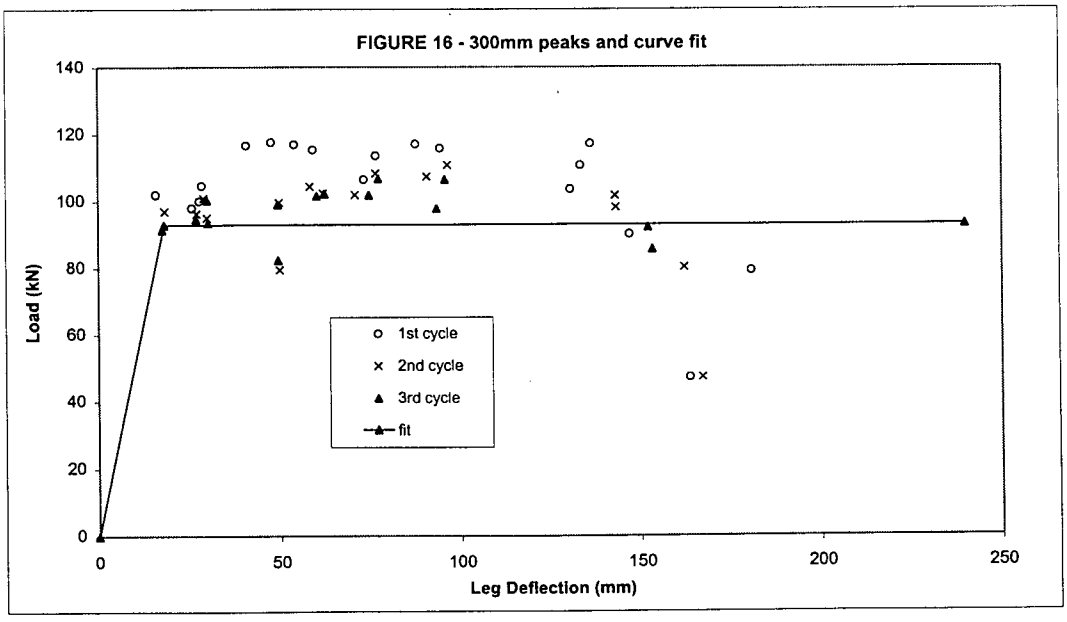
FIGURE 16 - 300mm peaks and curve fit
Load (kN)
Leg Deflection (mm)
1st cycle
2nd cycle
3rd cycle
fit

TABLE 9 - ULTIMATE FLEXURAL CAPACITY OF LEG

ASSUMING BOTTOM 3 LAYERS OF STEEL YIELD:

fc' (MPa)= 30 Ect(MPa) = 30124.7 ult strain = -0.00199

fr (MPa) =	0.00
str@cracking	0
alpha1=	0.7
alpha2=	1

Depth to bot strain (mm)= 740
Width of C flange (mm) = 190
d to bot of flange (mm) = 800
Width of web (mm) = 190
Depth to CA (mm) = 400

Top strain -3.50000E-03
Bot.strain 2.06427E-02
Beta1 0.902342126
Alpha1 0.806718693
c (mm) 107.2788048
phi 3.263E-05

Axial force (N)

conc C	-446699
conc T	0
steel	446702
	3.217E+0

Moments (Nmm)

conc C	157027225
conc T	000.00E+0
steel	155345338
	312372563

Moments (kNm) = 312.37

CONCRETE FORCES

Comp (N) -445.125E+3 (rectangular stress block)

10 LAYERS OF CONCRETE IN COMPRESSION: Shrinkage strain: 0.00E+00

Layer	Depth	strain cf	f (MPa)	d to bot of layer	Area	N (N)	lever (mm)	M (Nmm)
1	5.4	-3.33E-3	-16.6	10.7	2038	-33747	-395	13317890
2	16.1	-3.0E-3	-22.7	21.5	2038	-46245	-384	17753988
3	26.8	-2.6E-3	-27.0	32.2	2038	-54967	-373	20512584
4	37.5	-2.3E-3	-29.4	42.9	2038	-59912	-362	21715220
5	48.3	-1.9E-3	-30.0	53.6	2038	-61080	-352	21483441
6	59.0	-1.6E-3	-28.7	64.4	2038	-58472	-341	19938792
7	69.7	-1.2E-3	-25.6	75.1	2038	-52087	-330	17202817
8	80.5	-875.0E-6	-20.6	85.8	2038	-41926	-320	13397059
9	91.2	-525.0E-6	-13.7	96.6	2038	-27988	-309	8643063
10	101.9	-175.0E-6	-5.0	107.3	2038	-10273	-298	3062373
					20.38E+3	-446.70E+3		157027225

TENSILE FORCES - See C&M P135 for equation &143 for area

zone	d to cent.	strain cf	f (MPa)	Area	N (N)	lever (mm)	M (Nmm)
1	740	0.0206427	0.000	32300	0	340	0
2	520	0.0134651	0.000	43700	0	120	0
3	280	0.0056351	0.000	43700	0	-120	0
4	60	-0.0015425	0.000	32300	0	-340	0
5		-0.0035	0.000	0	0	-400	0
6		-0.0035	0.000	0	0	-400	0
7		-0.0035	0.000	0	0	-400	0
					000.00E+0		000.00E+0

STEEL FORCES

Layer	AREA	fy	Depth	strain from phi	strain sf	MPa	N (N)	lever (mm)	M (Nmm)
1	600	453	740	0.020643	0.020643	453.0	271800	340	92412000
2	400	450	520	0.013465	0.013465	450.0	180000	120	21600000
3	400	450	280	0.005635	0.005635	450.0	180000	-120	-21600000
4	600	453	60	-0.001542	-0.001542	-308.5	-185098	-340	62933338
				-0.003500	-0.003500	0.0	0	-400	0
				-0.003500	-0.003500	0.0	0	-400	0
				-0.003500	-0.003500	0.0	0	-400	0
				-0.003500	-0.003500	0.0	0	-400	0
				-0.003500	-0.003500	0.0	0	-400	0
				-0.003500	-0.003500	0.0	0	-400	0
				-0.003500	-0.003500	0.0	0	-400	0
							4.47E+05		1.55E+08

The ultimate moment was found to be 312 kNm. Using a lever arm of 2.9m the ultimate load is found to be 107 kN. Since this is the strength which would likely be used in the design, it is the strength which the leg would have to maintain while in the ductile range. Furthermore the displacement which corresponds to this load should be used as the "yield displacement" in the displacement ductility calculation. Assuming a linear range with an elastic stiffness based on the calculations of section 7.3, the displacement corresponding to a load of 107 kN was found to be 21.1 mm.

Since the 100 mm and 200 mm tie spacing specimens maintain strengths substantially larger than the first yield strength, it is appropriate to utilize this strength in design and to also use it as the threshold strength which the third cycle peaks must exceed while in the ductile range. Thus for the 100 mm and 200 mm tie spacing specimens the bi-linear curve consisted firstly of a line from the origin to the point defined by a load of 107 kN and displacement of 21.1 mm and secondly of a horizontal line starting from this point and extending in the direction of increasing displacements. The ultimate displacement will be assumed to be where a line connecting the third cycle peaks crosses the horizontal portion of the bi-linear plot. Thus the ultimate displacements for the 100 mm (see Figure 14) and 200 mm (see Figure 15) tie spacings were taken as 200 mm and 130 mm respectively.

Referring to Figure 16 it is observed that the third cycle peaks for the 300 mm specimens generally do not reach the ultimate strength of 107 kN. If 107 kN was taken to be the threshold strength, the 300 mm specimens would have no ductility at all. Thus it seems that the full ultimate strength cannot be attained with a tie spacing of 300 mm. Therefore the design strength should be assumed to be the first yield strength for sections with ties at 300 mm while an ultimate strength based on a compressive concrete strain of 0.0035 can be used when ties are spaced at 100 mm or 200 mm. This idea of having different design strengths is similar to the method used in a number of steel design codes in which, depending on the class of section, different design assumptions are used.

For the 300 mm tie spacings the bi-linear curve consisted firstly of a line from the origin to the point defined by a load of 93 kN and displacement of 18.3 mm and secondly of a horizontal line starting from this point and extending in the direction of increasing displacement. An ultimate displacement of 140 mm was obtained from Figure 16. To obtain the plastic displacement of the legs, the yield displacement was subtracted from the ultimate displacement.

7.5 Calculation of displacement ductility and corresponding force reduction factors

7.5.1 Displacement ductility defined

Displacement ductility, μ_d, is defined as follows:

$$\mu_{displacement} = \frac{d_{max}}{d_{yield}} \qquad \text{(Equation 7.5.1.1)}$$

Therefore to calculate displacement ductility, the yield displacement of the frame and the ultimate displacement of the frame are required:

7.5.2 Determination of yield displacement of frame

A linear elastic analysis of the frame shown in Figure I-1a of Appendix I was done using a basic structural analysis computer program. In order to run the program stiffness' for the frame members were required. Using the leg yield displacement and corresponding yield load found in section 7.3, the elastic stiffness of the leg of the frame was estimated, using equation 7.5.2.1, to be 41.3 x 10^6 N.m^2 .

$$d = \frac{PL^3}{3EI} \qquad \text{(Equation 7.5.1.1)}$$

The elastic stiffness of the beam was obtained from the moment curvature plot generated from the beam strain readings electronically recorded during the testing, and was calculated to be 237.7 x 10^6 N.m^2 (see Figure 13). Using the above mentioned stiffness' for the leg and the beam in the computer analysis, the frame yield displacement was calculated to be 33 mm. The full frame analysis at first yield is contained in Appendix II. The loads used and the corresponding bending moment diagram are also shown on Figure I-1b of Appendix I. Note that the moments in the top of the legs are, on average, approximately equal to the leg first yield moment of 271 kNm. Thus the frame displacement obtained from this analysis was the frame first yield displacement and was used as the yield displacement in the displacement ductility calculation for the 300 mm tie spacing calculation. A second analysis, contained in Appendix VII was done in which the loads were increased until the moments in the tops of the legs were equal to the ultimate moment of 312 kNm, see Table 9. The frame displacement obtained from this analysis was the ultimate moment displacement and was used in the displacement ductility calculation for the 100 mm and 200 mm tie spacings.

Apart from the hinge action which spread into the joint regions, there was relatively little cracking and therefore relatively little joint deformation in the tests. Therefore the joints were modeled using infinitely rigid short frame members for the computer analyses.

7.5.3 Determination of ultimate displacement of frame

It is assumed that after yielding begins in the leg, all subsequent displacement is a result of plastic rotation of the hinge i.e. assume the plastic displacement of the frame equals the plastic displacement of leg.

Therefore the ultimate displacement of the frame is assumed to equal the yield displacement of the frame (from the computer analysis) plus the plastic displacement of the leg.

Since the plastic displacement of the leg can be obtained from the leg load deflection plots, the ultimate displacement of the frame, and therefore the displacement ductility, can now be calculated.

7.5.4 Calculation of μ_d and corresponding force reduction factors, R

The natural period of vibration of buildings using tilt-up wall panels as the lateral load resistance system would be in the order of 0.2 seconds i.e. typically two storey buildings. Therefore the natural period of vibration would be less than the peak spectral period which is approximately 0.5 seconds. Therefore the equal displacement principle is not applicable and the equal energy rule should be applied. The following relationship between displacement ductility, μ_d, and the force reduction factor, R, is obtained when the equal energy rule is applied:

$$R = \sqrt{2\mu_{displacement} - 1} \qquad \text{(Equation 7.5.4.1)}$$

The calculation of the displacement ductilites and corresponding force reduction factors is shown below in Table 10.

Table 10 – Calculation of ductilities and force reduction factors

Hinge zone tie spacing:	100 mm	200 mm	300 mm
Leg ultimate displacement (mm).	200	130	140
Plastic displacement (mm)[(a)]	179	109	122
Frame yield displacement (mm)	38	38	33
Frame ultimate displacement (mm)[(b)]	217	147	155
μ_d[(c)]	5.7	3.9	4.7
R[(d)]	3.3	2.6	2.9

(a) Subtract leg yield displacement (18 mm for 300 mm spacing and 21 mm for 100 mm and 200 mm spacings) from maximum leg displacement.

(b) Frame yield displacement plus plastic displacement.

(c) Displacement ductility, calculated using equation 7.5.1.1.

(d) Force reduction factor, calculated using equation 7.5.4.1.

The relative magnitudes of the displacement ductilities and the force reduction factors are discussed in chapter 8.

8 CONCLUSIONS AND RECOMMENDATIONS

8.1 Mode of failure

The results of the tests done on the six tilt-up frame panels tested indicated that flexural hinges will form in the top of the first storey legs before failure of the panel takes place. The hinge region was found to be approximately equal to the depth of the leg. It was further found that hinging extends up into the joint region. Although there was significant cracking in the joint region and in the ends of the beams at failure, yielding of the beam steel did not appear to have occurred when failure of the leg took place. Diagonal shear cracks did form in both the legs and beams of the test specimens, but in no case did shear failure occur. Shear cracking was more severe in the specimens with larger tie spacings. The 100 mm specimens indicated that tie spacing can effect the mode of ultimate failure. In each of the 100 mm specimens the ties held the core together very effectively, the result being that failure occurred via either longitudinal beam steel pullout or local buckling of the entire reinforcement cage.

8.2 Effect of tie spacing on ultimate strength attained

As explained in section 7.4, in order for a specimen to be considered to have attained a particular strength, it is necessary for it to obtain that strength even on the third cycle of a given load sequence. Two maximum strengths were considered; ultimate strength of 312 kNm (force of 107 kN) and first yielding strength of 271 kNm (force of 93 kN). It is evident from figures 14 and 15 that the 100 mm and 200 mm tie spacing specimens both attained and maintained the ultimate load of 107 kN. The 300 mm specimen however did not attain the ultimate strength of 107 kN. It is therefore concluded that in design, if the tie spacing is small, less than 200 mm, then it is appropriate to calculate the leg flexural strength assuming a maximum compressive concrete strain of 0.0035 and account for the resistance offered by the distributed bars which are likely also yielding. However if the tie spacing is large, greater than 200 mm, then the ultimate strength should be considered to be equal to the strength at first yielding of the bottom reinforcement. This type of approach is commonly used in steel design i.e. the design assumptions are dependent on the class of section.

8.3 Effect of tie spacing on ductility and buckling of longitudinal reinforcement

Hinge zone tie spacing determines the mode of failure and has a significant effect on panel ductility. Table 10 indicates that larger ductilities can be expected from a 300 mm tie spacing than from a 200 mm spacing. This does not mean that the performance of the 300 mm spacing specimens was better than that of the 200 mm spacing specimens, in fact the opposite is true. A higher threshold load was used to calculate the ductility for the 200 mm specimens i.e. the end of the ductile range for the 200 mm specimens was assumed to occur when the load dropped below 107 kN, while the end of the ductile range for the 300 mm specimens was assumed to occur when the load dropped below 93 kN.

The ductilities calculated in table 10 for the 100 mm (5.7) and 200 mm (3.9) tie spacings can be directly compared because they were calculated using the same assumptions. From this comparison it is clear that decreasing the tie spacing from 200 mm to 100 mm had a significant positive effect on ductility.

A force reduction factor of 2 is currently prescribed in CSA A23.3[1] for the design of tilt-up panels. The testing done in this research indicates that this force reduction factor is appropriate for tie spacings up to 200 mm even if the full ultimate strength is assumed to be the strength retained during the ductile range. However, if the tie spacing is greater than 200 mm, a force reduction factor of 2 would be unconservative unless the maximum strength is assumed to be equal to the strength at first yielding of the longitudinal steel.

Previous research[9,10,11] has found that, depending on the tie stiffness, buckling can occur over multiple tie spacings. Scribner and Wight[9] suggested that ties as large as the longitudinal steel may be required to prevent buckling over multiple tie spacings. All buckling observed in these tests occurred over single tie spacings. Therefore these tests indicate that ties which are half of the size of the longitudinal bars are adequately stiff to prevent buckling over multiple tie spacings.

Previous researchers[5,6,7,8,1213,14] have observed buckling of flexural reinforcement in a number of different test setups. The S/D ratios recommended where buckling of longitudinal reinforcement is required, range between 5 and 8. The 100 mm tie spacing was sufficiently close to prevent buckling of the longitudinal bars after loss of the cover concrete. For the 100 mm tie spacing specimen which failed via local buckling of the whole hinge zone reinforcement cage, failure was initiated by out of plane buckling of the distribution reinforcement bars and not by buckling of the edge face bars which the rectangular ties were restraining. Therefore these tests indicate that a S/D ratio of 5 is adequate to prevent buckling of the longitudinal bars in compression.

The out of plane buckling failure of the 100 mm tie spacing specimen could be delayed by using cross ties to restrain the distributed reinforcement bars in the hinge region. For the 100 mm tie spacing specimen in which failure resulted from pullout of the bottom longitudinal beam bar, the failure could be delayed by hooking the ends of the bars which pulled out. However, since in the two specimens tested each failure was observed once, it is concluded that if either one of the failure modes is prevented, then failure would simply occur via the other mode at approximately the same time. Therefore if failure is to be significantly delayed, cross ties should be added and the bottom longitudinal beam bars should be hooked.

8.4 Effectiveness of test setup and testing procedure

Apart from the initial problems experienced with the sliding of the supports in test #1, the test setup performed well. Given that the area of hinging extended into the joint region, it is concluded that it was worthwhile to test the full "1/4 frame" panel because it modeled the joint region well. The ability to observe the level of damage in the beam when failure occurred in the leg, and the opportunity to record strain values from the beam also made the testing of the 1/4 frame model worthwhile.

The displacement data recording system worked well, however the strain recording method only worked well while until yielding began. A better means of obtaining strains would be to attach strain gauges to the longitudinal reinforcing steel where site conditions enable this.

8.5 Recommendations

The tests done clearly indicate that the maximum load attained and the ductility depend on the tie spacing. It is therefore recommended that when designing the legs of tilt-up frame panels, the method used to calculate the maximum flexural strength of the legs be dependent on the spacing of the ties in the hinge region. Further testing would be required in order to obtain accurate knowledge of what strength would be appropriate to assume for each tie spacing. Based on these tests the following recommendations are made: If the hinge zone tie spacing is less than 200 mm, the ultimate strength may be calculated assuming a maximum compressive concrete strain of 0.0035 and the resistance offered by the distributed bars, which are likely yielding, should be included. If the tie spacing is greater than 200 mm, the ultimate strength should be considered to be the strength at first yielding of the bottom steel and the resistance offered by the distributed bars, which would not have yet yielded, should be included. Thus in all cases a layer analysis should be done. If the above ultimate strengths, for members with hinge zone tie spacings greater and less than 200 mm respectively, are used as the "elastic strengths" of the tilt-up frame members, the results of this research indicate that it would then be appropriate to use a force reduction factor, R, of two in design.

Since the spalling of cover extended 400 mm up into the joint region and 700 mm down the leg, these tests indicate that "hinge zone tie spacing" should be applied from a distance equal to the member depth below the joint, up to the top of the joint.

BIBLIOGRAPHY:

1. CSA Committee A23.3, *Design of Concrete Structures*, Canadian Standards Association, Rexdale, Canada, 1994
2. *Concrete Design Handbook*, Canadian Portland Cement Association, Ottawa, 1995
3. ACI Committee 318, *Building Code Requirements for Structural Concrete*, American Concrete Institute, Farmington Hills, 1999
4. Agrawal, L Tulin, K. Gerstle (1965), *"Response of doubly reinforced concrete beams to cyclic loading"* Journal of American Concrete Institute, 62-51, P823-834
5. Burns, C. Seiss (1966), *"Plastic hinging in reinforced concrete"* Journal of Structural Engineering, ASCE, vol. 92 # ST5, Oct. P45-64
6. Burns, C. Seiss (1966),*"Repeated and reverse loading in reinforced concrete"* Journal of Structural Engineering, ASCE vol. 92 #ST5, Oct. P65-78
7. Brown, J Jirsa (1971), *"Reinforced concrete beams under load reversals"* Journal of American Concrete Institute, 68-39, P380-390
8. Gosain, R. Brown, J. Jirsa (1977), *"Shear requirements for load reversal in reinforced concrete members"* Journal of Structural Engineering, ASCE, vol. 103 #ST4, July, P1461
9. C. Scribner, J. Wight (1980), *"Strength decay of reinforced concrete beams under load reversal"* Journal of Structural Engineering, ASCE, vol. 106 #ST4, April, P861
10. C. Scribner (1986), *"Reinforcement buckling in reinforced concrete flexural members"* Journal of American Concrete Institute, 83-85, P966-973
11. Papia, G. Russo, G. Zingone (1988), *"Instability of longitudinal bars in RC columns"* Journal of Structural Engineering, ASCE, vol. 112 #2, P445
12. Saatcioglu, G Ozcebe (1989), *"Response of RC columns to simulated seismic loading"* Structural Journal of American Concrete Institute, 86-s1, P3-12
13. Mau, (1990), *"Effect of tie spacing on inelastic buckling of reinforcing bars"* Structural Journal of American Concrete Institute, 87-S69, P671-677
14. Monti, C Nuti (1992), *"Non-linear cyclic behavior of reinforcement bars including buckling"* Journal of Structural Engineering, ASCE, vol. 112 #12, P3268
15. Azizinamini, S. Baum Kuska, P. Brungardt, E. Hatfield (1994), *"Seismic behavior of square high strength concrete columns"* Structural Journal of American Concrete Institute, 91-S33, P336-345
16. Ruiz, G. Winter (1969), *"Reinforced concrete beams under repeated loads"* Journal of Structural Engineering, ASCE vol. 95 #ST6, June, P1189
17. Wight, M. Sozen (1975), *"Strength decay of reinforced concrete columns under shear reversals"* Journal of Structural Engineering, ASCE, vol. 101 #ST5, May, P1053
18. Scott, R. Park, M. Priestley (1982), *"Stress strain behavior of concrete confined by overlapping hoops at low and high strain rates"* Journal of American Concrete Institute, 79-2, P13-27
19. Pantazopoula (1998), *"Detailing for reinforcement stability in RC members"* Journal of Structural Engineering, ASCE, vol. 124 #6, P623-P641
20. Canadian Portland Cement Association, *"Concrete Design Handbook"* 1995, 116 Albert Street, Ottawa, Ontario, Canada
21. Collins and Mitchell, "Prestressed Concrete Basics." 1987, first edition, Canadian Prestressed Concrete Institute, 85 Albert Street, Ottawa, Ontario, Canada
22. Response 2000, layer analysis computer program used to predict the flexural response of reinforced concrete sections. Developed at the University of toronto under the supervision of Professor Michael Collins. A version of the program can be downloaded from *www.ecf.utoronto.ca/~bentz/r2k.htm*

APPENDIX I

FIGURES FREQUENTLY REFERENCED

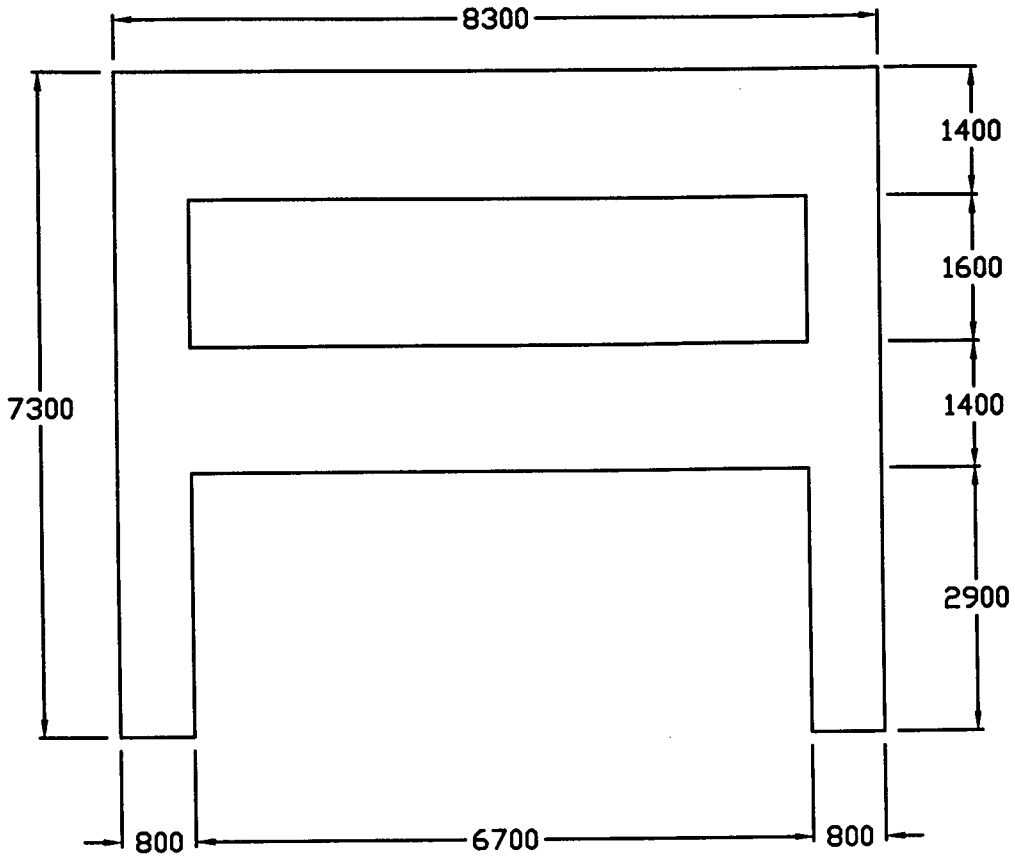

Figure I-1a - Frame Dimensions

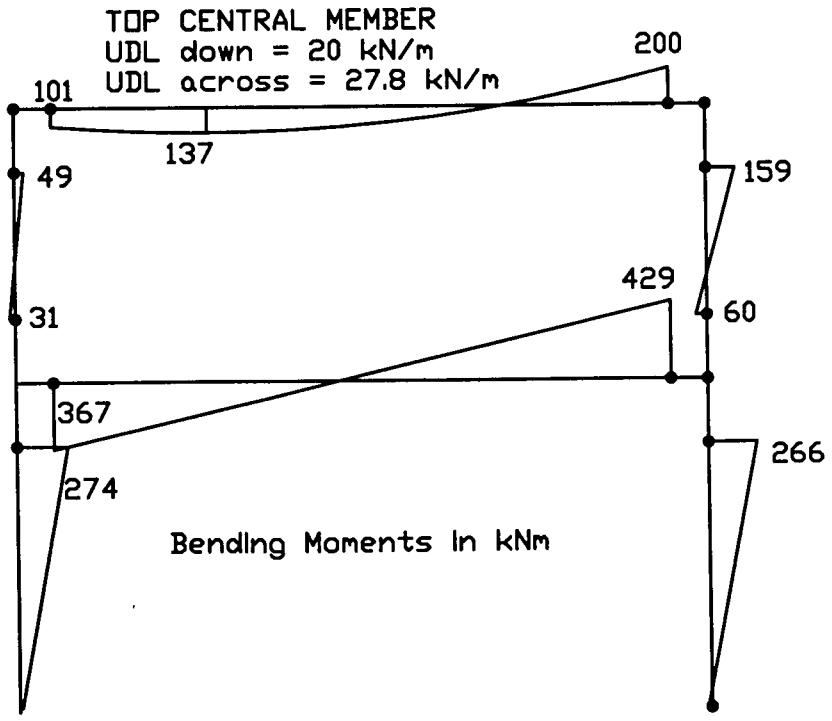

Figure I-1b - Bending Moment Diagram

FIGURE I-1

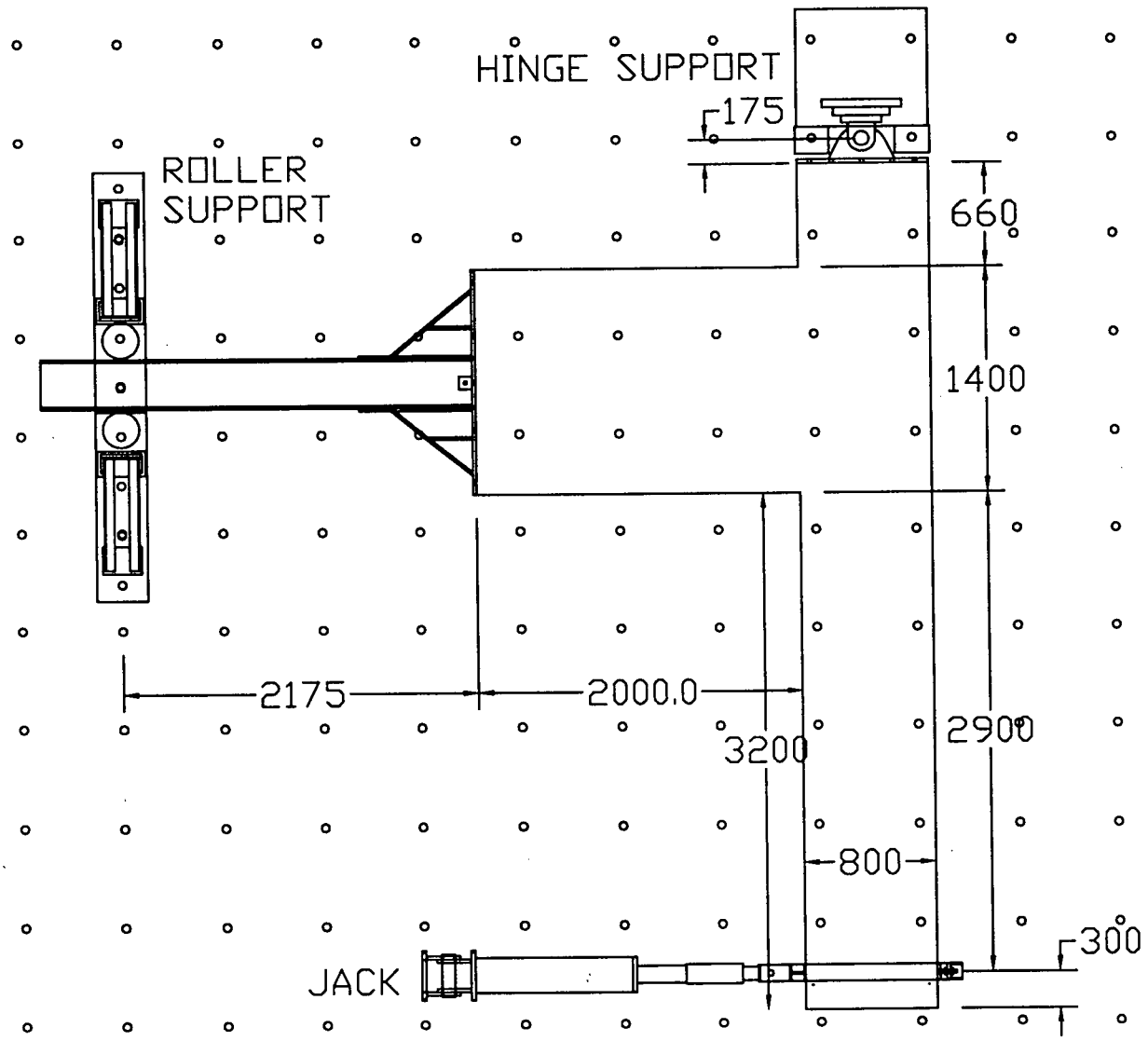

Figure I-2 - Test Setup

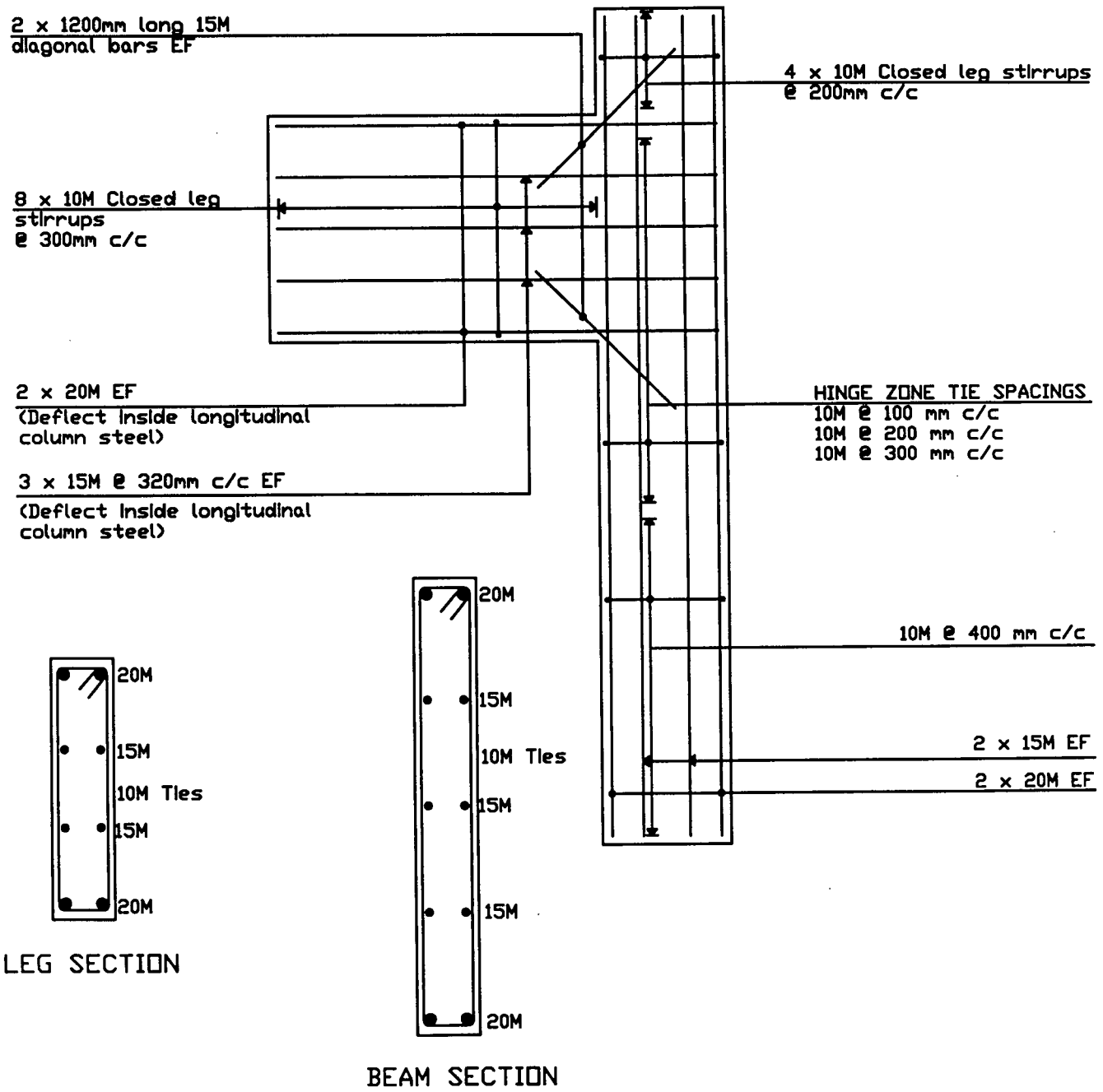

Figure I-3 - Reinforcement Details

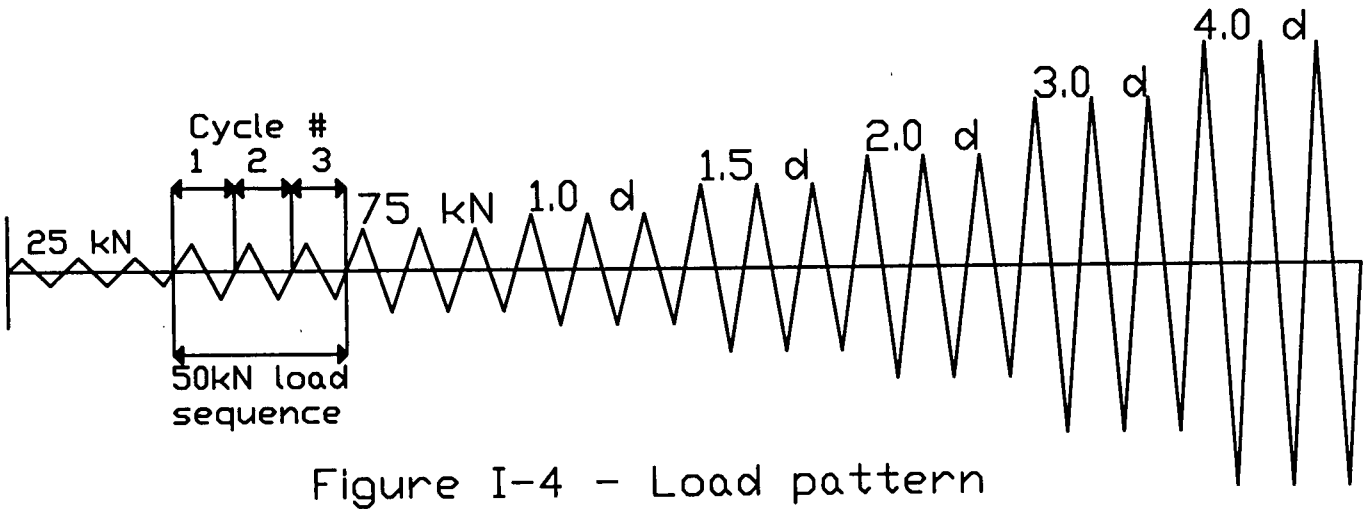

Figure I-4 - Load pattern

Figure I-5 - Load vs. Leg Deflection - Tests 2 - 6

Figure I-5a
Jack Load vs LEG Deflection - Test 2, 100mm Ties

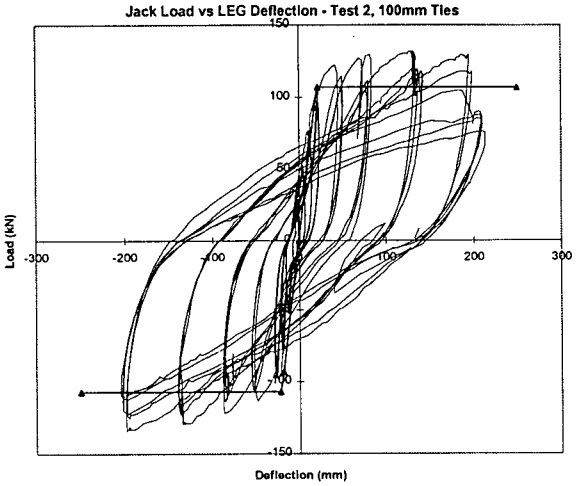

Figure I-5b
Jack Load vs LEG Deflection - Test 5, 100mm Ties

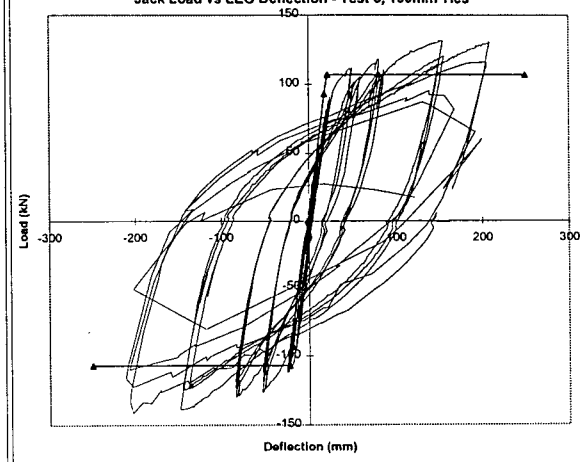

Figure I-5c
Jack Load vs LEG Deflection - Test 6, 200mm Ties

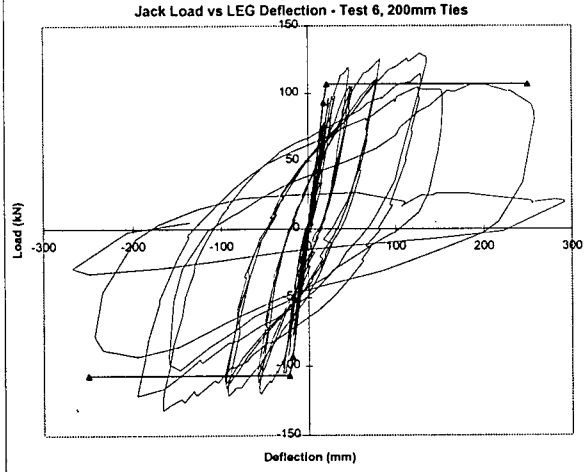

Figure I-5d - Bi-linear Plots

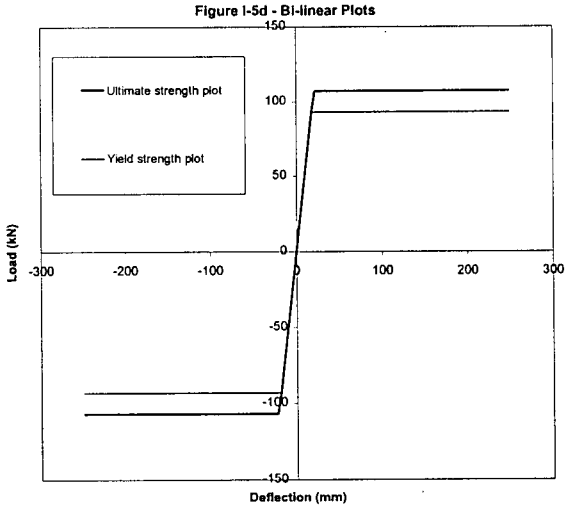

Figure I-5e
Jack Load vs LEG Deflection - Test 3, 300mm Ties

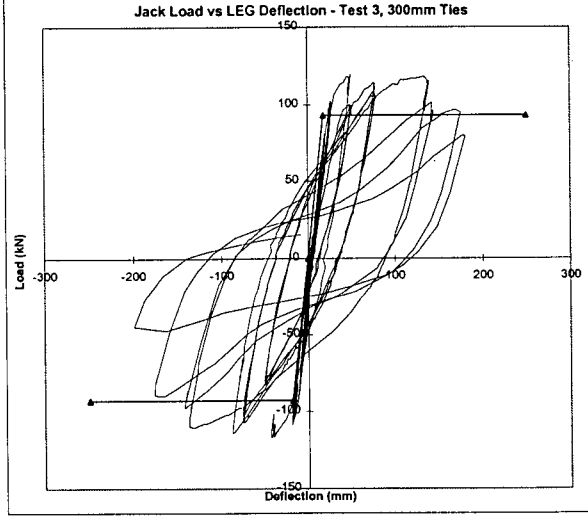

Figure I-5f
Jack Load vs LEG Deflection - Test 4, 300mm Ties

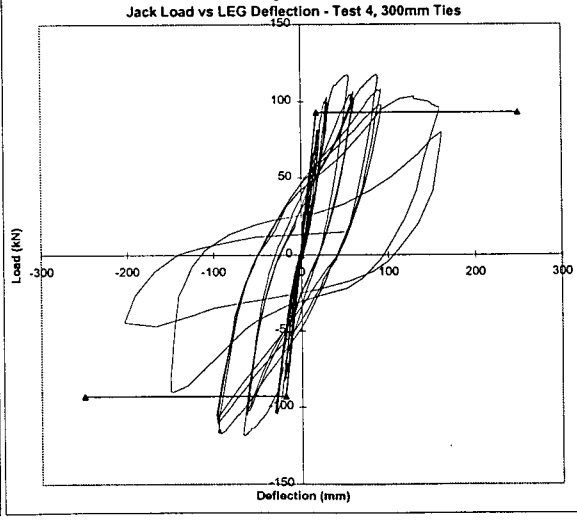

APPENDIX II

FRAME ANALYSIS AT YIELD

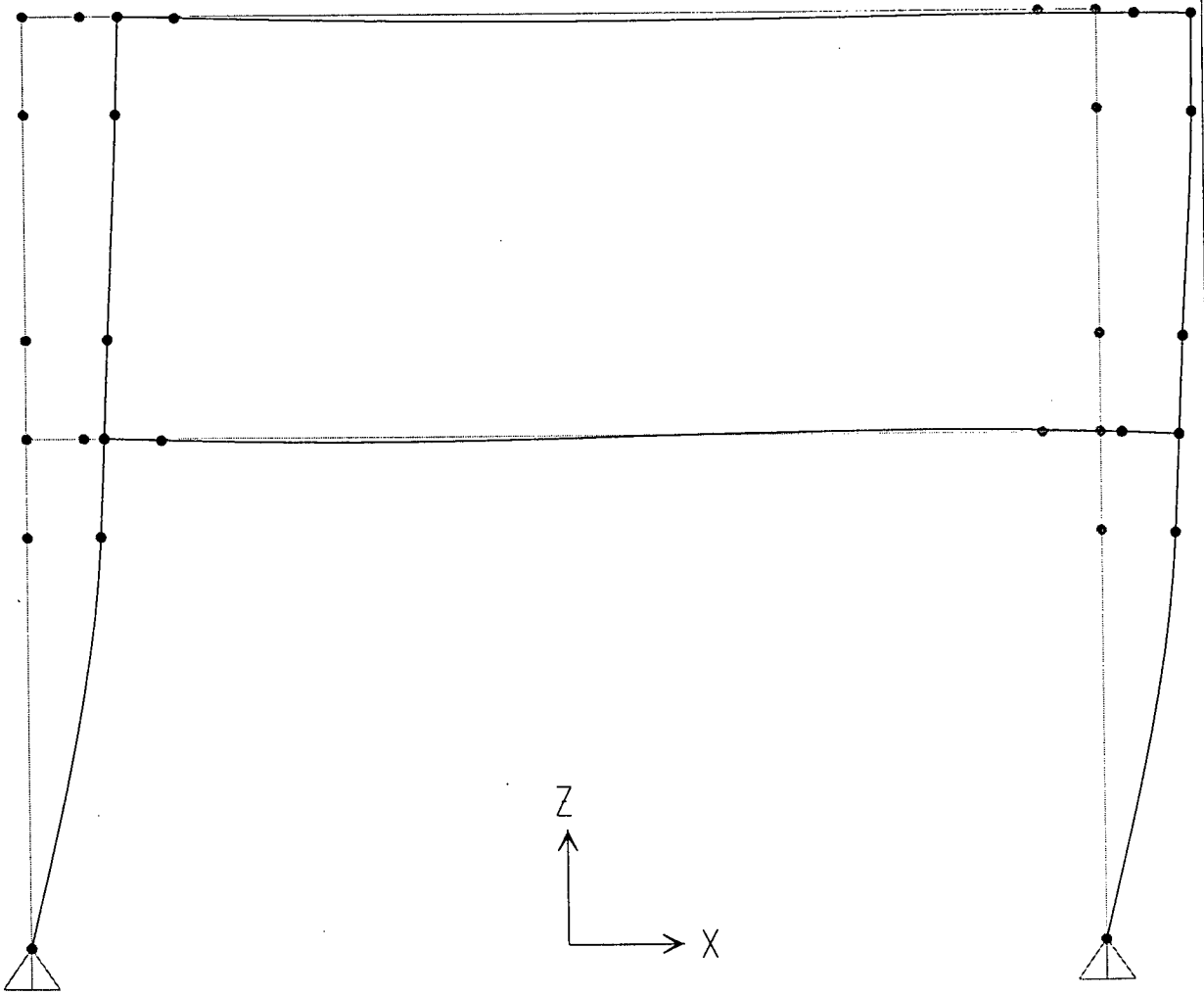
Z
X

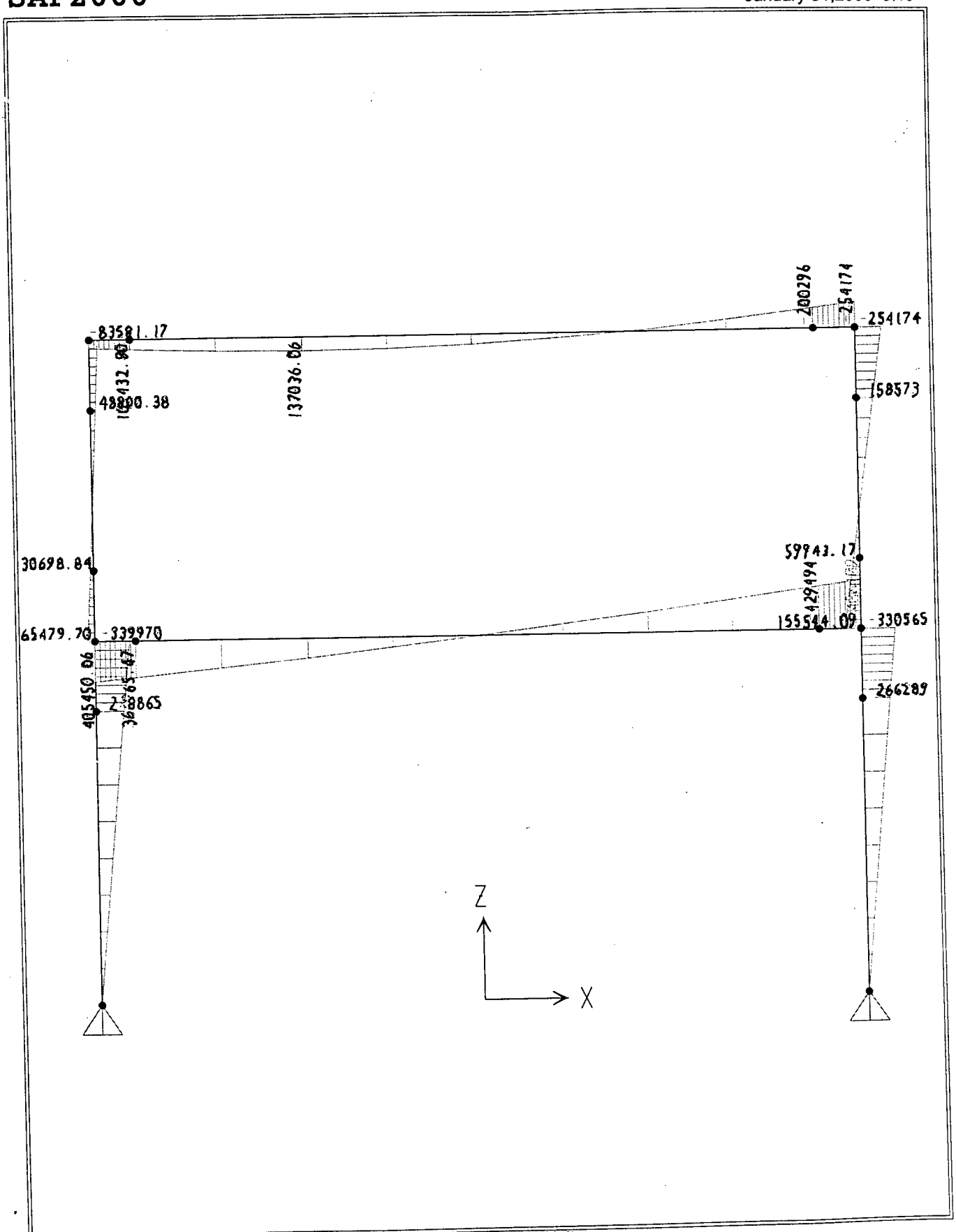
-83581.17
48800.38
137036.06
200296
254174
-254174
158573
30698.84
59743.17
65479.70
-339970
155544.09
-330565
-266289
Z
X

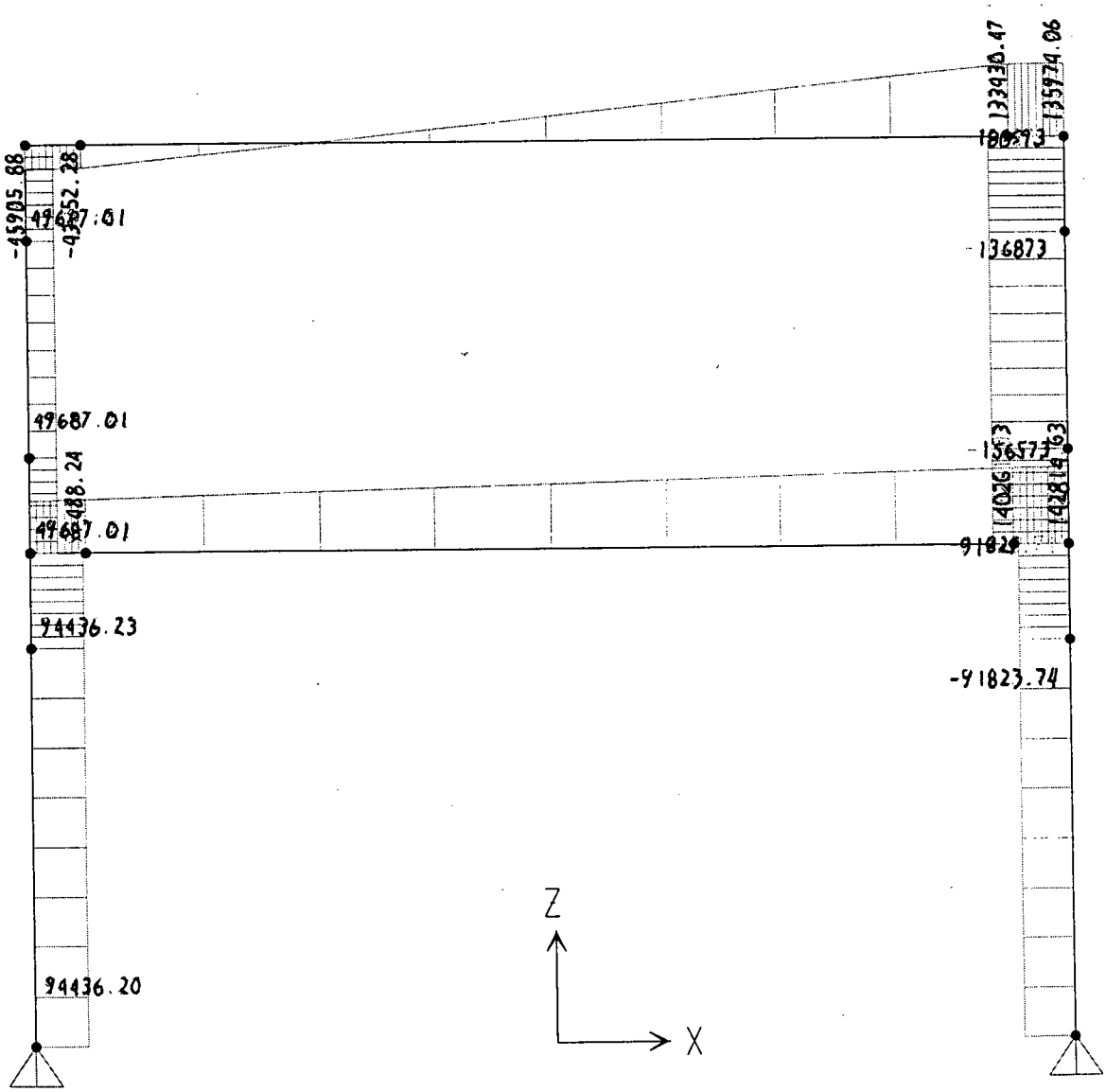
-45905.88
-43552.28
49687.01
49687.01
49687.01
94436.23
94436.20
-136873
-91823.74
Z
X

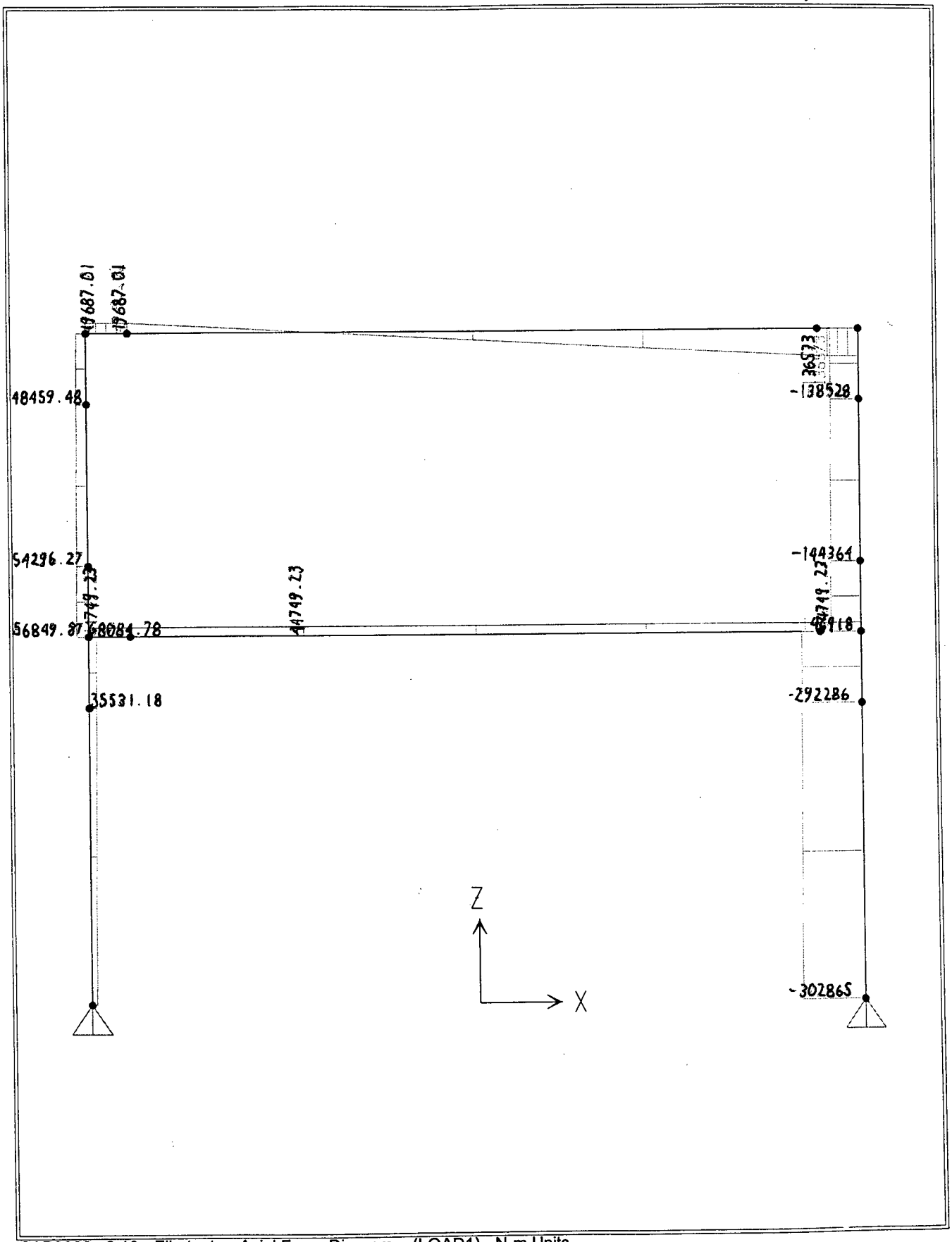
19687.01
19687.01
48459.48
54296.27
44749.23
44749.23
56849.87
68084.78
35531.18
-138528
-144364
-292286
-302865
Z
X

J O I N T D I S P L A C E M E N T S

JOINT	LOAD	UX	UY	UZ	RX	RY	RZ
1	LOAD1	0.0000	0.0000	0.0000	0.0000	0.0117	0.0000
2	LOAD1	0.0257	0.0000	1.132E-04	0.0000	2.092E-03	0.0000
3	LOAD1	0.0271	0.0000	1.140E-04	0.0000	1.959E-03	0.0000
4	LOAD1	0.0285	0.0000	1.127E-04	0.0000	1.980E-03	0.0000
5	LOAD1	0.0321	0.0000	6.660E-06	0.0000	1.630E-03	0.0000
6	LOAD1	0.0332	0.0000	5.574E-06	0.0000	1.601E-03	0.0000
7	LOAD1	0.0332	0.0000	-6.350E-04	0.0000	1.597E-03	0.0000
8	LOAD1	0.0330	0.0000	-1.337E-03	0.0000	2.082E-04	0.0000
9	LOAD1	0.0330	0.0000	-1.419E-03	0.0000	2.187E-04	0.0000
10	LOAD1	0.0328	0.0000	-1.416E-03	0.0000	3.078E-04	0.0000
11	LOAD1	0.0288	0.0000	-1.124E-03	0.0000	2.217E-03	0.0000
12	LOAD1	0.0273	0.0000	-1.120E-03	0.0000	2.171E-03	0.0000
13	LOAD1	0.0257	0.0000	-1.114E-03	0.0000	2.299E-03	0.0000
14	LOAD1	0.0000	0.0000	0.0000	0.0000	0.0116	0.0000
15	LOAD1	0.0271	0.0000	-6.638E-04	0.0000	1.941E-03	0.0000
16	LOAD1	0.0273	0.0000	-2.598E-04	0.0000	2.149E-03	0.0000

F R A M E E L E M E N T F O R C E S

FRAME	LOAD	LOC	P	V2	V3	T	M2	M3
1	LOAD1							
		0.00	24951.98	94436.23	0.00	0.00	0.00	0.00
		1.45	30241.58	94436.23	0.00	0.00	0.00	-136932.50
		2.90	35531.18	94436.23	0.00	0.00	0.00	-273865.00
2	LOAD1							
		0.00	35531.18	94436.23	0.00	0.00	0.00	-273865.00
		3.5E-01	36807.98	94436.23	0.00	0.00	0.00	-306917.69
		7.0E-01	38084.78	94436.23	0.00	0.00	0.00	-339970.34
3	LOAD1							
		0.00	44749.23	94934.64	0.00	0.00	0.00	405450.06
		1.0E-01	44749.23	95573.05	0.00	0.00	0.00	395924.69
		2.0E-01	44749.23	96211.45	0.00	0.00	0.00	386335.44
		3.0E-01	44749.23	96849.84	0.00	0.00	0.00	376682.38
		4.0E-01	44749.23	97488.24	0.00	0.00	0.00	366965.47
4	LOAD1							
		0.00	44749.23	97488.24	0.00	0.00	0.00	366965.47
		1.67	44749.23	108181.44	0.00	0.00	0.00	194717.17
		3.35	44749.23	118874.64	0.00	0.00	0.00	4557.76
		5.02	44749.23	129567.84	0.00	0.00	0.00	-203512.75
		6.70	44749.23	140261.03	0.00	0.00	0.00	-429494.34
5	LOAD1							
		0.00	44749.23	140261.03	0.00	0.00	0.00	-429494.34
		1.0E-01	44749.23	140899.44	0.00	0.00	0.00	-443552.34
		2.0E-01	44749.23	141537.83	0.00	0.00	0.00	-457674.16
		3.0E-01	44749.23	142176.23	0.00	0.00	0.00	-471859.84
		4.0E-01	44749.23	142814.63	0.00	0.00	0.00	-486109.34
6	LOAD1							
		0.00	-289732.69	-91823.71	0.00	0.00	0.00	-330565.25
		3.5E-01	-291009.47	-91823.71	0.00	0.00	0.00	-298426.97
		7.0E-01	-292286.28	-91823.71	0.00	0.00	0.00	-266288.66
7	LOAD1							
		0.00	-292286.28	-91823.71	0.00	0.00	0.00	-266288.66
		1.45	-297575.88	-91823.71	0.00	0.00	0.00	-133144.33
		2.90	-302865.47	-91823.71	0.00	0.00	0.00	0.00
8	LOAD1							
		0.00	-56849.87	49687.01	0.00	0.00	0.00	65479.70
		3.5E-01	-55573.07	49687.01	0.00	0.00	0.00	48089.27
		7.0E-01	-54296.27	49687.01	0.00	0.00	0.00	30698.84

F R A M E E L E M E N T F O R C E S

FRAME	LOAD	LOC	P	V2	V3	T	M2	M3
9	LOAD1							
		0.00	-54296.27	49687.01	0.00	0.00	0.00	30698.84
		8.0E-01	-51377.88	49687.01	0.00	0.00	0.00	-9050.74
		1.60	-48459.48	49687.01	0.00	0.00	0.00	-48800.32
10	LOAD1							
		0.00	-48459.48	49687.01	0.00	0.00	0.00	-48800.32
		3.5E-01	-47182.68	49687.01	0.00	0.00	0.00	-66190.74
		7.0E-01	-45905.88	49687.01	0.00	0.00	0.00	-83581.17
11	LOAD1							
		0.00	49687.01	-45905.88	0.00	0.00	0.00	83581.17
		1.0E-01	49687.01	-45267.48	0.00	0.00	0.00	88139.84
		2.0E-01	49687.01	-44629.08	0.00	0.00	0.00	92634.66
		3.0E-01	49687.01	-43990.68	0.00	0.00	0.00	97065.66
		4.0E-01	49687.01	-43352.28	0.00	0.00	0.00	101432.80
12	LOAD1							
		0.00	49687.01	-43352.28	0.00	0.00	0.00	101432.80
		1.67	3122.02	840.91	0.00	0.00	0.00	137036.06
		3.35	-43442.96	45034.09	0.00	0.00	0.00	98615.76
		5.02	-90007.95	89227.28	0.00	0.00	0.00	-13828.11
		6.70	-136572.94	133420.47	0.00	0.00	0.00	-200295.55
13	LOAD1							
		0.00	-136572.94	133420.47	0.00	0.00	0.00	-200295.55
		1.0E-01	-136572.94	134058.86	0.00	0.00	0.00	-213669.47
		2.0E-01	-136572.94	134697.27	0.00	0.00	0.00	-227107.25
		3.0E-01	-136572.94	135335.66	0.00	0.00	0.00	-240608.86
		4.0E-01	-136572.94	135974.06	0.00	0.00	0.00	-254174.31
14	LOAD1							
		0.00	-135974.06	-136572.94	0.00	0.00	0.00	-254174.31
		3.5E-01	-137250.86	-136572.94	0.00	0.00	0.00	-206373.86
		7.0E-01	-138527.66	-136572.94	0.00	0.00	0.00	-158573.39
15	LOAD1							
		0.00	-138527.66	-136572.94	0.00	0.00	0.00	-158573.39
		8.0E-01	-141446.06	-136572.94	0.00	0.00	0.00	-49315.11
		1.60	-144364.45	-136572.94	0.00	0.00	0.00	59943.17
16	LOAD1							
		0.00	-144364.45	-136572.94	0.00	0.00	0.00	59943.17
		3.5E-01	-145641.25	-136572.94	0.00	0.00	0.00	107743.63
		7.0E-01	-146918.05	-136572.94	0.00	0.00	0.00	155544.09

J O I N T D A T A

JOINT	GLOBAL-X	GLOBAL-Y	GLOBAL-Z	RESTRAINTS	ANGLE-A	ANGLE-B	ANGLE-C
1	-3.75000	3.75000	0.00000	1 1 1 0 0 0	0.000	0.000	0.000
2	-3.75000	3.75000	2.90000	0 0 0 0 0 0	0.000	0.000	0.000
3	-3.75000	3.75000	3.60000	0 0 0 0 0 0	0.000	0.000	0.000
4	-3.75000	3.75000	4.30000	0 0 0 0 0 0	0.000	0.000	0.000
5	-3.75000	3.75000	5.90000	0 0 0 0 0 0	0.000	0.000	0.000
6	-3.75000	3.75000	6.60000	0 0 0 0 0 0	0.000	0.000	0.000
7	-3.35000	3.75000	6.60000	0 0 0 0 0 0	0.000	0.000	0.000
8	3.35000	3.75000	6.60000	0 0 0 0 0 0	0.000	0.000	0.000
9	3.75000	3.75000	6.60000	0 0 0 0 0 0	0.000	0.000	0.000
10	3.75000	3.75000	5.90000	0 0 0 0 0 0	0.000	0.000	0.000
11	3.75000	3.75000	4.30000	0 0 0 0 0 0	0.000	0.000	0.000
12	3.75000	3.75000	3.60000	0 0 0 0 0 0	0.000	0.000	0.000
13	3.75000	3.75000	2.90000	0 0 0 0 0 0	0.000	0.000	0.000
14	3.75000	3.75000	0.00000	1 1 1 0 0 0	0.000	0.000	0.000
15	-3.35000	3.75000	3.60000	0 0 0 0 0 0	0.000	0.000	0.000
16	3.35000	3.75000	3.60000	0 0 0 0 0 0	0.000	0.000	0.000

F R A M E E L E M E N T D A T A

FRAME	JNT-1	JNT-2	SECTION	ANGLE	RELEASES	SEGMENTS	R1	R2	FACTOR	LENGTH
1	1	2	LEG	0.000	000000	2	0.000	0.000	1.000	2.900
2	2	3	JNTLEG	0.000	000000	2	0.000	0.000	1.000	0.700
3	3	15	JNTBM	0.000	000000	4	0.000	0.000	1.000	0.400
4	15	16	BEAM	0.000	000000	4	0.000	0.000	1.000	6.700
5	16	12	JNTBM	0.000	000000	4	0.000	0.000	1.000	0.400
6	12	13	JNTLEG	0.000	000000	2	0.000	0.000	1.000	0.700
7	13	14	LEG	0.000	000000	2	0.000	0.000	1.000	2.900
8	3	4	JNTLEG	0.000	000000	2	0.000	0.000	1.000	0.700
9	4	5	LEG	0.000	000000	2	0.000	0.000	1.000	1.600
10	5	6	JNTLEG	0.000	000000	2	0.000	0.000	1.000	0.700
11	6	7	JNTBM	0.000	000000	4	0.000	0.000	1.000	0.400
12	7	8	BEAM	0.000	000000	4	0.000	0.000	1.000	6.700
13	8	9	JNTBM	0.000	000000	4	0.000	0.000	1.000	0.400
14	9	10	JNTLEG	0.000	000000	2	0.000	0.000	1.000	0.700
15	10	11	LEG	0.000	000000	2	0.000	0.000	1.000	1.600
16	11	12	JNTLEG	0.000	000000	2	0.000	0.000	1.000	0.700

F R A M E S P A N D I S T R I B U T E D L O A D S Load Case LOAD1

FRAME	TYPE	DIRECTION	DISTANCE-A	VALUE-A	DISTANCE-B	VALUE-B
12	FORCE	GLOBAL-Z	0.0000	-20000.0000	1.0000	-20000.0000
12	FORCE	GLOBAL-X	0.0000	27800.0000	1.0000	27800.0000
12	FORCE	GLOBAL-X	0.0000	40000.0000	1.0000	40000.0000
12	FORCE	GLOBAL-X	0.0000	-40000.0000	1.0000	-40000.0000

STATIC LOAD CASES

STATIC CASE	CASE TYPE	SELF WT FACTOR
LOAD1	DEAD	1.0000

MATERIAL PROPERTY DATA

MAT LABEL	MODULUS OF ELASTICITY	POISSON'S RATIO	THERMAL COEFF	WEIGHT PER UNIT VOL	MASS PER UNIT VOL
STEEL	1.999E+11	0.300	1.170E-05	76819.547	7827.101
CONC	2.482E+10	0.200	9.900E-06	23561.609	2400.680
LEGMAT	5.098E+09	0.200	0.000	24000.000	2400.000
BEAMMAT	5.472E+09	0.200	0.000	24000.000	2400.000
JNTMAT	2.000E+11	0.300	0.000	24000.000	2400.000

MATERIAL DESIGN DATA

MAT LABEL	DESIGN CODE	STEEL FY	CONCRETE FC	REBAR FY	CONCRETE FCS	REBAR FYS
LEGMAT	N					
BEAMMAT	N					
JNTMAT	N					

FRAME SECTION PROPERTY DATA

SECTION LABEL	MAT WEB LABEL	SECTION FLANGE TYPE	DEPTH	FLANGE WIDTH TOP	FLANGE THICK TOP	FLANGE THICK BOTTOM	FLANGE WIDTH BOTTOM	FLANGE THICK
BEAM	BEAMMAT		1.400	0.190	0.000	0.000	0.000	0.000
LEG	LEGMAT		0.800	0.190	0.000	0.000	0.000	0.000
JNTLEG	JNTMAT		0.800	0.190	0.000	0.000	0.000	0.000
JNTBM	JNTMAT		1.400	0.190	0.000	0.000	0.000	0.000

FRAME SECTION PROPERTY DATA

SECTION LABEL	AREA	TORSIONAL INERTIA	MOMENTS OF INERTIA I33	I22	SHEAR AREAS A2	A3
BEAM	0.266	2.927E-03	4.345E-02	8.002E-04	0.222	0.222
LEG	0.152	1.555E-03	8.107E-03	4.573E-04	0.127	0.127
JNTLEG	0.152	1.555E-03	8.107E-03	4.573E-04	0.127	0.127
JNTBM	0.266	2.927E-03	4.345E-02	8.002E-04	0.222	0.222

FRAME SECTION PROPERTY DATA

SECTION LABEL	SECTION MODULII S33	S22	PLASTIC MODULII Z33	Z22	RADII OF GYRATION R33	R22
BEAM	6.207E-02	8.423E-03	9.310E-02	1.263E-02	0.404	5.485E-02
LEG	2.027E-02	4.813E-03	3.040E-02	7.220E-03	0.231	5.485E-02
JNTLEG	2.027E-02	4.813E-03	3.040E-02	7.220E-03	0.231	5.485E-02
JNTBM	6.207E-02	8.423E-03	9.310E-02	1.263E-02	0.404	5.485E-02

FRAME SECTION PROPERTY DATA

SECTION LABEL	TOTAL WEIGHT	TOTAL MASS
BEAM	85545.570	8554.558
LEG	32831.984	3283.198
JNTLEG	15321.587	1532.159
JNTBM	10214.391	1021.439

APPENDIX III

TEST HARDWARE

COMPLETE EXTENSION BEAM

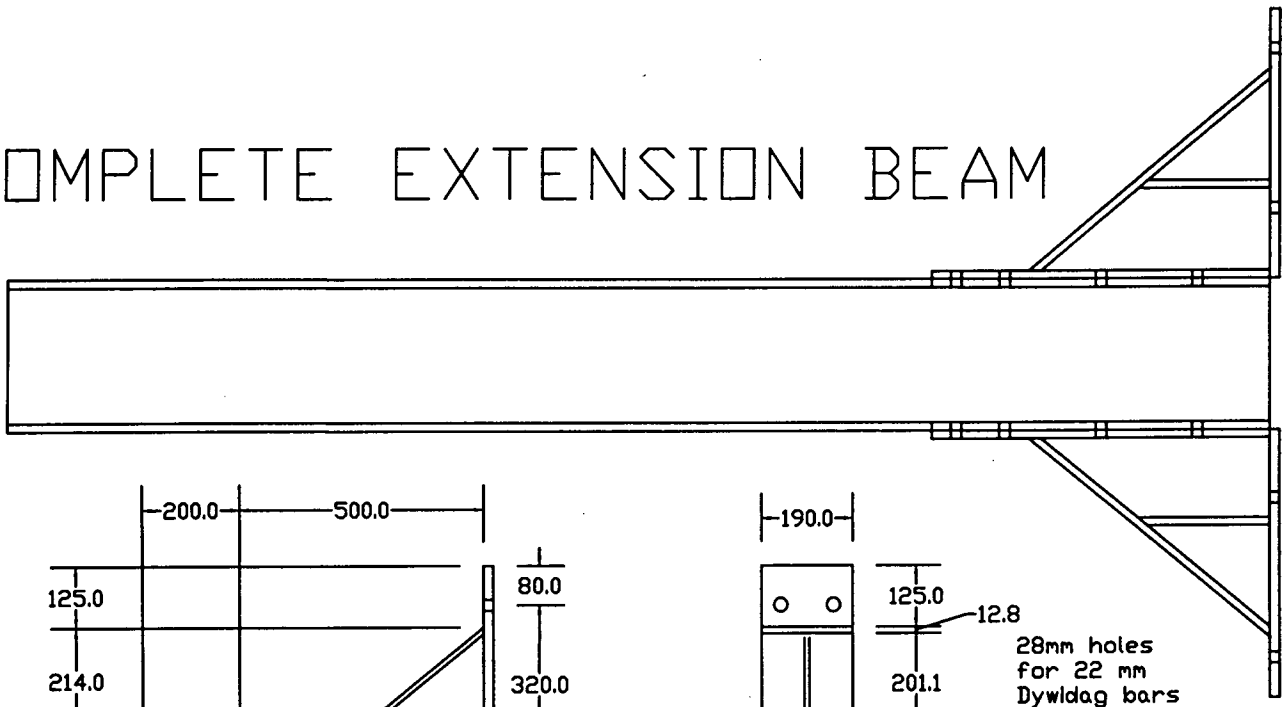

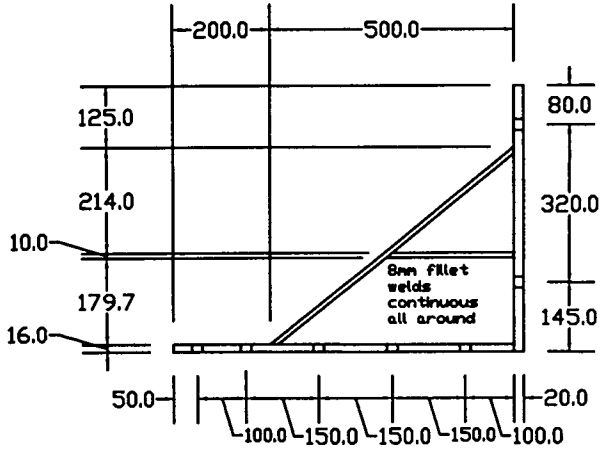

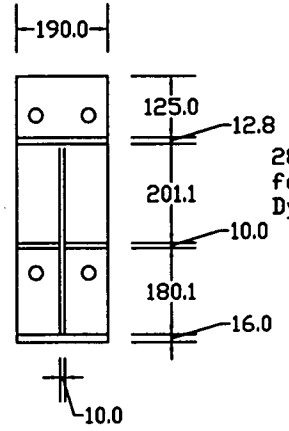

28mm holes for 22 mm Dywidag bars

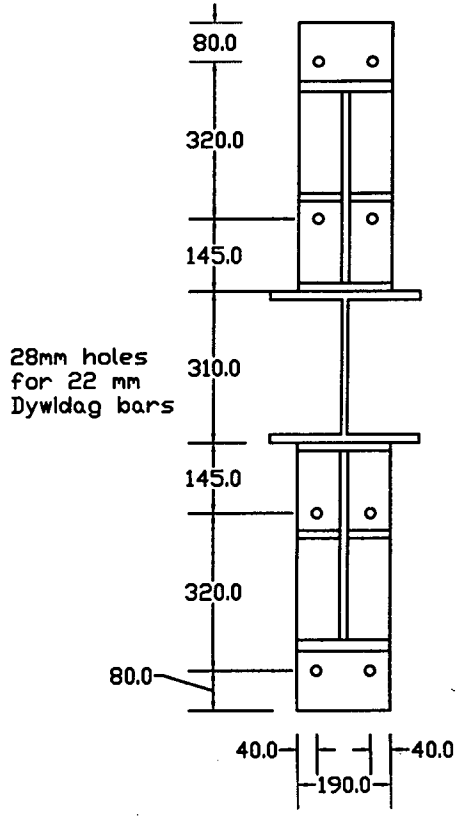

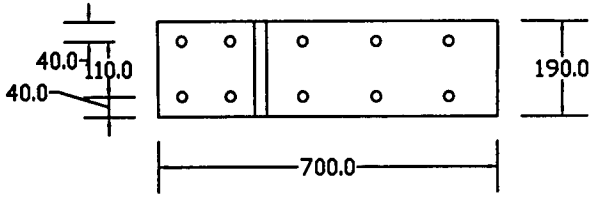

21mm holes for 3/4" bolts

All plate at least grade 300W.

8mm fillet welds continuous all around.

Weld using E480XX electrode (metric) or E70XX electrode (imperial) or equivalent

WEB ATTACHMENT

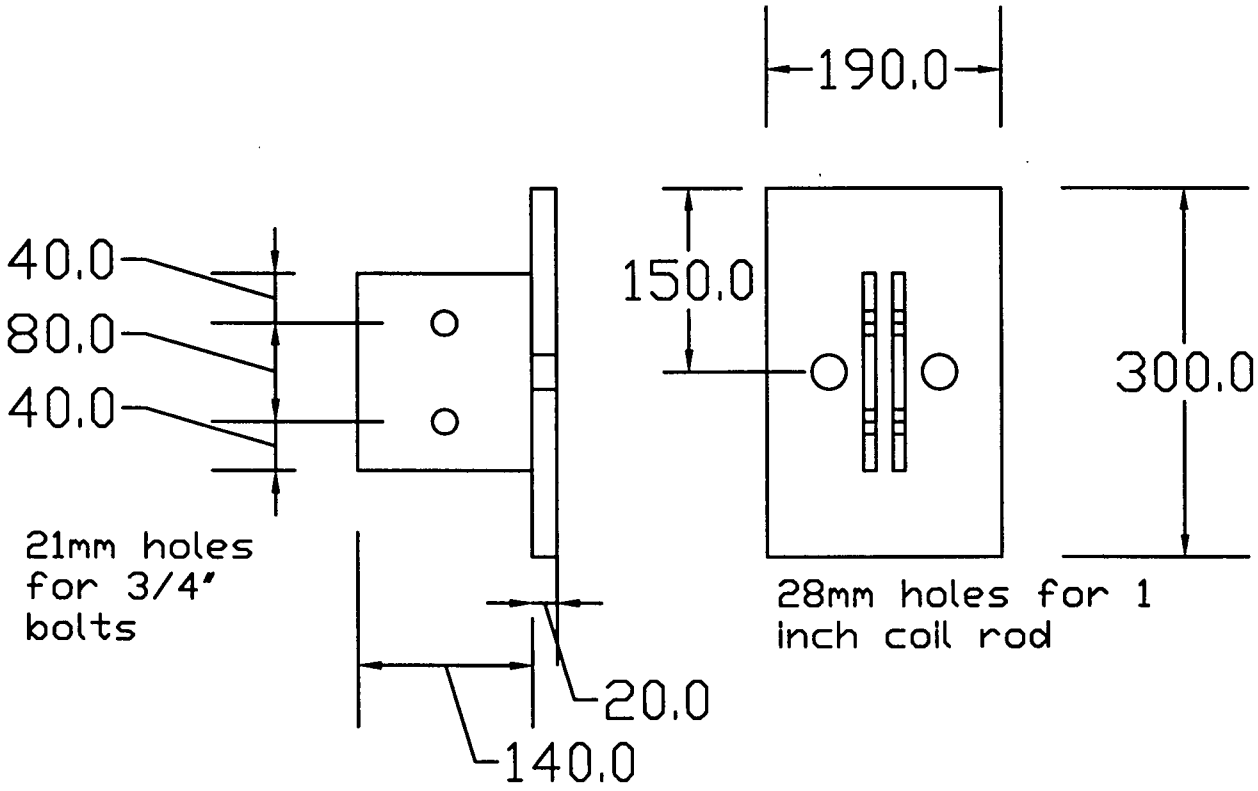

All plate at least grade 300W.

8mm fillet welds continuous all around.

Weld using E480XX electrode (metric) or E70XX electrode (imperial) or equivalent

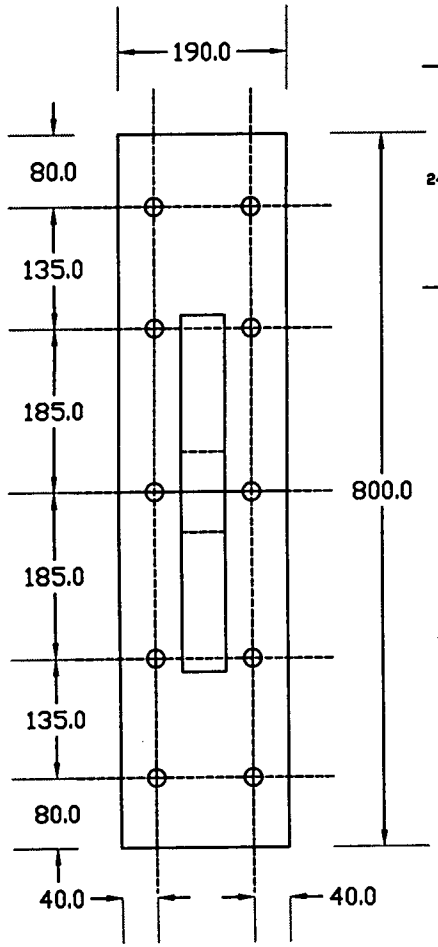

28mm diameter holes for 1 inch coil rod

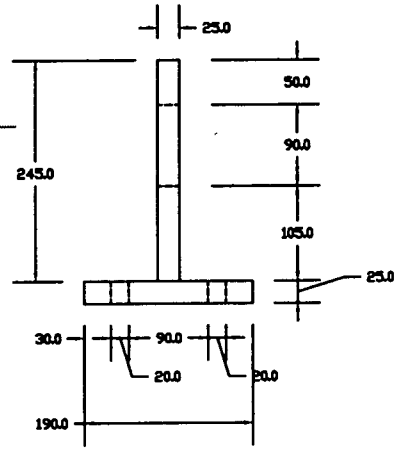

All plate at least grade 300 W

10mm fillet welds continuous all around

Weld using E480XX electrode (metric) or E70XX electrode (Imperial) or equivalent.

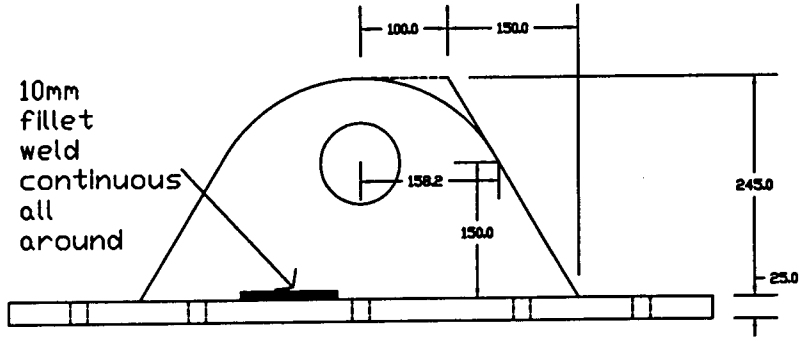

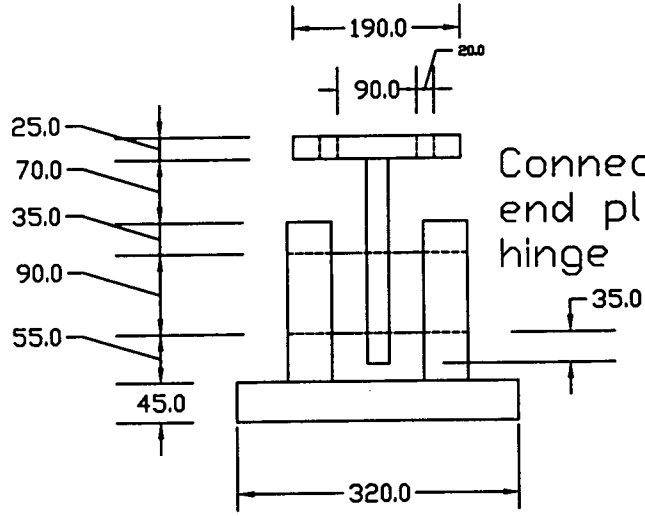

Connection of end plate to hinge

HINGE CONNECTION PLATE TO BE BOLTED TO COIL RODS CAST INTO SPECIMEN

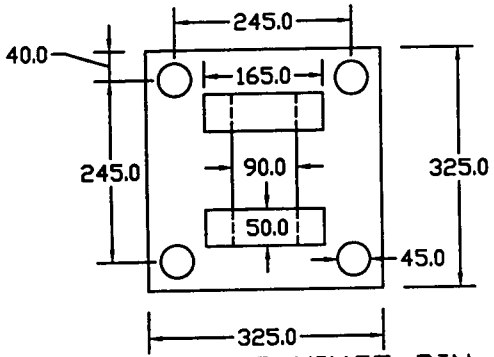

EXISTING HINGE PIN:

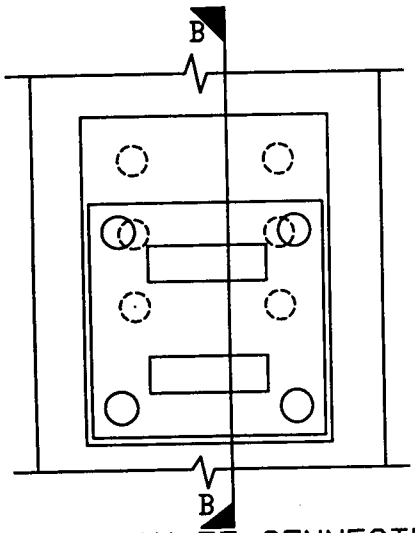

OVERLAY OF CONNECTED PLATES

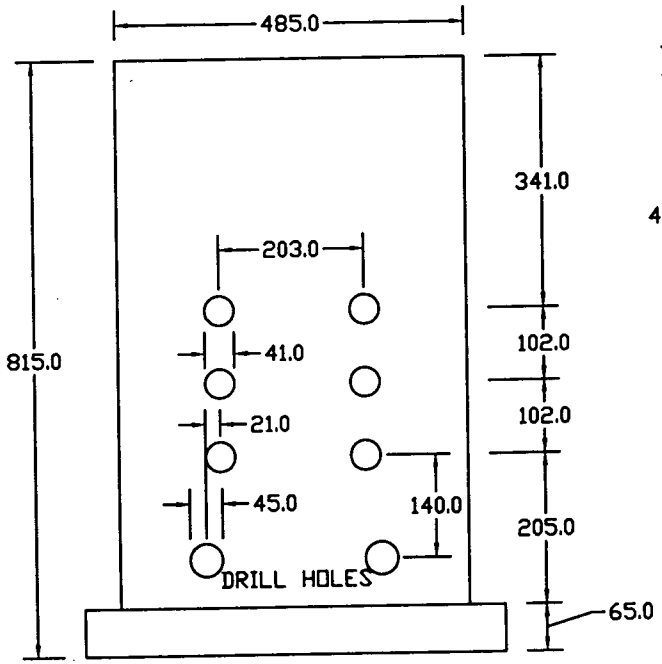

EXISTING THRUST SUPPORT:

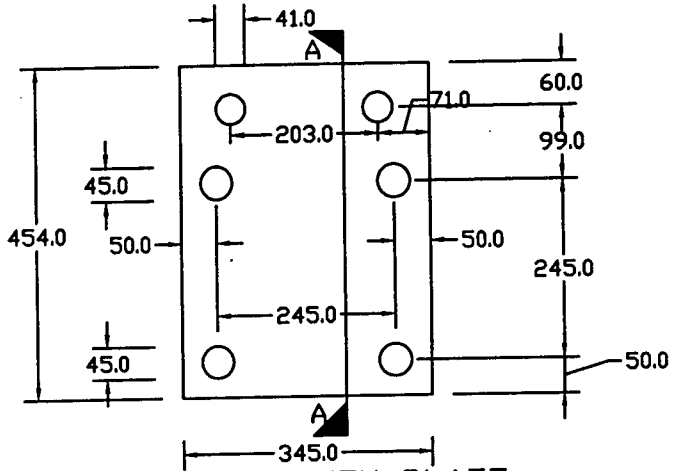

CONNECTION PLATE (TO BE MADE UP)

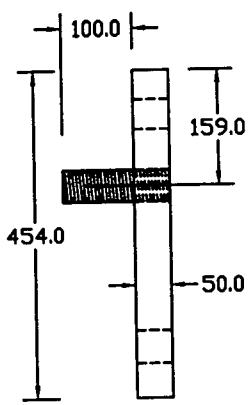

SECTION A-A

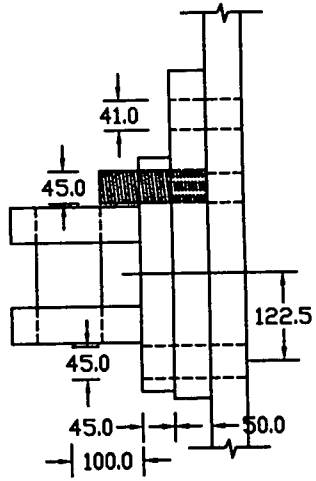

SECTION B-B

HINGE CONNECTION DETAIL

JACK SET-UP:

PLAN VIEW

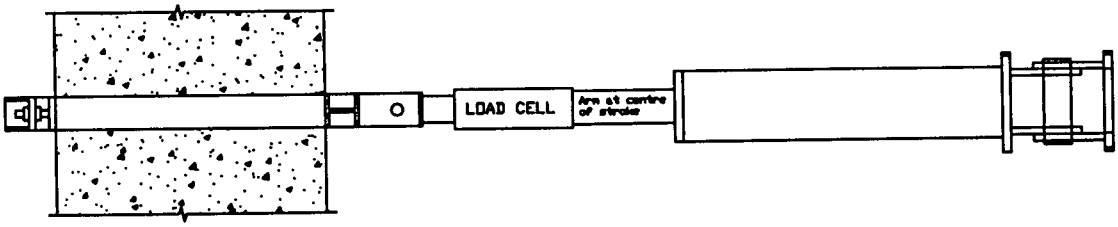

ELEVATION

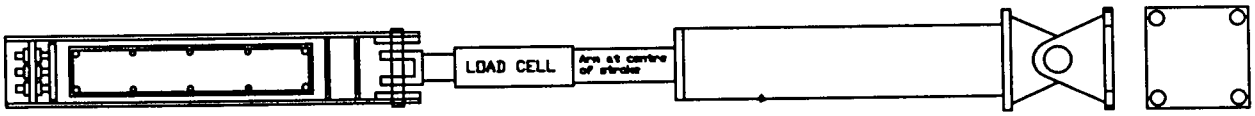

CONNECTION TO LEG DETAIL:

PLAN VIEW

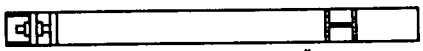

ELEVATION

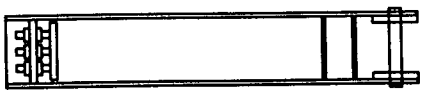

APPENDIX IV

TEST PHOTOGRAPHS

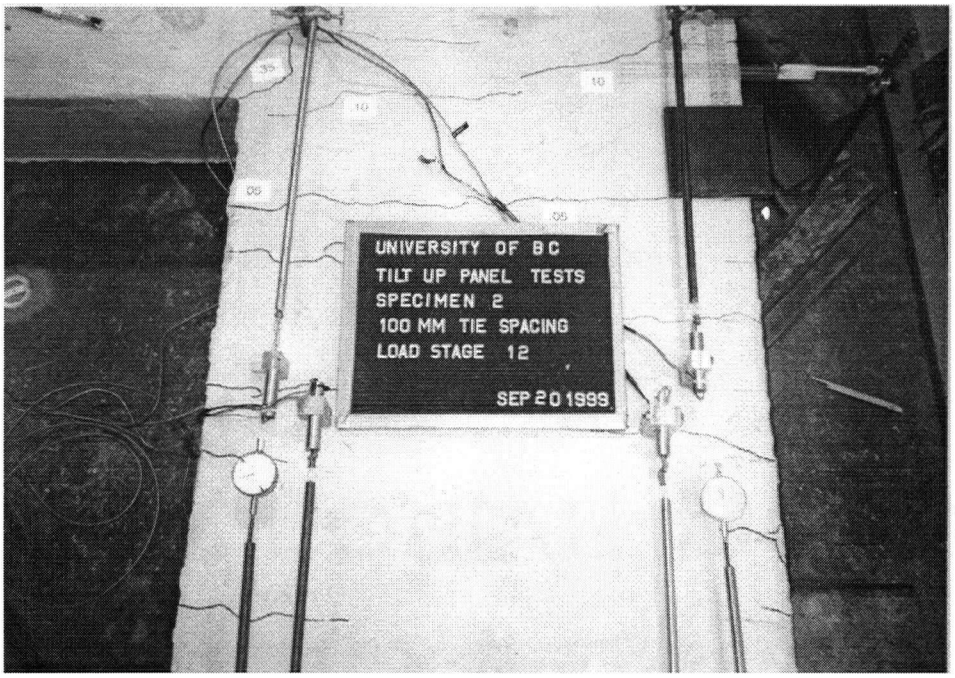

FIGURE IV-1

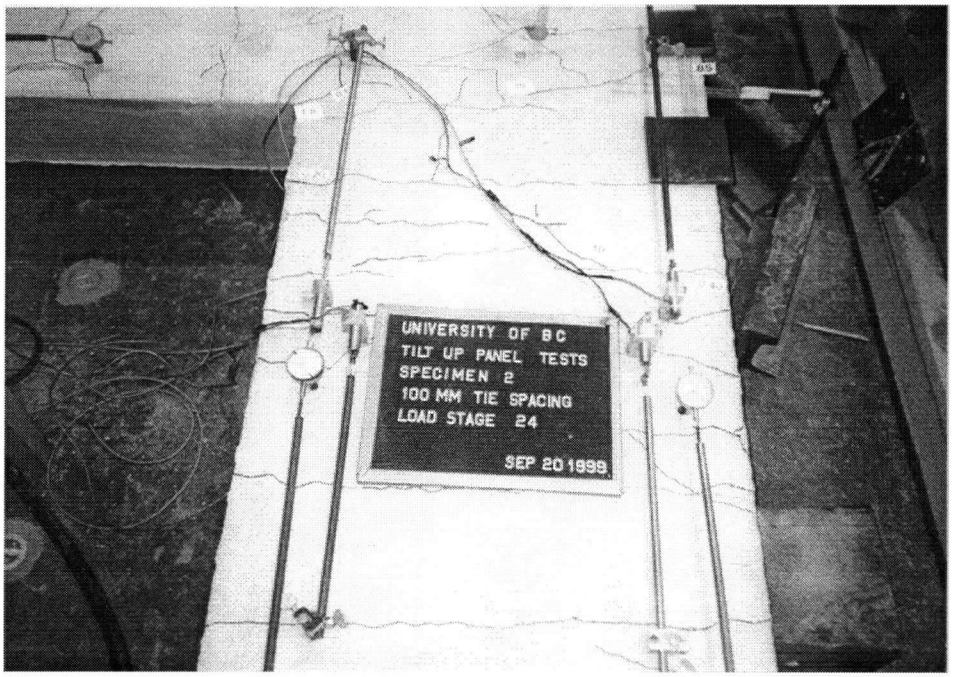

FIGURE IV-2

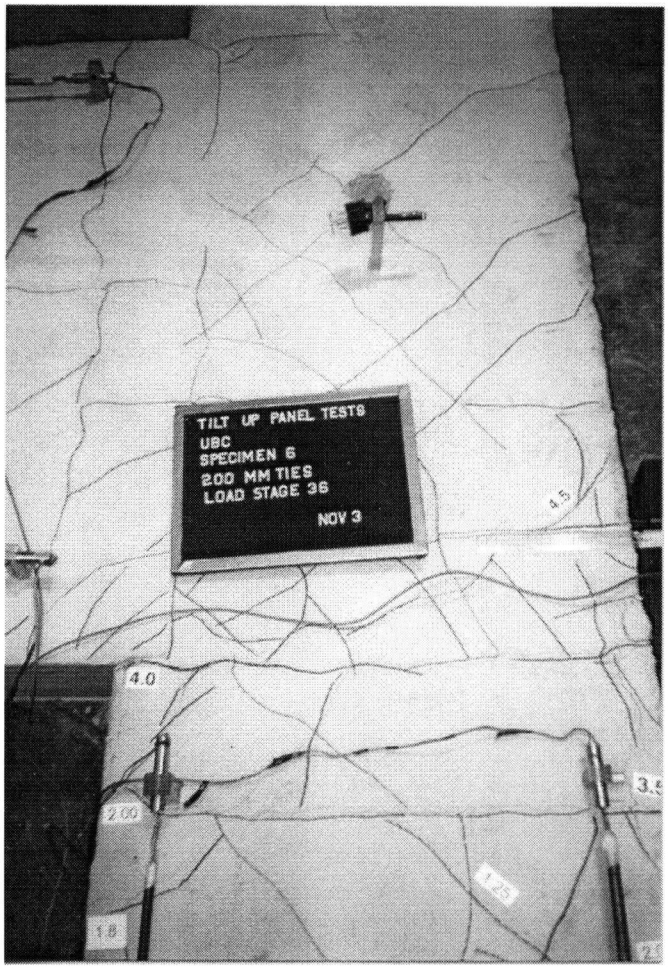
TILT UP PANEL TESTS
UBC
SPECIMEN 6
200 MM TIES
LOAD STAGE 36
NOV 3
4.0
4.5
2.00
1.25
1.8

FIGURE IV-3

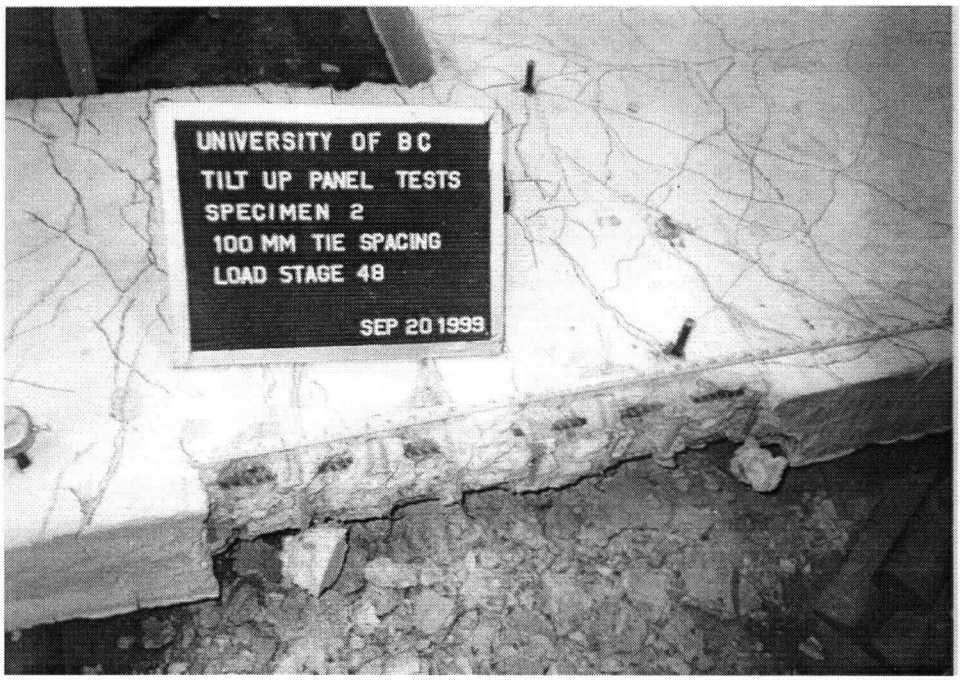
UNIVERSITY OF BC
TILT UP PANEL TESTS
SPECIMEN 2
100 MM TIE SPACING
LOAD STAGE 48
SEP 20 1999

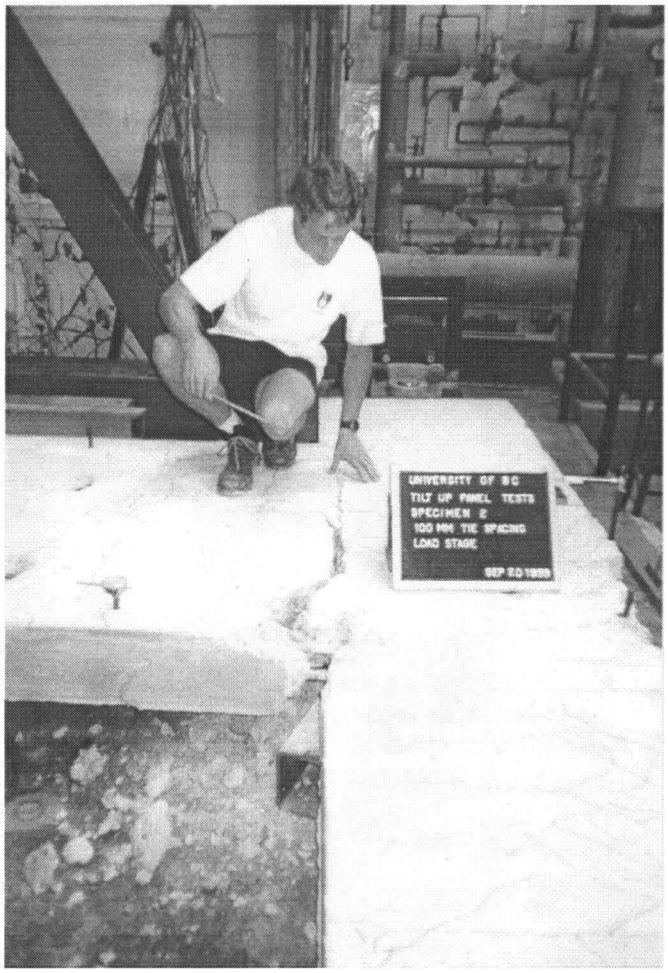
UNIVERSITY OF BC
TILT UP PANEL TESTS
SPECIMEN 2
100 MM TIE SPACING
LOAD STAGE
SEP 20 1999

FIGURE IV-5


UNIVERSITY OF BC
TILT UP PANEL TESTS
SPECIMEN 2
100 MM TIE SPACING
LOAD STAGE
SEP 20 1999

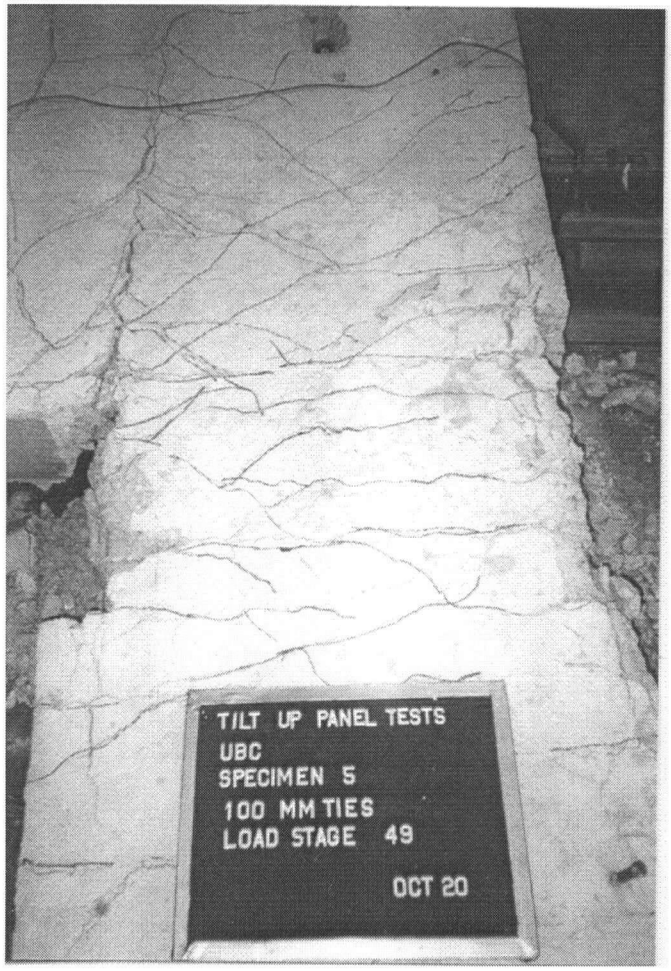
TILT UP PANEL TESTS
UBC
SPECIMEN 5
100 MM TIES
LOAD STAGE 49
OCT 20

FIGURE IV-7

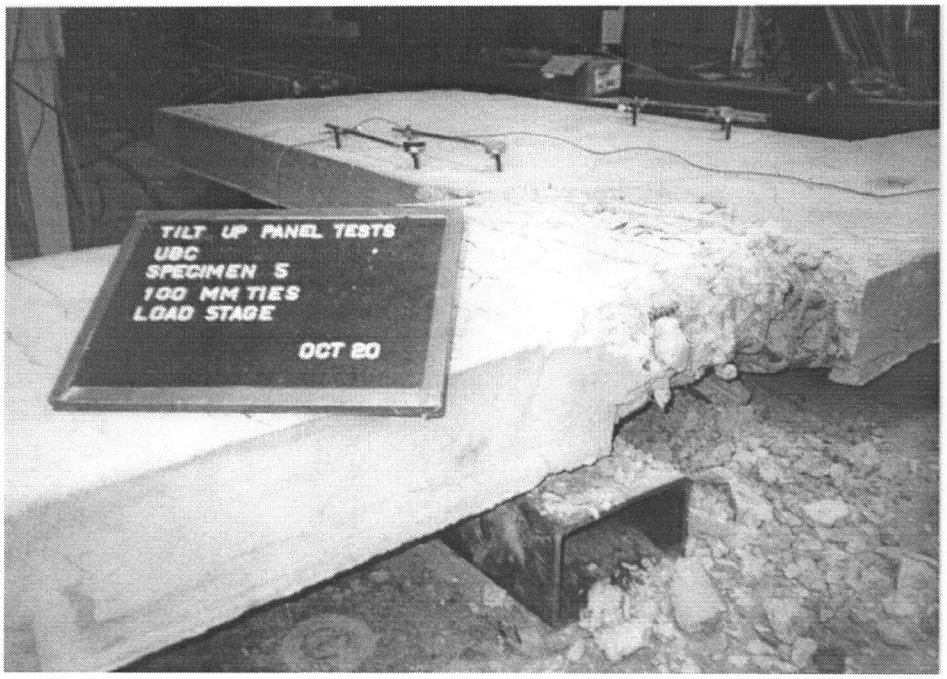
TILT UP PANEL TESTS
UBC
SPECIMEN 5
100 MM TIES
LOAD STAGE
OCT 20

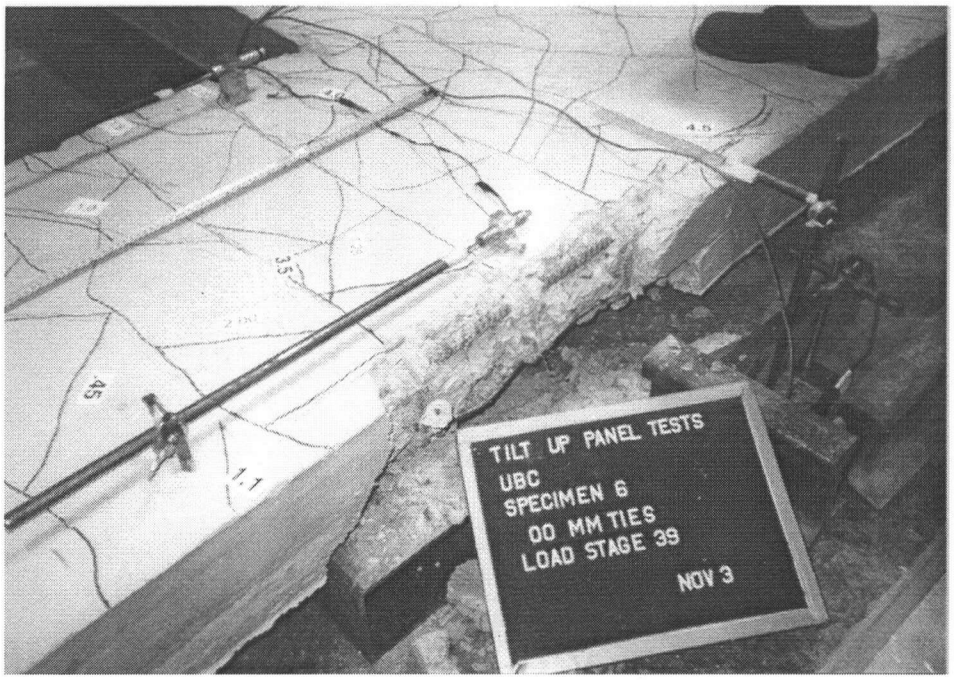

FIGURE IV-9

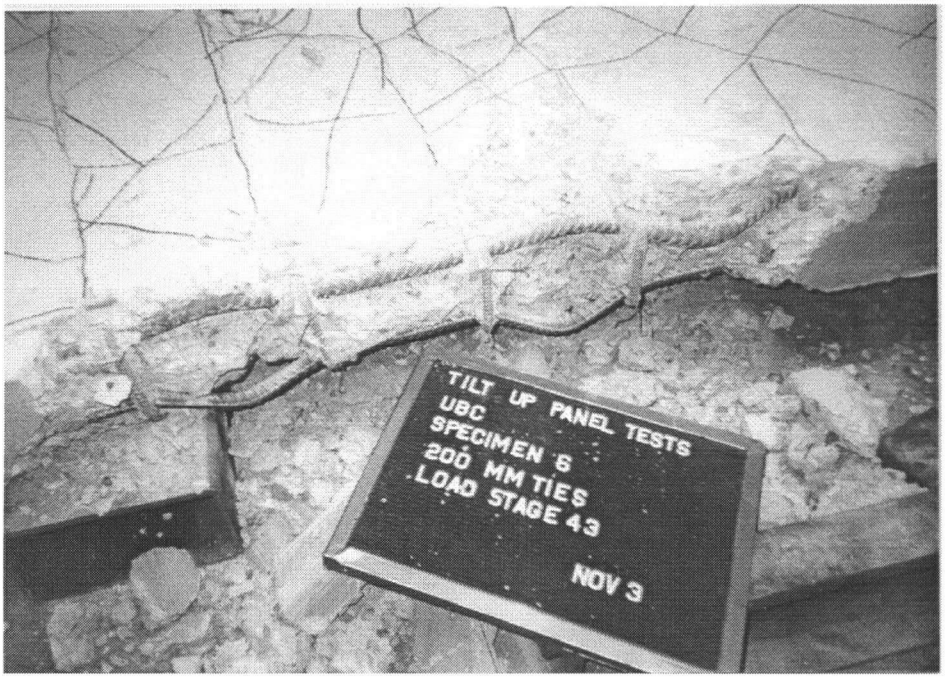

FIGURE IV-10

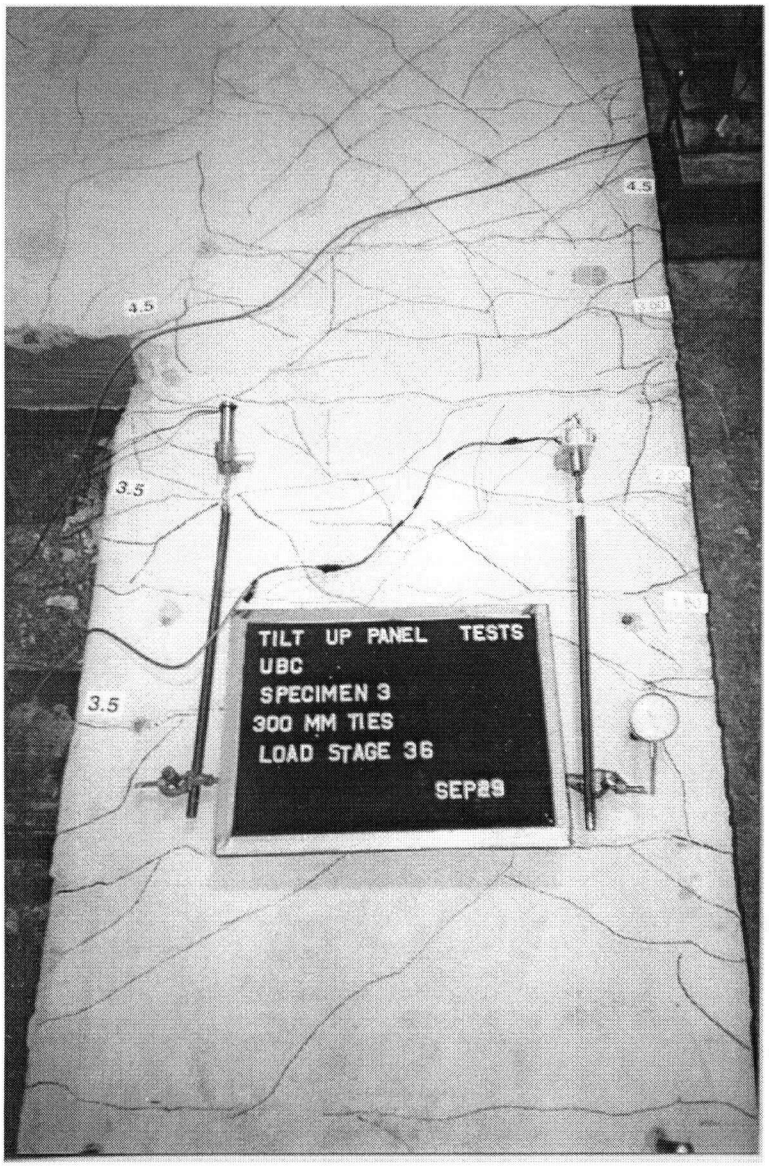

FIGURE IV-11

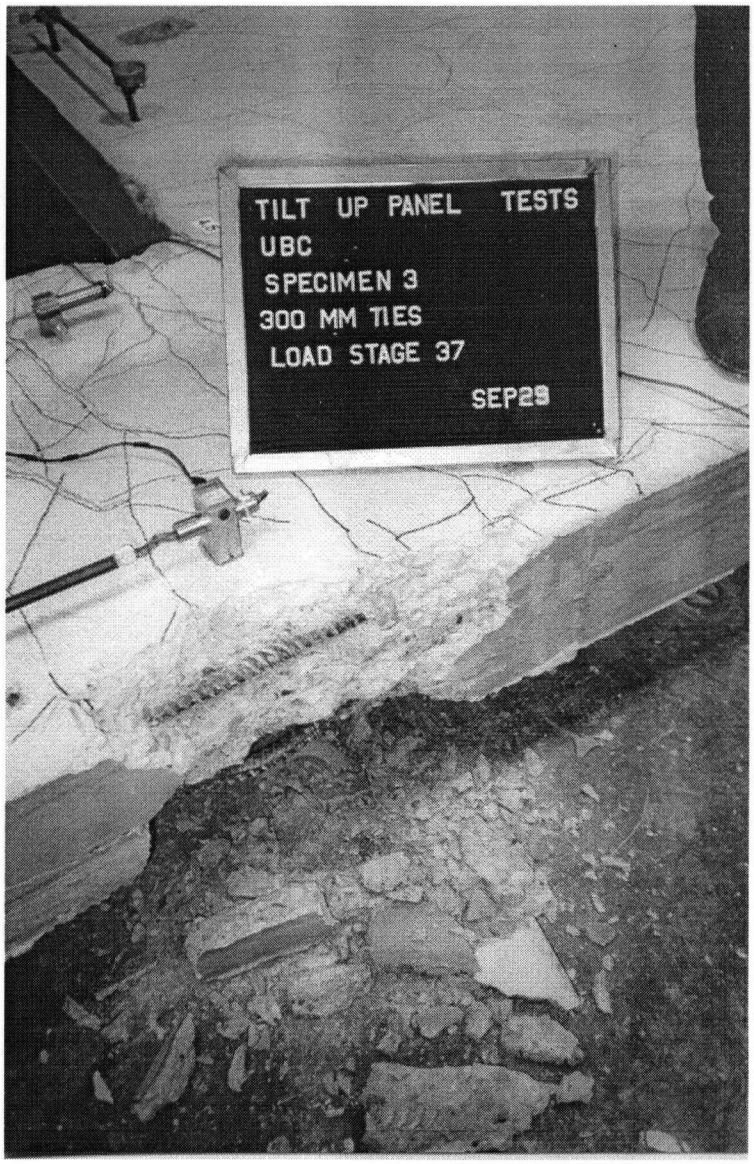

FIGURE IV-12

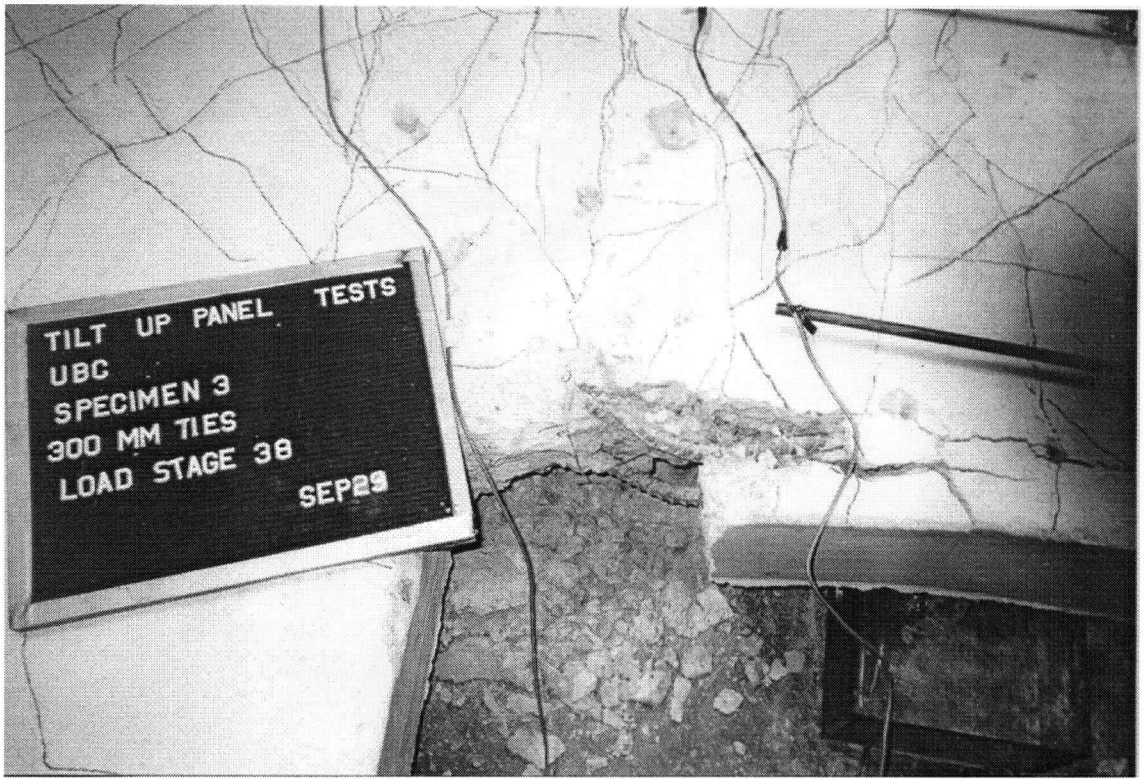

FIGURE IV-13

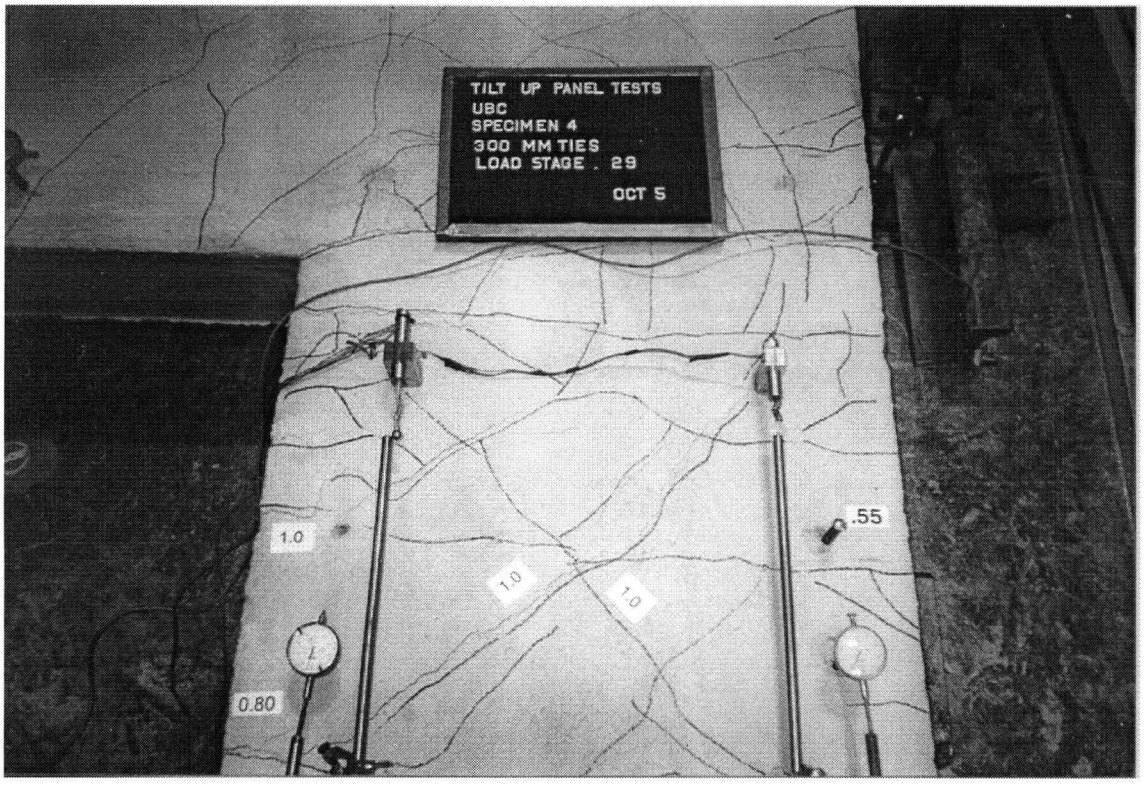

FIGURE IV-14

FIGURE IV-15

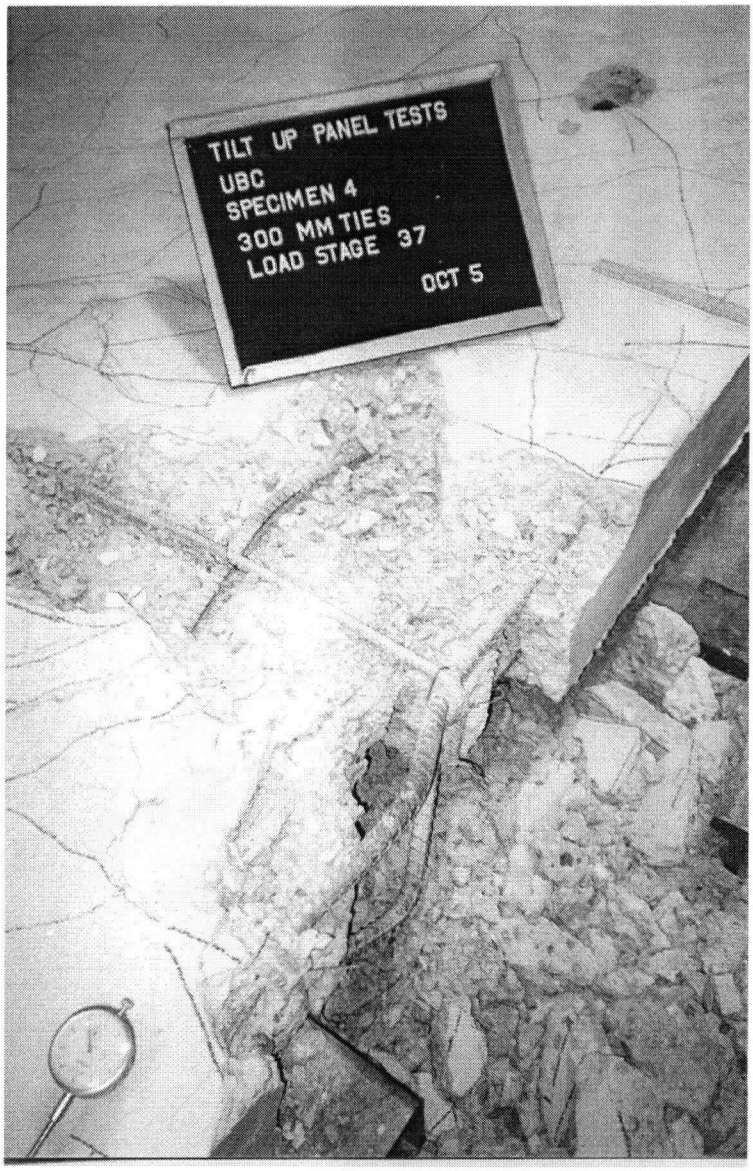

FIGURE IV-16

APPENDIX V

TEST DATA

ELECTRONICALLY RECORDED TEST DATA

The following measurements were electronically recorded:

- Jack load (kN), all tests.
- Jack Displacement (mm), all tests.
- Deflection at top of leg (mm), tests 3 to 6.
- Strain on top face of beam, test 6.
- Strain on bottom face of beam, test 6.

Since each test had up to 2000 recordings of each of the above measurements, the data has not been printed. Instead it is contained on a computer disk submitted with the thesis. The data is contained within an EXCEL spreadsheet and the columns containing the data are clearly labeled.

DATA RECORDED BY HAND DURING TESTING

The following data was recorded by hand during the tests:

- Jack Load (kN), all tests.
- Jack Displacement (mm), all tests.
- LVDT displacement at top of leg (mm), tests 3-6.
- Ruler measurements at joint and at the foot of the leg (mm), all tests.
- Position of laser dot on paper (mm), tests 2-6.

This data is contained in tables, one for each test, beginning on the following page.

SELECTED DATA USED FOR ANALYSIS

Load and corresponding deflection values at each of the post yielding cycle peaks for tests 2-6 were extracted from the electronically recorded data. Tables containing this data as well as plots of the data are given after the tables containing the data recorded by hand during the testing.

TEST 1 - 200mm TIE SPACING

LOAD STAGE	JACK DATA			Ruler Measurements							
	LOAD (kN		DISP.	Connection		Hinge		Top of leg	Foot		
	Push	Pull	(mm)	Left/Right	Up/Down	Left/Right	Up/Dow	Left/Right	Left/Right	Up/Down	
0			-2.2	150	150	150	150	150	150	150	
1	25		10.9	152	148	151	150	153	490	151	
2		25	-13.7	147	152	149	150	147	510	149	
3	25		10.9	152	148	150	150	153	490	151	
4		25	-14.7	147	152	149	150	147	512	149	
5	25		10.6	152	148	151	150	153	489	150	
6		25	-15.6	147	153	150	150	147	512	150	
7	50		26.5	155	145	152	150	157	475	152	
8		50	-31.9	144	155	149	150	143	528	149	
9	50		28.6	155	144	152	150	157	473	151	
10		50	-33.1	144	156	149	150	143	528	150	
11	50		30.3	156	144	152	150	158	471	152	
12		50	-33.5	144	156	148	150	142	529	149	
13	75		43.2	158	142	153	150	161	459	153	
14		75	-48.1	140	157	148	150	139	543	150	
15	75		44.5	158	142	153	150	161	458	154	
16		75	-50.2	140	158	147	150	139	545	149	
17	75		46.8	158	142	153	150	162	455	154	
18		75	-51.8	139	158	147	150	137	549	150	
Pushing direction roller support moved about 20mm at this stage, reference measurements re-taken											
0			14	157	142	152	150	156	484	151	
19	94		79	169	132	155	151	171	423	156	
20		96	-51	144	152	143	149	142	540	150	
21	96.8		79	168	132	155	150	170	429	156	
22		90	-51	144	153	146	150	140	545	150	
23	94		79	168	132	155	150	171	422	144	
Hinge Support moved significantly, by this stage plastic deformation had taken place											
and it was therefore not possible to "re-reference" the rulers											
	0		30								
24	96		106	180	140	167	161	185	397	147	
25	96		130	182				191			
26	124		157	182	137	170	162	192	345	152	83mm of plastic disp
27	128		170					192			
28	131		186					193			
29	133		200					193			
30	134		236					193			Crushing of concrete
31	138		254					194			
32											
33			-200								Bar rupture

TEST 2 - 100mm TIE SPACING

LOAD STAGE	JACK DATA LOAD (kN) Push	Pull	DISP. (mm)	Ruler Measurements Top of Hinge Left/Right	Up/Down	Foot Left/Right	Up/Down	d of dot (mm)
0			-2	150	150	500	150	
1	25		10.3	153	150	488	150	11
2		25	-11.6	149	151	507	150	-8
3	25		8.7	153	149	489	150	11
4		25	-12.5	147	150	508	150	-9
5	25		8.8	152	150	489	150	11
6		25	-12.8	146	151	508	150	-9
7	50		24.8	157	149	475	151	27
8		50	-29.2	142	151	523	150	-22
9	50		25.5	157	149	474	149	28
10		50	-30.8	141	151	524	150	-24
11	50		26.2	158	149	473	148	29
12		50	-31.5	141	151	525	150	-24
13	75		42.6	162	148	457	154	47
14		75	-45.2	138	153	538	150	-36
15	75		43.6	162	151	456	154	47
16		75	-46.9	137	157	540	150	-36
17	75		45	162	152	455	155	49
18		75	-48.4	137	158	542	150	-38
19	97		61	166	151	439	156	69
20		97.9	-61	134	159	554	150	-44
21	93.5		61	167	150	439	156	68
22		89.9	-61	134	158	553	150	-44
23	96.2		61	166	150	438	156	68
24		89	-61	135	158	553	151	-44
25	122		92	171	149	409	160	
26		108	-92	132	160	580	155	
27	101		92	170	149	406	165	
28		105	-92	132	160	581	155	
29	106		92	170	149	405	165	
30		104	-92	132	160	581	155	
31	95		122	172	149	380	170	
32		89	-122	132	162	609	157	
33	108		122	172	149	378	171	
34		106	-122	131	161	605	157	
35	105		122	172	149	380	171	
36		100	-122	131	162	608	157	
37	130		183					
38		129	-183					
39	117		183					
40		116	-183					
41	105		183					
42		119	-183					
43	128		244	192	2120mm			
44			-244	138	from pin			
45			244	190	i.e. at lvdt			
46			-244	138	stud			
47			244	200				
48			-244	175	1370mm			
49			245	225	from pin			
50			-245	175	i.e. at insert			
51			245	226				
52			-245					

TEST 3 - 300mm TIE SPACING

LOAD STAGE	JACK DATA LOAD (kN) Push	Pull	DISP. (mm)	LVDT @joint (mm)	Ruler Measurements Top of Hinge Left/Right	Foot Left/Right	Up/Down	d of dot on board (mm)
0				52.9	150	500	150	
1	25		20.05	49.4	153	485	151	17
2		-25	-6.04	54.6	149	509	150	-7
3	25		21.1	49	154	486	151	20
4		-25	-6.34	54.7	148	509	150	-7
5	25		21.9	48.9	154	485	151	19
6		-25	-8.9	55.2	147	511	150	-7
7	50		39.6	45	157	468	152	37
8		-50	-17.9	57.8	145	522	150	-20
9	50		40.2	45	157	467	152	36
10		-50	-25.7	59.7	144	528	150	-23
11	50		42.3	44.5	158	467	151	36
12		-50	-23.1	58.6	144	528	150	-23
13	75		57.3	41.3	161	451	154	50
14		-75	-36	61	141	542	150	-34
15	75		58	41.1	161	450	155	50
16		-75	-38.6	61.6	141	543	150	-34
17	75		59.2	41	161	450	155	50
18		-75	-38.6	61.5	141	543	150	-34
19	94		74	38.2	165	434	157	59
20		-98	-54	64.5	139	558	150	-42
21	94		74	38.5	164	435	158	59
22		-97	-54	64	138	557	150	-42
23	92		74	38	163	435	157	59
24		-91	-54	64	138	556	150	-42
25	117		106	35.6	166	405	163	71
26		-117	-86	66.4	136	591	151	-50
27	100		106	36.3	166	406	166	71
28		-80	-86	63.7	139	588	153	-42
29	99		106	36.2	166	405	166	69
30		-82	-86	63.8	138	588	154	-42
31	112		138	34.7	167	373	172	76
32		-106	-118	66.3	137	620	155	-50
33	104		138	34.7	167	375	172	76
34		-68	-118	64.2	137	620	156	-46
35	106		138	34.8	167	374	172	76
36		-100	-118	66	136	618	157	-50
37	112		202	33.8	167	310	181	76

TEST 4 - 300mm TIE SPACING

LOAD STAGE	JACK DATA LOAD (kN) Push	Pull	DISP. (mm)	LVDT @joint (mm)	Ruler Measurements Top of Hinge Left/Right	Foot Left/Right	Up/Down	d of dot on board (mm)
0			-2	57.3	150	500	150	
1	25		9.73	54.9	153	490	150	10
2		25	-12	60.2	147	511	150	-12
3	25		10.1	54.8	153	490	150	10
4		25	-13.8	60.6	147	512	150	-12
5	25		10.6	54.8	152	490	151	10
6		25	-15.3	60.9	147	513	150	-12
7	50		28.15	50.7	156	473	153	27
8		50	-31.8	64.7	143	529	150	-27
9	50		31.8	50.4	157	470	153	32
10		50	-34	65.5	142	530	150	27
11	50		31.8	50.4	158	470	153	32
12		50	-34	65.8	142	533	150	-31
13	75		48.7	46.4	161	452	155	48
14		75	-51	69.4	138	549	149	-45
15	75		50.8	46.4	161	451	155	48
16		75	-54	69.8	138	549	150	-45
17	75		52	46.2	161	450	156	48
18		75	-58	70.9	137	552	150	-51
19	100		70	42.8	165	432	157	62
20		-98	-74	73	135	566	150	-61
21	94		70	43.4	163	435	158	59
22		-98	-74	73	135	568	150	-61
23	92		70	43.5	165	435	158	59
24		-96	-74	73	135	570	150	-61
25	117		106	39.6	167	398	165	75
26		-114	-110	75	132	605	152	-70
27	104		106	40.8	167	400	166	72
28		-105	-110	74.2	134	602	152	-65
29	101		106	41.3	166	398	166	72
30		-100	-110	73.9	134	604	152	-65
31	117		142	38	168	365	173	79
32		-117	-146	75.3	132	639	155	-72
33	107		142	39.4	167	366	176	77
34		-107	-146	74.5	133	635	155	-70
35	92		142	40	166	367	175	75
36		-104	-146	74.5	133	636	157	-70

Failed on the way pushing to 214mm

TEST 5 - 100mm TIE SPACING

LOAD STAGE	JACK DATA			LVDT	Ruler Measurements			d of dot on board
	LOAD (kN)		DISP.	@joint	Top of Hinge	Foot		
	Start	@DG	(mm)	(mm)	Left/Right	Left/Right	Up/Down	(mm)
0	0	0	0	62.9	150	500	100	
1	25	25	14.6	59.4	153	486	101	16
2	25	25	-11.8	65.8	147	512	100	-12
3	25	25	17.5	58.7	154	484	101	20
4	25	25	-13	66.2	147	513	100	-14
5	25	25	17.4	58.7	154	484	101	20
6	25	25	-13	66.7	147	513	100	-14
7	50	50	37	54.6	158	164	102	39
8	50	50	-26	69.3	144	528	100	-26
9	50	50	40.7	54	159	462	105	42
10	50	50	-28.5	70.1	143	529	100	-27
11	50	50	41.7	54	159	463	104	42
12	50	50	-28.7	70.1	144	528	100	-27
13	75	75	58.4	50.8	162	445	105	57
14	75	75	-44.3	73.3	139	545	100	-40
15	75	75	59	50.5	163	444	106	58
16	75	75	-46	73.5	140	546	99	-40
17	75	75	61	50.3	162	442	107	61
18	75	75	-51	74.7	139	550	99	-42
19	87	87	69	48.7	164	436	107	65
20	-99	-99	-69	76.6	137	569	99	-53
21	83	80	69	49	164	435	108	65
22	-99	-93	-69	76	136	567	100	-53
23	83	77	69	49	164	435	108	65
24	-98	-91	-69	76	136	567	100	-49
25	111	110	104	45	166	403	114	70
26	-123	-110	-104	79	136	598	101	-61
27	98	93	104	46.7	166	402	111	77
28	-113	-113	-104	79	135	598	102	-58
29	91	82	104	47.8	165	404	116	77
30	-110	-110	-104	78	135	598	103	-58
31	118	118	138	45	167	369	122	80
32	-129	-111	-138	79	134	633	104	-63
33	109	104	138	46	167	370	125	80
34	-121	-105	-138	79	134	631	105	-63
35	106	107	138	46	166	369	125	81
36	-116	-100	-138	79	135	630	105	-62
37			207					
38	-138		-207					
39			207					
40	-121		-207					
41	112		207					
42	-123		-207					
43	129		276					

TEST 6 - 200mm TIE SPACING

LOAD	JACK DATA		LVDT	Ruler Measurements			Dial Gauges		d of dot
STAGE	LOAD	DISP.	@joint	Hinge	Foot		Beam Outer		
	(kN)	(mm)	(mm)	L/R	L/R	Up/Down	Top	Bottom	(mm)
0		0.15	66.2	150	500	150	4.82	5.21	
1	25	14.8	61.7	155	488	151	4.86	5.22	15
2	-25	-11.5	69.5	146	513	150	4.77	5.22	-12
3	25	15.4	61.7	155	488	151	4.87	5.22	15
4	-25	-12	69	146	513	151	4.78	5.22	-12
5	25	15.1	61.7	155	488	151	4.87	5.22	15
6	-25	-13	70	146	514	150	4.78	5.22	-14
7	50	35	56	161	469	152	4.94	5.17	34
8	-50	-30	74	141	530	150	4.7	5.25	-26
9	50	37	56	161	467	152	4.97	5.14	36
10	-50	-32	74	141	532	150	4.69	5.26	-30
11	50	36	56	161	467	152	4.98	5.13	36
12	-50	-33	75	141	533	150	4.68	5.26	-30
13	75	53	52	165	450	153	5.06	4.84	49
14	-75	-44	77	139	543	150	4.51	5.3	-37
15	75	54	52	165	450	155	5.08	4.8	49
16	-75	-47	79	138	545	150	4.48	5.31	-40
17	75	56	52	165	449	155	5.09	4.78	52
18	-75	-51	78	137	549	151	4.47	5.32	-43
19	94	68	49	168	436	155	5.16	4.64	61
20	-101	-68	81	134	565	152	4.38	5.35	-53
21	91	68	49	168	437	155	5.15	4.63	61
22	-100	-68	81	135	565	152	4.4	5.35	-53
23	74	68	49	167	437	156	5.14	4.65	59
24	-100	-68	81	135	566	152	4.41	5.35	-53
25	118	102	44	172	404	161	5.21	4.36	77
26	-117	-102	83	133	598	155	4.32	5.37	-59
27	104	102	46	171	402	162	5.2	4.42	73
28	-111	-102	83	133	599	155	4.34	5.37	-59
29	101	102	46	171	403	164	5.19	4.44	73
30	-108	-102	83	133	599	155	4.36	5.36	-59
31	107	136	45	173	370	170	5.22	4.36	80
32	-119	-136	83	132	630	160	4.3	5.38	-62
33	106	136	44	173	370	170	5.21	4.4	80
34	-114	-136	82	132	631	160	4.33	5.37	-62
35	105	136	43	173	370	170	5.21	4.42	80
36	-107	-136	81	133	632	160	4.35	5.37	-62
37	123	204	40	176	305	184	5.25	4.24	93
38	-118	-204	81	132	697	165	4.27	5.36	-66
39	109	204	37				5.24	4.31	89

POST YIELDING CYCLE PEAKS - 100 mm tie spacing

TEST TWO

Load Stage	Jack def.	Load (kN)	leg deflection (mm)
19	d	100.833	20.34
20	-d	-97.9	-25.33
21	d	97.428	20.8
22	-d	-97.238	-26.33
23	d	97.144	21.65
24	-d	-97.238	-27.66
25	1.5d	121.643	42.82
26	-1.5d	-113.508	-49.41
27	1.5d	114.832	49.92
28	-1.5d	-106.414	-53.09
29	1.5d	106.319	48.26
30	-1.5d	-104.333	-53.31
31	2d	126.94	69.78
32	-2d	-120.035	-81.48
33	2d	110.292	76.71
34	-2d	-108.022	-81.79
35	2d	105.468	77.78
36	-2d	-104.806	-82.71
37	3d	131.858	129.23
38	-3d	-129.493	-133
39	3d	120.318	132.81
40	-3d	-121.17	-136.31
41	3d	115.305	135.08
42	-3d	-119.278	-137.94
43	4d	128.831	190.49
44	-4d	-133.088	-193.09
45	4d	116.156	196.65
46	-4d	-123.629	-197.7
47	4d	90.333	206.37
48	-4d	-122.305	-197.92
49	4d	88.063	208.29
50	-4d	-111.711	-202.09
51	4d	84.847	209.7
52	-4d	-109.535	-205.45
53	4d	75.672	213.31

TEST FIVE

Load stage	Jack def.	Load (kN)	d of leg (mm)
19	d	86.171	22.86
20	-d	-109.819	-21.08
21	d	83.334	23.11
22	-d	-101.306	-21.67
23	d	85.509	24.57
24	-d	-97.806	-21.87
25	1.5d	111.616	47.89
26	-1.5d	-122.967	-49.73
27	1.5d	99.603	50.18
28	-1.5d	-113.319	-50.93
29	1.5d	101.968	54.78
30	-1.5d	-109.44	-51.28
31	2d	117.102	79.31
32	-2d	-129.021	-81.38
33	2d	110.292	76.71
34	-2d	-108.022	-81.79
35	2d	105.278	81.84
36	-2d	-116.251	-82.53
37	3d	128.831	140.4
38	-3d	-138.29	-142.42
39	3d	115.683	142.83
40	-3d	-124.102	-138.13
41	3d	112.846	142.69
42	-3d	-124.196	-143.23
43	4d	129.115	204.4
44	-4d	-141.317	-203.25
45	4d	116.346	204.85
46	-4d	-122.588	-202.97
47	4d	91.752	156.41
48	-4d	-110.008	-207.42
49	4d	65.551	192.12
50	-4d	-51.173	-202.23
51	4d	17.405	121.66

First cycle load peaks

		load (kN)	Leg d (mm)
19	d	100.833	20.34
20	-d	-97.9	-25.33
19	d	86.171	22.86
20	-d	-109.819	-21.08
25	1.5d	121.643	42.82
26	-1.5d	-113.508	-49.41
25	1.5d	111.616	47.89
26	-1.5d	-122.967	-49.73
31	2d	126.94	69.78
32	-2d	-120.035	-81.48
31	2d	117.102	79.31
32	-2d	-129.021	-81.38
37	3d	131.858	129.23
38	-3d	-129.493	-133
37	3d	128.831	140.4
38	-3d	-138.29	-142.42
43	4d	128.831	190.49
44	-4d	-133.088	-193.09
43	4d	129.115	204.4
44	-4d	-141.317	-203.25

Second cycle load peaks

		load (kN)	Leg d (mm)
21	d	97.428	20.80
22	-d	-97.238	-26.33
21	d	83.334	23.11
22	-d	-101.306	-21.67
27	1.5d	114.832	49.92
28	-1.5d	-106.414	-53.09
27	1.5d	99.603	50.18
28	-1.5d	-113.319	-50.93
33	2d	110.292	76.71
34	-2d	-108.022	-81.79
33	2d	110.292	76.71
34	-2d	-108.022	-81.79
39	3d	120.318	132.81
40	-3d	-121.17	-136.31
39	3d	115.683	142.83
40	-3d	-124.102	-138.13
45	4d	116.156	196.65
46	-4d	-123.629	-197.70
45	4d	116.346	204.85
46	-4d	-122.588	-202.97

Third cycle load peaks

		load (kN)	Leg d (mm)
23	d	97.144	21.65
24	-d	-97.238	-27.66
23	d	85.509	24.57
24	-d	-97.806	-21.87
29	1.5d	106.319	48.26
30	-1.5d	-104.333	-53.31
29	1.5d	101.968	54.78
30	-1.5d	-109.44	-51.28
35	2d	105.468	77.78
36	-2d	-104.806	-82.71
35	2d	105.278	81.84
36	-2d	-116.251	-82.53
41	3d	115.305	135.08
42	-3d	-119.278	-137.94
41	3d	112.846	142.69
42	-3d	-124.196	-143.23
47	4d	90.333	206.37
48	-4d	-122.305	-197.92
48	-4d	-110.008	-207.42
49	4d	88.063	208.29
50	-4d	-111.711	-202.09
49	4d	65.551	192.12
50	-4d	-51.173	-202.23
51	4d	84.847	209.70
52	-4d	-109.535	-205.45
53	4d	75.672	213.31

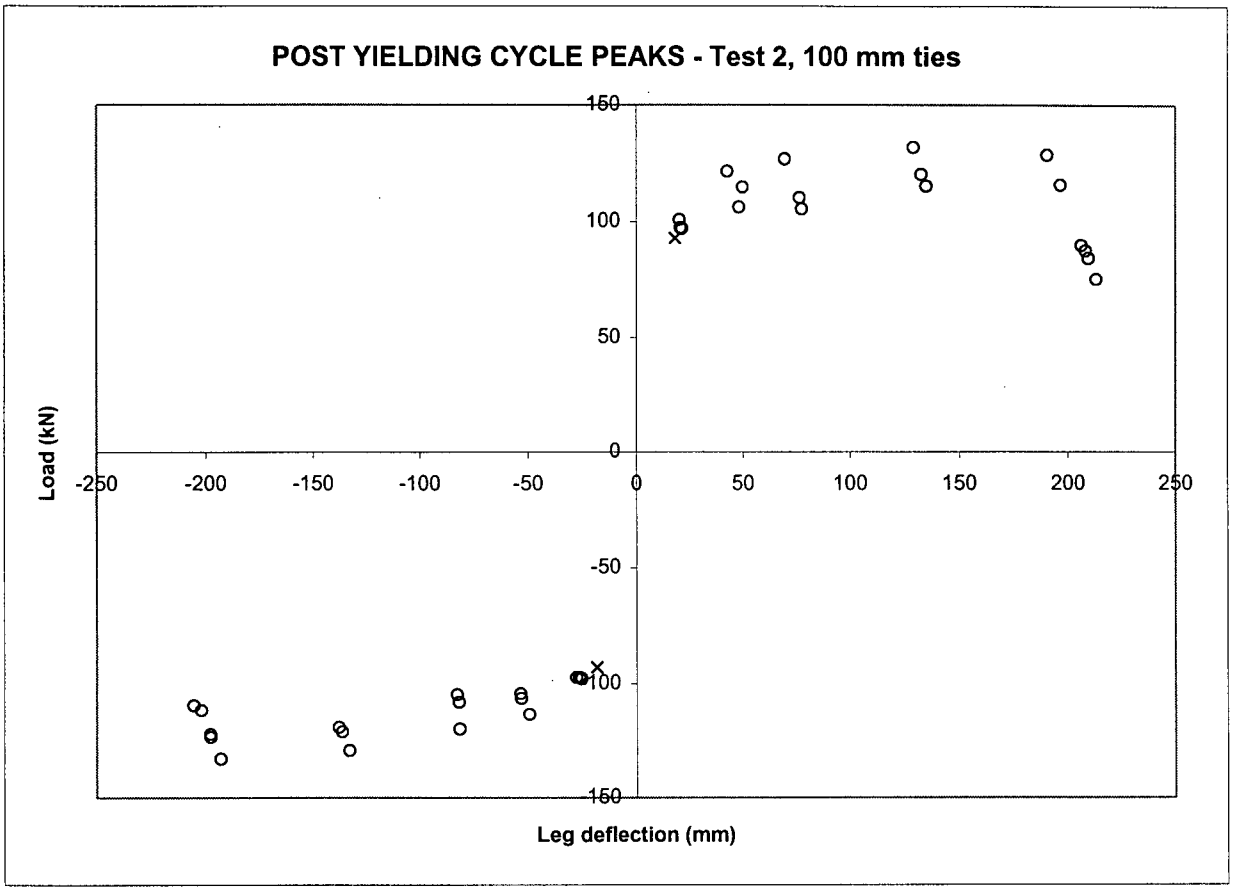
POST YIELDING CYCLE PEAKS - Test 2, 100 mm ties
Load (kN)
150
100
50
0
-50
-100
-150
-250
-200
-150
-100
-50
0
50
100
150
200
250
Leg deflection (mm)

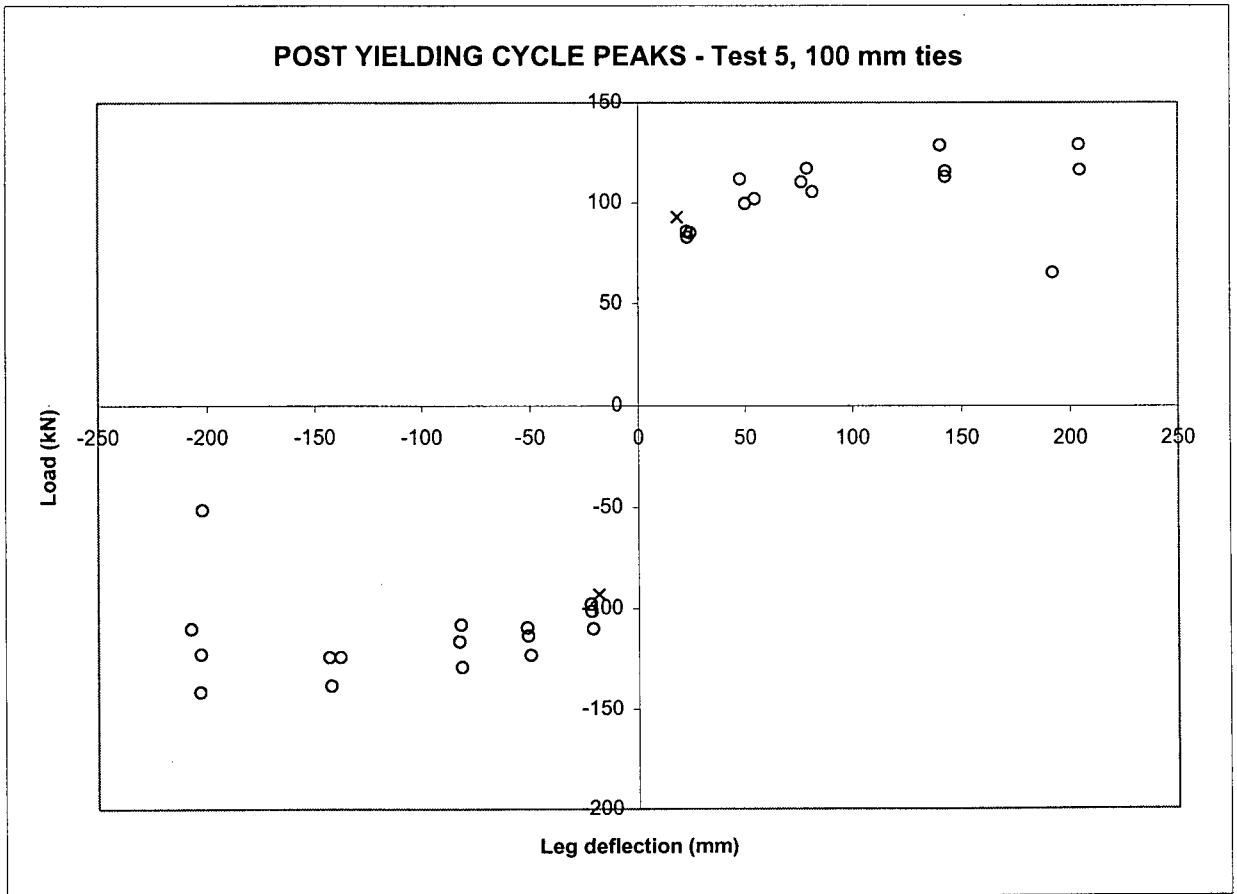
POST YIELDING CYCLE PEAKS - Test 5, 100 mm ties
Load (kN)
150
100
50
0
-50
-100
-150
-200
-250
-200
-150
-100
-50
0
50
100
150
200
250
Leg deflection (mm)

POST YIELDING CYCLE PEAKS - 200mm Tie spacing specimen

TEST 6

Load stage	Jack def.	Load (kN)	d of leg (mm)
19	d	96.387	24.0
20	-d	-105.184	-29.7
21	d	92.603	24.2
22	-d	-101.4	-29.2
23	d	82.009	23.8
24	-d	-99.509	-28.5
25	1.5d	119.089	47.1
26	-1.5d	-120.129	-55.0
27	1.5d	105.657	48.4
28	-1.5d	-112.089	-58.7
29	1.5d	105.468	51.2
30	-1.5d	-108.495	-58.6
31	2d	125.426	83.3
32	-2d	-121.832	-92.5
33	2d	107.927	75.9
34	-2d	-116.156	-95.0
35	2d	108.967	78.6
36	-2d	-112.373	-94.8
37	3d	127.413	134.2
38	-3d	-131.953	-166.4
39	3d	114.832	129.1
40	-3d	-95.63	-187.1
41	3d	104.995	126.6
42	-3d	-102.819	-147.5
43	4d	101.306	228.0
44	-4d	-88.158	-234.0

First cycle peaks

19	d	96.387	24.0
20	-d	-105.2	-29.7
25	1.5d	119.09	47.1
26	-1.5d	-120.1	-55.0
31	2d	125.43	83.3
32	-2d	-121.8	-92.5
37	3d	127.41	134.2
38	-3d	-132	-166.4
43	4d	101.31	228.0
44	-4d	-88.16	-234.0

Second cycle peaks

21	d	92.603	24.2
22	-d	-101.4	-29.2
27	1.5d	105.66	48.4
28	-1.5d	-112.1	-58.7
33	2d	107.93	75.9
34	-2d	-116.2	-95.0
39	3d	114.83	129.1
40	-3d	-95.63	-187.1

Third cycle peaks

23	d	82.009	23.8
24	-d	-99.51	-28.5
29	1.5d	105.47	51.2
30	-1.5d	-108.5	-58.6
35	2d	108.97	78.6
36	-2d	-112.4	-94.8
41	3d	105	126.6
42	-3d	-102.8	-147.5

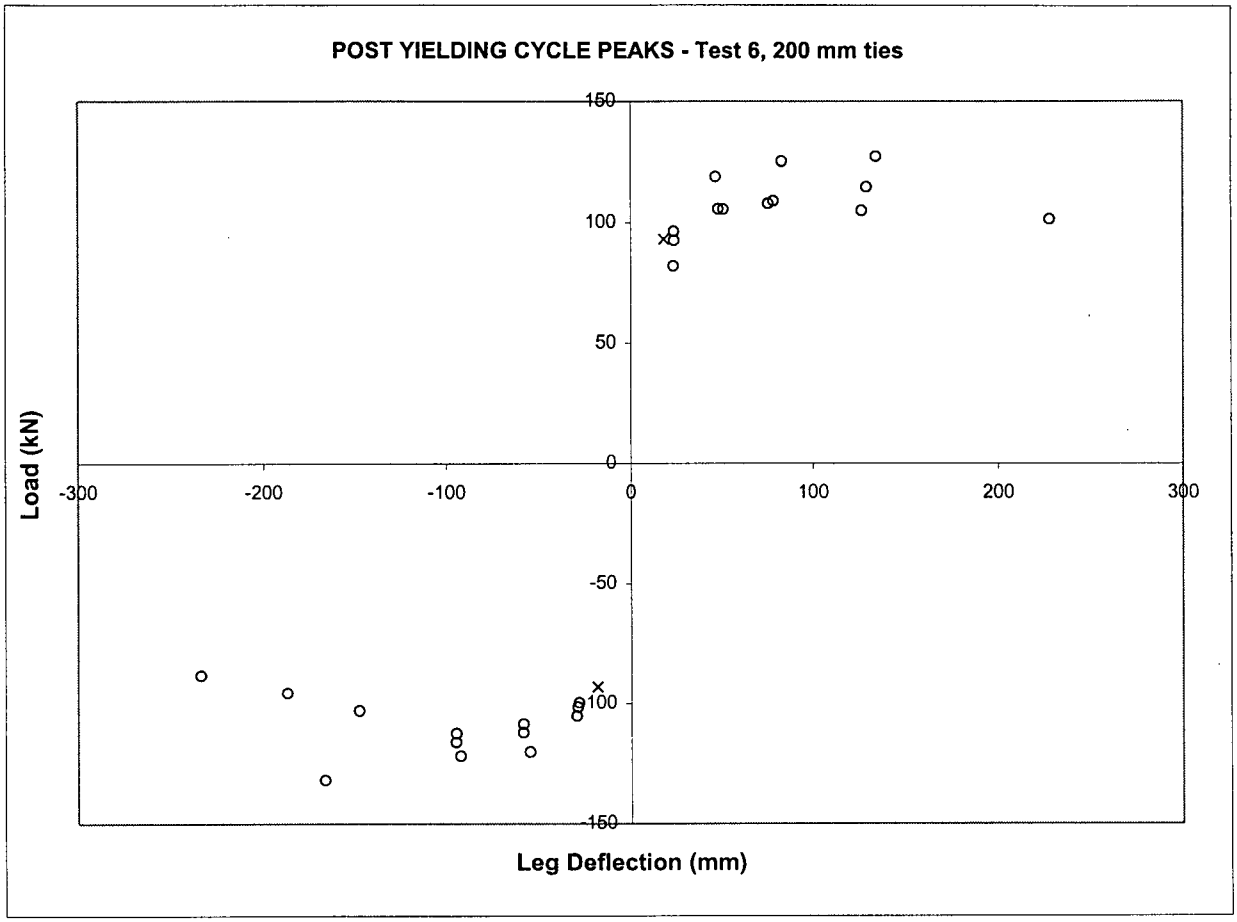
POST YIELDING CYCLE PEAKS - Test 6, 200 mm ties
Load (kN)
Leg Deflection (mm)
150
100
50
0
-50
-100
-150
-300
-200
-100
0
100
200
300

POST YIELDING CYCLE PEAKS - 300 mm tie spacing

TEST THREE

Load Stage	Jack def.	Load (kN)	leg def (mm)
19	d	98.09	25.92
20	-d	-102.062	-16.02
21	d	96.292	27.16
22	-d	-97.049	-18.48
23	d	94.684	27.02
24	-d	-91.563	-17.79
25	1.5d	117.67	47.78
26	-1.5d	-116.724	-40.91
27	1.5d	99.603	49.80
28	-1.5d	-79.361	-49.96
29	1.5d	99.036	49.47
30	-1.5d	-82.388	-49.61
31	2d	113.697	76.67
32	-2d	-106.508	-73.40
33	2d	108.305	76.59
34	-2d	-101.873	-70.92
35	2d	106.792	77.33
36	-2d	-101.873	-74.75
37	3d	117.197	136.29
38	-3d	-110.67	-133.55
39	3d	101.589	143.11
40	-3d	-98.09	-143.31
41	3d	92.131	152.06
42	-3d	-85.509	-153.27
43	4d	79.077	180.53
44	-4d	-47.106	-163.48

TEST FOUR

Load Stage	Jack def.	Load (kN)	d of leg (mm)
19	d	100.076	28.01
20	-d	-104.711	-28.73
21	d	95.063	30.02
22	-d	-100.927	-29.12
23	d	93.549	30.31
24	-d	-100.36	-30.07
25	1.5d	117.008	54.12
26	-1.5d	-115.4	-59.33
27	1.5d	104.333	58.37
28	-1.5d	-102.346	-62.08
29	1.5d	101.589	60.31
30	-1.5d	-102.252	-62.42
31	2d	117.102	87.73
32	-2d	-115.873	-94.51
33	2d	107.359	90.76
34	-2d	-110.765	-96.59
35	2d	97.806	93.44
36	-2d	-106.508	-95.76
37	3d	103.481	130.68
38	-3d	-90.05	-147
39	3d	80.023	162
40	-3d	-47.106	-166.93

First cycle peaks

19	d	98.09	25.92
20	-d	-102.062	-16.02
19	d	100.076	28.01
20	-d	-104.711	-28.73
25	1.5d	117.67	47.78
26	-1.5d	-116.724	-40.91
25	1.5d	117.008	54.12
26	-1.5d	-115.4	-59.33
31	2d	113.697	76.67
32	-2d	-106.508	-73.40
31	2d	117.102	87.73
32	-2d	-115.873	-94.51
37	3d	117.197	136.29
38	-3d	-110.67	-133.55
37	3d	103.481	130.68
38	-3d	-90.05	-147
43	4d	79.077	180.53
44	-4d	-47.106	-163.48

Second cycle peaks

21	d	96.292	27.16
22	-d	-97.049	-18.48
21	d	95.063	30.02
22	-d	-100.927	-29.12
27	1.5d	99.603	49.80
28	-1.5d	-79.361	-49.96
27	1.5d	104.333	58.37
28	-1.5d	-102.346	-62.08
33	2d	108.305	76.59
34	-2d	-101.873	-70.92
33	2d	107.359	90.76
34	-2d	-110.765	-96.59
39	3d	101.589	143.11
40	-3d	-98.09	-143.31
39	3d	80.023	162
40	-3d	-47.106	-166.93

Third cycle peaks

23	d	94.684	27.02
24	-d	-91.563	-17.79
23	d	93.549	30.31
24	-d	-100.36	-30.07
29	1.5d	99.036	49.47
30	-1.5d	-82.388	-49.61
29	1.5d	101.589	60.31
30	-1.5d	-102.252	-62.42
35	2d	106.792	77.33
36	-2d	-101.873	-74.75
35	2d	97.806	93.44
36	-2d	-106.508	-95.76
41	3d	92.131	152.06
42	-3d	-85.509	-153.27

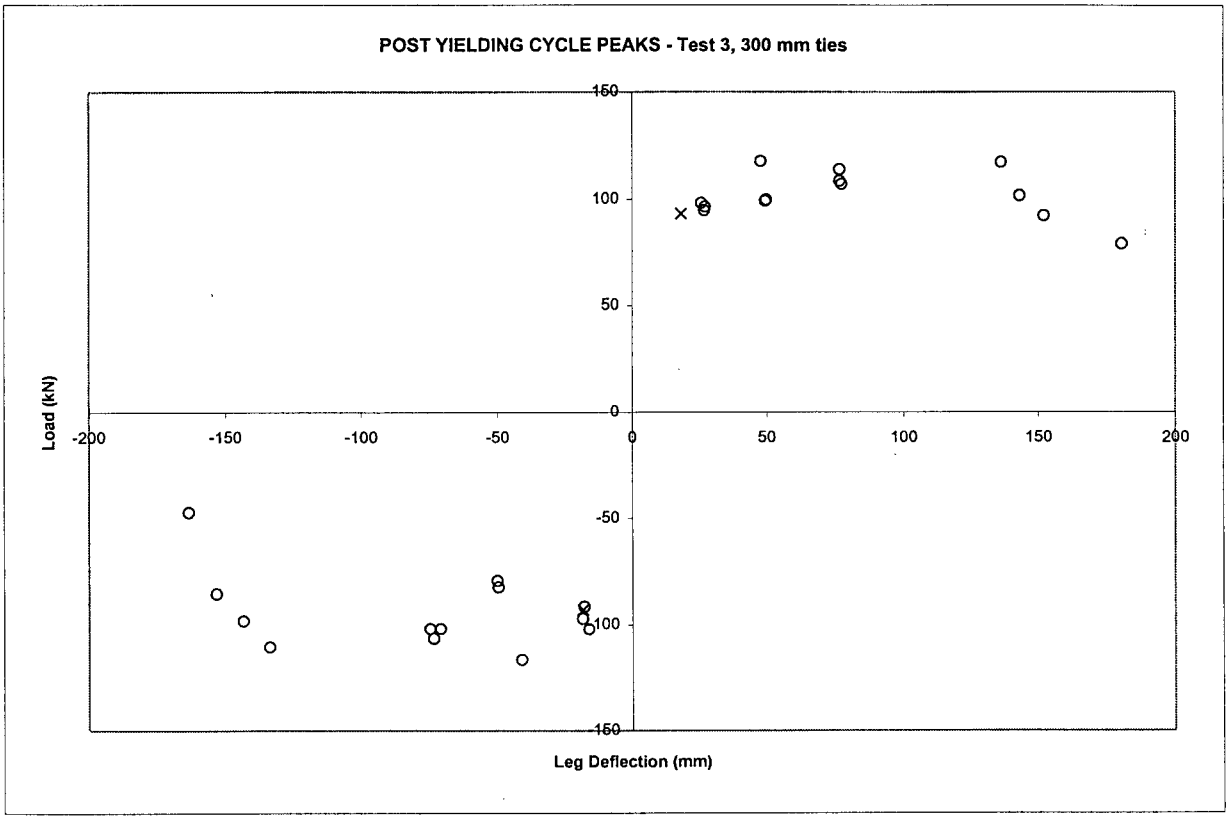
POST YIELDING CYCLE PEAKS - Test 3, 300 mm ties
Load (kN)
150
100
50
0
-50
-100
-150
-200
-150
-100
-50
0
50
100
150
200
Leg Deflection (mm)

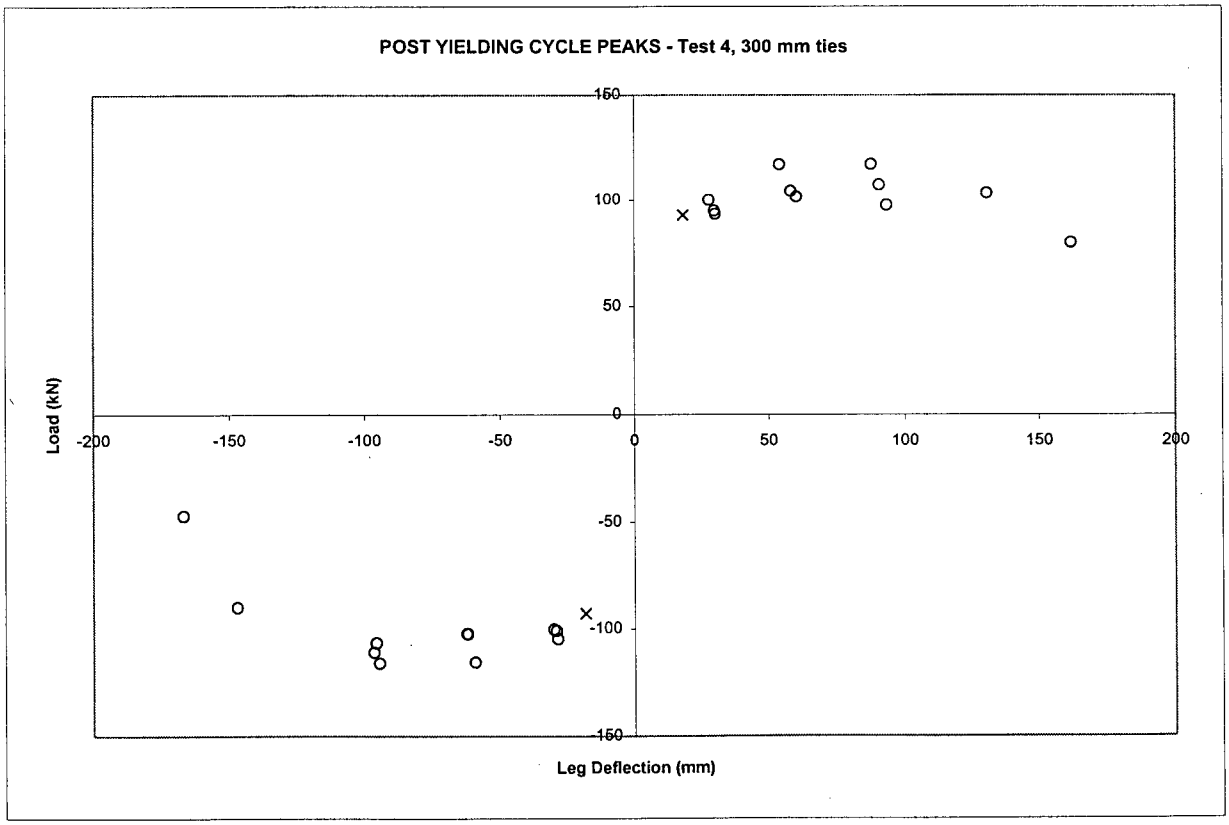
POST YIELDING CYCLE PEAKS - Test 4, 300 mm ties
Load (kN)
150
100
50
0
-50
-100
-150
-200
-150
-100
-50
0
50
100
150
200
Leg Deflection (mm)

APPENDIX VI

FRAME ANALYSIS FOR DISPLACEMENT AT ULTIMATE STRENGTH

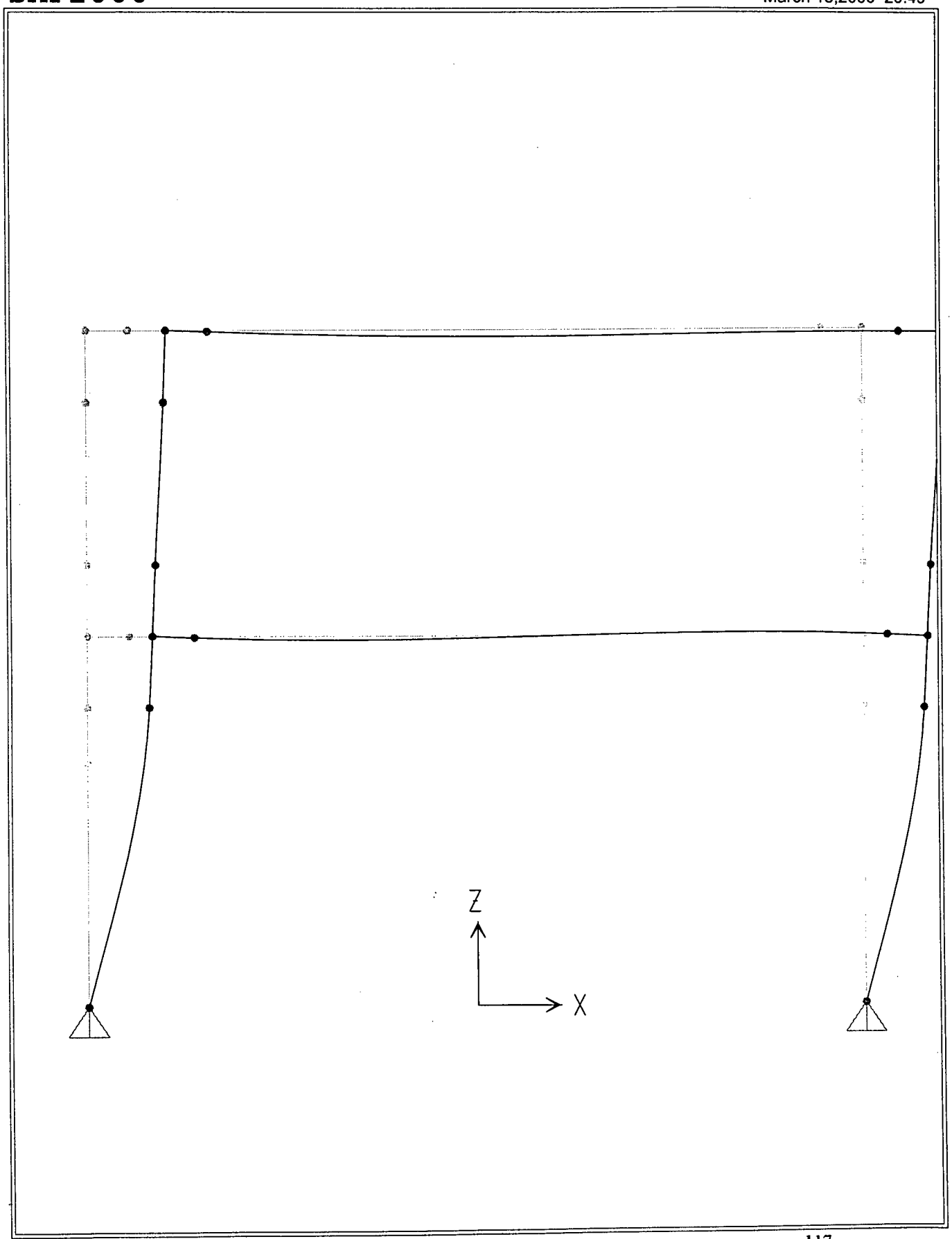
Z
X

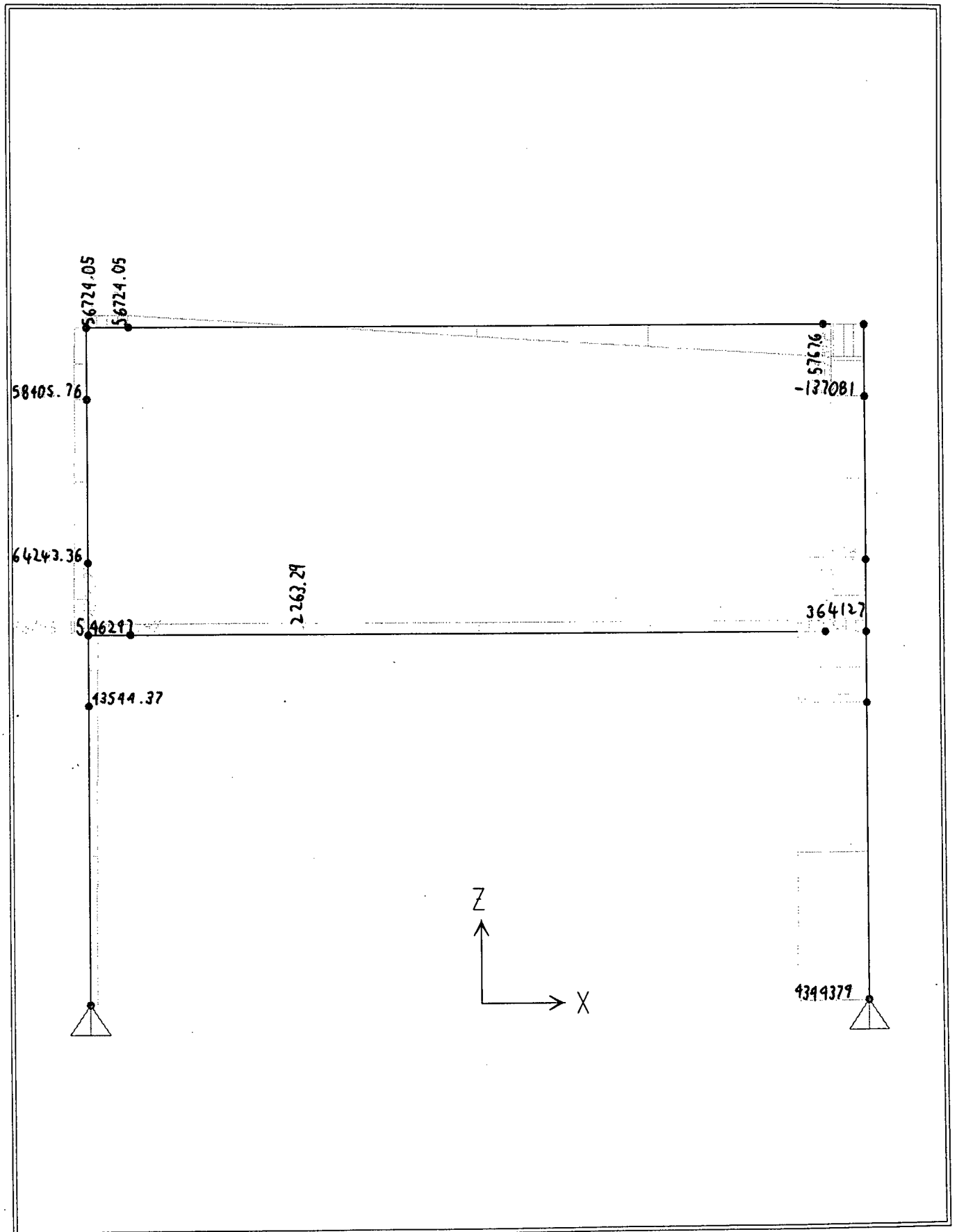
56724.05
56724.05
58405.76
64243.36
2263.29
546297
13544.37
-157676
-137081
364127
4349379
Z
X

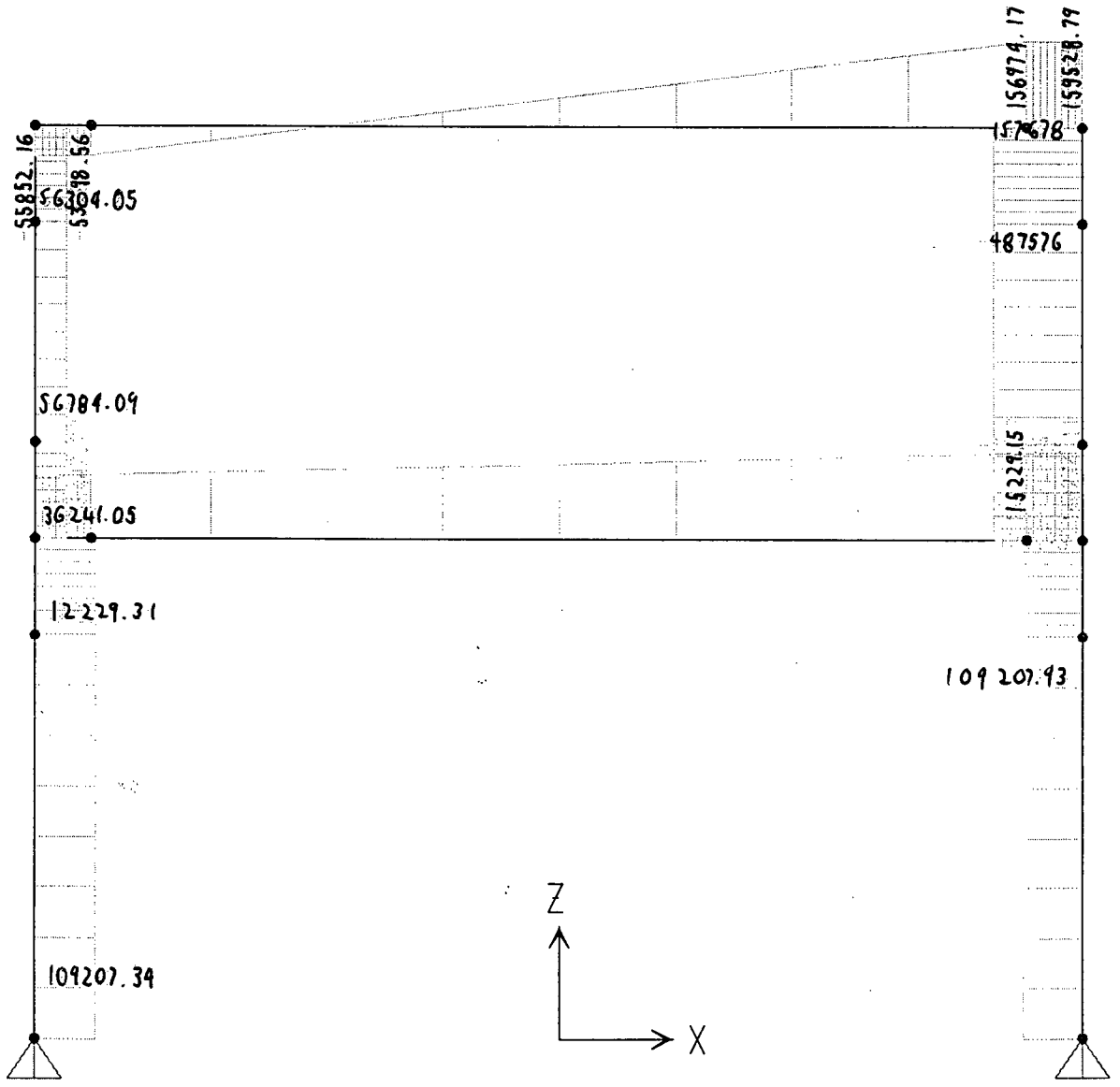
156974.17
159528.79
157678
55852.16
53398.56
56204.05
487576
56784.09
36241.05
152291.15
12229.31
109207.93
109207.34
Z
X

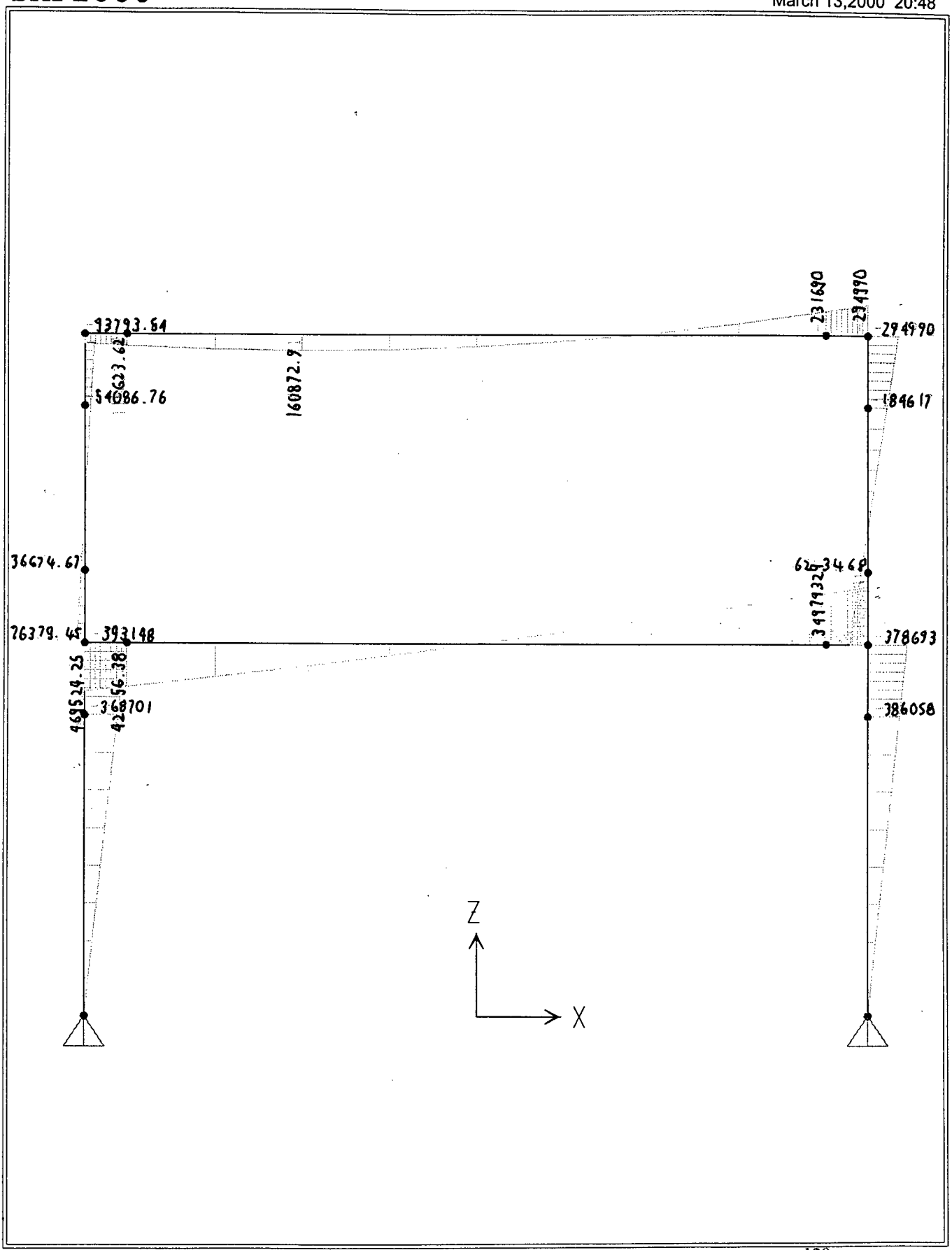
93793.64
54086.76
160872.9
231690
294990
294990
184617
36674.67
76379.45
393148
378693
386058
Z
X

SAP2000 v6.10 File: TEST2 N-m Units March 13, 2000 20:37

JOINT DISPLACEMENTS

JOINT	LOAD	UX	UY	UZ	RX	RY	RZ
1	LOAD1	0.0000	0.0000	0.0000	0.0000	0.0135	0.0000
2	LOAD1	0.0296	0.0000	1.432E-04	0.0000	2.378E-03	0.0000
3	LOAD1	0.0312	0.0000	1.442E-04	0.0000	2.225E-03	0.0000
4	LOAD1	0.0327	0.0000	1.427E-04	0.0000	2.249E-03	0.0000
5	LOAD1	0.0369	0.0000	1.607E-05	0.0000	1.912E-03	0.0000
6	LOAD1	0.0382	0.0000	1.475E-05	0.0000	1.880E-03	0.0000
7	LOAD1	0.0382	0.0000	-7.377E-04	0.0000	1.875E-03	0.0000
8	LOAD1	0.0380	0.0000	-1.545E-03	0.0000	2.022E-04	0.0000
9	LOAD1	0.0380	0.0000	-1.625E-03	0.0000	2.143E-04	0.0000
10	LOAD1	0.0378	0.0000	-1.621E-03	0.0000	3.179E-04	0.0000
11	LOAD1	0.0332	0.0000	-1.281E-03	0.0000	2.582E-03	0.0000
12	LOAD1	0.0314	0.0000	-1.277E-03	0.0000	2.529E-03	0.0000
13	LOAD1	0.0296	0.0000	-1.269E-03	0.0000	2.676E-03	0.0000
14	LOAD1	0.0000	0.0000	0.0000	0.0000	0.0134	0.0000
15	LOAD1	0.0312	0.0000	-7.389E-04	0.0000	2.204E-03	0.0000
16	LOAD1	0.0314	0.0000	-2.739E-04	0.0000	2.505E-03	0.0000

JOINT REACTIONS

JOINT	LOAD	F1	F2	F3	M1	M2	M3
1	LOAD1	-109207	0.0000	-32965.1758	0.0000	0.0000	0.0000
14	LOAD1	-105193	0.0000	344378.6563	0.0000	0.0000	0.0000

FRAME ELEMENT FORCES

FRAME	LOAD	LOC	P	V2	V3	T	M2	M3
1	LOAD1							
		0.00	32965.18	109207.34	0.00	0.00	0.00	0.00
		1.45	38254.77	109207.34	0.00	0.00	0.00	-158350.58
		2.90	43544.37	109207.34	0.00	0.00	0.00	-316701.16
2	LOAD1							
		0.00	43544.37	109207.34	0.00	0.00	0.00	-316701.16
		3.5E-01	44821.17	109207.34	0.00	0.00	0.00	-354923.75
		7.0E-01	46097.97	109207.34	0.00	0.00	0.00	-393146.31
3	LOAD1							
		0.00	52483.29	112894.13	0.00	0.00	0.00	469524.75

1.0E-01	52483.29	113532.52	0.00	0.00	0.00	458203.44
2.0E-01	52483.29	114170.92	0.00	0.00	0.00	446818.25
3.0E-01	52483.29	114809.32	0.00	0.00	0.00	435369.25
4.0E-01	52483.29	115447.72	0.00	0.00	0.00	423856.38
4 LOAD1						
0.00	52483.29	115447.72	0.00	0.00	0.00	423856.38
1.67	52483.29	126140.92	0.00	0.00	0.00	221525.97
3.35	52483.29	136834.11	0.00	0.00	0.00	1284.44
5.02	52483.29	147527.31	0.00	0.00	0.00	-236868.19
6.70	52483.29	158220.52	0.00	0.00	0.00	-492931.91
5 LOAD1						
0.00	52483.29	158220.52	0.00	0.00	0.00	-492931.91
1.0E-01	52483.29	158858.91	0.00	0.00	0.00	-508785.84
2.0E-01	52483.29	159497.31	0.00	0.00	0.00	-524703.63
3.0E-01	52483.29	160135.70	0.00	0.00	0.00	-540685.25
4.0E-01	52483.29	160774.11	0.00	0.00	0.00	-556730.69
6 LOAD1						
0.00	-331245.88	-105192.60	0.00	0.00	0.00	-378693.25
3.5E-01	-332522.66	-105192.60	0.00	0.00	0.00	-341875.84
7.0E-01	-333799.47	-105192.60	0.00	0.00	0.00	-305058.44
7 LOAD1						
0.00	-333799.47	-105192.60	0.00	0.00	0.00	-305058.44
1.45	-339089.06	-105192.60	0.00	0.00	0.00	-152529.22
2.90	-344378.66	-105192.60	0.00	0.00	0.00	0.00
8 LOAD1						
0.00	-66796.15	56724.05	0.00	0.00	0.00	76378.45
3.5E-01	-65519.35	56724.05	0.00	0.00	0.00	56525.06
7.0E-01	-64242.55	56724.05	0.00	0.00	0.00	36671.67
9 LOAD1						
0.00	-64242.55	56724.05	0.00	0.00	0.00	36671.67
8.0E-01	-61324.16	56724.05	0.00	0.00	0.00	-8707.55
1.60	-58405.76	56724.05	0.00	0.00	0.00	-54086.76
10 LOAD1						
0.00	-58405.76	56724.05	0.00	0.00	0.00	-54086.76
3.5E-01	-57128.96	56724.05	0.00	0.00	0.00	-73940.15
7.0E-01	-55852.16	56724.05	0.00	0.00	0.00	-93793.54

11 LOAD1

0.00	56724.05	-55852.16	0.00	0.00	0.00	93793.54
1.0E-01	56724.05	-55213.76	0.00	0.00	0.00	99346.84
2.0E-01	56724.05	-54575.36	0.00	0.00	0.00	104836.30
3.0E-01	56724.05	-53936.96	0.00	0.00	0.00	110261.91
4.0E-01	56724.05	-53298.56	0.00	0.00	0.00	115623.69

12 LOAD1

0.00	56724.05	-53298.56	0.00	0.00	0.00	115623.69
1.67	3124.07	-730.38	0.00	0.00	0.00	160872.91
3.35	-50475.91	51837.81	0.00	0.00	0.00	118070.45
5.02	-104075.90	104405.99	0.00	0.00	0.00	-12783.69
6.70	-157675.88	156974.17	0.00	0.00	0.00	-231689.52

13 LOAD1

0.00	-157675.88	156974.17	0.00	0.00	0.00	-231689.52
1.0E-01	-157675.88	157612.58	0.00	0.00	0.00	-247418.81
2.0E-01	-157675.88	158250.97	0.00	0.00	0.00	-263211.97
3.0E-01	-157675.88	158889.38	0.00	0.00	0.00	-279068.94
4.0E-01	-157675.88	159527.77	0.00	0.00	0.00	-294989.75

14 LOAD1

0.00	-159527.77	-157675.88	0.00	0.00	0.00	-294989.75
3.5E-01	-160804.56	-157675.88	0.00	0.00	0.00	-239803.27
7.0E-01	-162081.36	-157675.88	0.00	0.00	0.00	-184616.80

15 LOAD1

0.00	-162081.36	-157675.88	0.00	0.00	0.00	-184616.80
8.0E-01	-164999.77	-157675.88	0.00	0.00	0.00	-58476.16
1.60	-167918.16	-157675.88	0.00	0.00	0.00	67664.46

16 LOAD1

0.00	-167918.16	-157675.88	0.00	0.00	0.00	67664.46
3.5E-01	-169194.95	-157675.88	0.00	0.00	0.00	122850.95
7.0E-01	-170471.77	-157675.88	0.00	0.00	0.00	178037.42

S T A T I C L O A D C A S E S

STATIC CASE	CASE TYPE	SELF WT FACTOR
LOAD1	DEAD	1.0000

J O I N T D A T A

JOINT	GLOBAL-X	GLOBAL-Y	GLOBAL-Z	RESTRAINTS
	ANGLE-A	ANGLE-B	ANGLE-C	
1	-3.75000	3.75000	0.00000	1 1 1 0 0 0
0.000	0.000	0.000		
2	-3.75000	3.75000	2.90000	0 0 0 0 0 0
0.000	0.000	0.000		
3	-3.75000	3.75000	3.60000	0 0 0 0 0 0
0.000	0.000	0.000		
4	-3.75000	3.75000	4.30000	0 0 0 0 0 0
0.000	0.000	0.000		
5	-3.75000	3.75000	5.90000	0 0 0 0 0 0
0.000	0.000	0.000		
6	-3.75000	3.75000	6.60000	0 0 0 0 0 0
0.000	0.000	0.000		
7	-3.35000	3.75000	6.60000	0 0 0 0 0 0
0.000	0.000	0.000		
8	3.35000	3.75000	6.60000	0 0 0 0 0 0
0.000	0.000	0.000		
9	3.75000	3.75000	6.60000	0 0 0 0 0 0
0.000	0.000	0.000		
10	3.75000	3.75000	5.90000	0 0 0 0 0 0
0.000	0.000	0.000		
11	3.75000	3.75000	4.30000	0 0 0 0 0 0
0.000	0.000	0.000		
12	3.75000	3.75000	3.60000	0 0 0 0 0 0
0.000	0.000	0.000		
13	3.75000	3.75000	2.90000	0 0 0 0 0 0
0.000	0.000	0.000		
14	3.75000	3.75000	0.00000	1 1 1 0 0 0
0.000	0.000	0.000		
15	-3.35000	3.75000	3.60000	0 0 0 0 0 0
0.000	0.000	0.000		
16	3.35000	3.75000	3.60000	0 0 0 0 0 0
0.000	0.000	0.000		

F R A M E E L E M E N T D A T A

FRAME	JNT-1	JNT-2	SECTION	ANGLE	RELEASES	SEGMENTS
	R1	R2	FACTOR	LENGTH		
1	1	2	LEG	0.000	000000	2
0.000	0.000	1.000	2.900			
2	2	3	JNTLEG	0.000	000000	2
0.000	0.000	1.000	0.700			
3	3	15	JNTBM	0.000	000000	4
0.000	0.000	1.000	0.400			
4	15	16	BEAM	0.000	000000	4
0.000	0.000	1.000	6.700			
5	16	12	JNTBM	0.000	000000	4
0.000	0.000	1.000	0.400			
6	12	13	JNTLEG	0.000	000000	2
0.000	0.000	1.000	0.700			
7	13	14	LEG	0.000	000000	2
0.000	0.000	1.000	2.900			
8	3	4	JNTLEG	0.000	000000	2
0.000	0.000	1.000	0.700			

```
9        4        5        LEG      0.000     000000          2
0.000      0.000      1.000        1.600
10       5        6      JNTLEG      0.000     000000          2
0.000      0.000      1.000        0.700
11       6        7       JNTBM      0.000     000000          4
0.000      0.000      1.000        0.400
12       7        8        BEAM      0.000     000000          4
0.000      0.000      1.000        6.700
13       8        9       JNTBM      0.000     000000          4
0.000      0.000      1.000        0.400
14       9       10      JNTLEG      0.000     000000          2
0.000      0.000      1.000        0.700
15      10       11         LEG      0.000     000000          2
0.000      0.000      1.000        1.600
16      11       12      JNTLEG      0.000     000000          2
0.000      0.000      1.000        0.700
```

M A T E R I A L P R O P E R T Y D A T A

MAT LABEL	MODULUS OF ELASTICITY	POISSON'S RATIO	THERMAL COEFF	WEIGHT PER UNIT VOL	MASS PER UNIT VOL
STEEL	1.999E+11	0.300	1.170E-05	76819.547	7827.101
CONC	2.482E+10	0.200	9.900E-06	23561.609	2400.680
LEGMAT	5.098E+09	0.200	0.000	24000.000	2400.000
BEAMMAT	5.472E+09	0.200	0.000	24000.000	2400.000
JNTMAT	2.000E+11	0.300	0.000	24000.000	2400.000

M A T E R I A L D E S I G N D A T A

MAT LABEL	DESIGN CODE	STEEL FY	CONCRETE FC	REBAR FY	CONCRETE REBAR FYS
STEEL	S	248211296			
CONC	C		27579030	413685504	27579030 275790304
LEGMAT	N				
BEAMMAT	N				
JNTMAT	N				

F R A M E S E C T I O N P R O P E R T Y D A T A

SECTION LABEL	MAT LABEL	SECTION TYPE	DEPTH	FLANGE WIDTH	FLANGE THICK	WEB THICK	FLANGE WIDTH TOP	FLANGE THICK TOP	FLANGE WIDTH BOTTOM	FLANGE THICK BOTTOM
BEAM	BEAMMAT		1.400	0.190	0.000	0.000	0.000	0.000		
LEG	LEGMAT		0.800	0.190	0.000	0.000	0.000	0.000		

JNTLEG	JNTMAT			0.800	0.190
0.000	0.000	0.000	0.000		
JNTBM	JNTMAT			1.400	0.190
0.000	0.000	0.000	0.000		

F R A M E S E C T I O N P R O P E R T Y D A T A

SECTION LABEL	AREA	TORSIONAL INERTIA	MOMENTS OF INERTIA I33	I22	SHEAR AREAS A2	A3
BEAM	0.266	2.927E-03	4.345E-02	8.002E-04	0.222	0.222
LEG	0.152	1.555E-03	8.107E-03	4.573E-04	0.127	0.127
JNTLEG	0.152	1.555E-03	8.107E-03	4.573E-04	0.127	0.127
JNTBM	0.266	2.927E-03	4.345E-02	8.002E-04	0.222	0.222

F R A M E S E C T I O N P R O P E R T Y D A T A

SECTION LABEL	SECTION MODULII S33	S22	PLASTIC MODULII Z33	Z22	RADII OF GYRATION R33	R22
BEAM	6.207E-02	8.423E-03	9.310E-02	1.263E-02	0.404	5.485E-02
LEG	2.027E-02	4.813E-03	3.040E-02	7.220E-03	0.231	5.485E-02
JNTLEG	2.027E-02	4.813E-03	3.040E-02	7.220E-03	0.231	5.485E-02
JNTBM	6.207E-02	8.423E-03	9.310E-02	1.263E-02	0.404	5.485E-02

F R A M E S E C T I O N P R O P E R T Y D A T A

SECTION LABEL	TOTAL WEIGHT	TOTAL MASS
BEAM	85545.570	8554.558
LEG	32831.984	3283.198
JNTLEG	15321.587	1532.159
JNTBM	10214.391	1021.439

S H E L L S E C T I O N P R O P E R T Y D A T A

SECTION LABEL	MAT LABEL	SHELL TYPE	MEMBRANE THICK	BENDING THICK	MATERIAL ANGLE
SSEC1	CONC	1	1.000	1.000	0.000

SAP2000 v6.10 File: TEST2 N-m Units PAGE 11
March 13, 2000 20:38

S H E L L S E C T I O N P R O P E R T Y D A T A

SECTION LABEL	TOTAL WEIGHT	TOTAL MASS
SSEC1	0.000	0.000

SAP2000 v6.10 File: TEST2 N-m Units PAGE 12
March 13, 2000 20:38

G R O U P M A S S D A T A

GROUP	M-X	M-Y	M-Z
ALL	14391.352	14391.352	14391.352

SAP2000 v6.10 File: TEST2 N-m Units PAGE 13
March 13, 2000 20:38

F R A M E S P A N D I S T R I B U T E D L O A D S Load Case LOAD1

FRAME	TYPE	DIRECTION	DISTANCE-A	VALUE-A	DISTANCE-B	VALUE-B
12	FORCE	GLOBAL-X	0.0000	32000.0000	1.0000	32000.0000
12	FORCE	GLOBAL-Z	0.0000	-25000.0000	1.0000	-25000.0000